P.N. Lebedev Physical **Institute RAS, Samara Branch,**
Chemical and Electric-Discharge Laser Laboratory

Novo-Sadovaya str., 221, Samara, **443011,** Russia, Fax: (8462)-355-600, e-mail:
<nikolaev@**fian.samara.ru** >;

The final technical report (contract F61775-99-WE032.)

The numeration of figures, tables and citation in each part of final report are independent.

Part 1.

1.4 kW COIL with 5 cm Gain Length and Nitrogen Dilution

ABSTRACT

The developed supersonic COIL with 5 cm gain length was driven by Verti Jet SOG having 0.28 liter of working volume. The oxygen was diluted by the primary nitrogen downstream from the JSOG. Two types of nozzles were tested: single throat nozzle with 10 mm throat height and double throat nozzle with total throat height 15 mm. The COIL with single throat nozzle operated at the primary nitrogen dilution O_2:N_2 = 1:1 and the chlorine flow rate less than 40 mmole/s to maintain the designed gas flow conditions in the reactor of JSOG. The maximum power 765 W has been achieved at 39 mmole/s of the chlorine molar flow rate. The using of double throat nozzle allowed to increase chlorine molar flow rate up to 75 mmole/s. In this case the maximum power 1.4 kW has been reached for primary nitrogen ratio O_2:N_2=1:1.28. The specific performances of 5 kW per 1 liter of the reactor volume, of 100 W/cm^2 per unit of the stream cross section area in the cavity and of 2,7W/(liter/s) of the pump capacity were obtained.

Specification

P_1- pressure in reactor
P_2- in the mixing chamber (plenum pressure),
P_3static pressure in the cavity,
P_4 -pressure in iodine measurement cell,
P_5 -total pressure in Pitot tube
P_6 -pressure in the vacuum duct downstream cavity
P_{I2}- iodine partial pressure in the measuring cell
G_c - chlorine molar flow rate,
G_{NP} -primary nitrogen molar flow rate,
G_{NS} -secondary nitrogen molar flow rate,
G_{I2}- iodine molar flow rate,
G_{NM}-the total nitrogen molar flow rate through mirrors tunnels (purging)
T_1 - the transmission of the output mirror,
T_2 - transmission of the second mirror.
W_1- laser power from output mirror
W- total laser power
η_c-chemical efficiency
M- Mach number of the flow from ratio $\frac{P_5}{P_3} = \frac{166.7M^7}{\left(7M^2-1\right)^{2.5}}$

1.1 Introduction

The large interest to a possibility of creation of the chemical oxygen-iodine laser (COIL) for various technological applications has increased now [1-3]. The special interest represents the use COIL with 10÷30 kW power level for the remote decontamination and decommissioning of nuclear reactors. On evaluations of the experts, the request of disassembling of nuclear reactors will increase sharply in the beginning of the next century, when the reactors created in 60-70 years will serve the term [3]. COIL can find applications in such areas, as cutting thick-walled steel in shipbuilding, the welding of aluminum constructions, welding and cutting under water. The good delivery of COIL radiation by optical fiber allows to roboticize the technology laser equipment on it base. For reduction of life-cycle cost of COIL energy the essential

REPORT DOCUMENTATION PAGE

Form Approved OMB No. 0704-0188

1. AGENCY USE ONLY (Leave blank)	2. REPORT DATE	3. REPORT TYPE AND DATES COVERED
	2000	Final Report

4. TITLE AND SUBTITLE

The Study Of Supersonic COIL With Generation Of Iodine Atoms From CH3I In DC And RF Discharges And New Methods Of Active Medium Preparation

5. FUNDING NUMBERS

F61775-99-WE

6. AUTHOR(S)

Dr. Valeri Nikolaev

7. PERFORMING ORGANIZATION NAME(S) AND ADDRESS(ES)

P. N. Lebedev Physical Institute, Samara branch
Novo-Sadovaya St., 221
Samara 443011
Russia

8. PERFORMING ORGANIZATION REPORT NUMBER

N/A

9. SPONSORING/MONITORING AGENCY NAME(S) AND ADDRESS(ES)

EOARD
PSC 802 BOX 14
FPO 09499-0200

10. SPONSORING/MONITORING AGENCY REPORT NUMBER

SPC 99-4032

11. SUPPLEMENTARY NOTES

12a. DISTRIBUTION/AVAILABILITY STATEMENT

Approved for public release; distribution is unlimited.

12b. DISTRIBUTION CODE

A

13. ABSTRACT (Maximum 200 words)

This report results from a contract tasking P. N. Lebedev Physical Institute, Samara branch as follows: The contractor will optimize the chemical oxygen-iodine laser (COIL) operation with advanced Verti-JSOG and dilution of oxygen by nitrogen buffer gas, and will study COIL operation with generation of iodine atoms from RI iodides by electrical discharge in RI-O2-buffer gas mixture.

14. SUBJECT TERMS

EOARD, Chemical lasers, COIL, High average power gas lasers

15. NUMBER OF PAGES

45

16. PRICE CODE

N/A

17. SECURITY CLASSIFICATION OF REPORT	18. SECURITY CLASSIFICATION OF THIS PAGE	19, SECURITY CLASSIFICATION OF ABSTRACT	20. LIMITATION OF ABSTRACT
UNCLASSIFIED	UNCLASSIFIED	UNCLASSIFIED	UL

significance has the decrease of the requested pump capacity and the cost of all chemicals and buffer gases [4]. To decrease of the requested vacuum pump capacity it is necessary to increase partial pressure of oxygen in the cavity. The use of nitrogen for dilution of COIL active medium is preferable because this gas is much cheaper than helium and can be stored in the liquid state. It was shown earlier, that the use of nitrogen in supersonic COIL makes possible to reach chemical efficiency comparable with it value at using helium as diluent [5]. The preliminary cooling of nitrogen up to 80°K increases chemical efficiency of laser on several percents. It's possible to supply laser directly from vessels with liquid nitrogen in this case that considerably will reduce weight-dimensional performances of a mobile laser set-up. The necessity of significant gasdynamic cooling of an active medium is not at using cold primary nitrogen because of the total pressure losses are less essentially for smaller Mach numbers. The request of a large gas velocity in the cavity is connected with the stretching of the gain zone. It is necessary for using of the effective optical resonators. The gas velocity at Mach number M=2 exceed sonic velocity only in 1.63 times at the same stagnation temperature, because it is enough to achieve the Mach number of the active gas in the cavity close to M=1. Up to the present possibility of reaching of high COIL chemical efficiency for nitrogen as diluent of active medium and high oxygen pressure in the cavity remained open. Recently in the work [3] the chemical efficiency η=15% has been obtained at chlorine flow rate 70mmole/s in COIL with 5 cm gain length. The main feature of the laser operation at nitrogen dilution of the active medium consists in the diminution of the duct conductivity «SOG - nozzle» and in the growth of all pressure in the duct and $O_2(^1\Delta)$ transportation time than at using helium as diluent. It is accompanied by $O_2(^1\Delta)$ quenching and losses and growth of the static pressure in the iodine mixing region. Therefore requests to the designs of the COIL duct and mixing units increase sharply. There is the necessity of the increase of the supersonic nozzle throat at using nitrogen. At the same time the increase of the nozzle throat is limited by the existing vacuum pump capacity. In the given work we have tried to take into account all these factors connected with COIL operation at high chlorine flow rate and nitrogen dilution of the active medium. JSOG allows to reach very good chlorine utilization and to obtain oxygen at pressures in tens torr with the high $O_2(^1\Delta)$ content [6]. The generator with output of oxygen stream vertically through a central orifice in the injector of the basic hydrogen peroxide (BHP) is the most advanced JSOG design from the viewpoint of it's scaling [7]. The investigated COIL with advanced JSOG design and gain length of 5 cm has practically the same widths of the stream in the reaction zone (34 mm) and in the cavity (30 mm). The configuration of gas stream in the given laser can be considered as one element of the stream in the high powerful COIL with grid nozzle.

1.2. EXPERIMENTAL COIL SET-UP AND MEASUREMENTS

The present COIL consists of the advanced JSOG (1), the chamber for mixing of primary nitrogen with oxygen (6) and the slit nozzle (Fig.1).

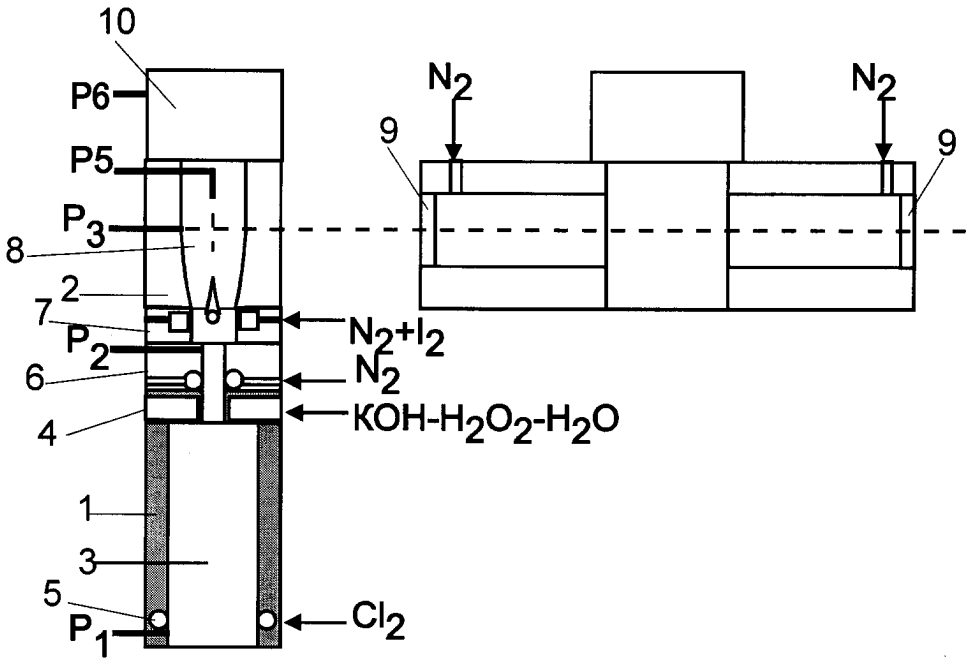

FIG.1 (just insert file fig.1-1)

Fig. 1. The scheme of COIL set-up

The JSOG consists of the counter-flow reactor (3), the nozzle bank for injection of BHP jets (4), the inlet for gaseous chlorine (5). The cross-section of the reactor is equal to 34×50mm^2. The design of JSOG was described in detail in final technical report according to contract SPC-98-4044. The new nozzle bank for injection of BHP jets was designed. It was

manufactured from plastic. The total number of nozzles drilled in nozzle bank was 296 and diameter of nozzles 0.7 mm. The thickness of nozzle bank plate is equal to 3 mm. The distance between the chlorine inlets and the oxygen outlet was equal to 165mm. The gas flow system consists of mixing chamber (6) of 60 mm in long where oxygen is mixed with primary nitrogen, iodine mixer (7), two supersonic nozzles (2), laser cavity (8) and vacuum duct (10). For preliminary cooling of O_2+N_2 mixture primary nitrogen was passed through a copper spiral placed into liquid nitrogen. Two slit nozzles were tested. The first iodine mixer + nozzle unit was identical to that described in [5] and had the single throat 10 mm in height and 50 mm along optical axis. The height of flow near optical axis was 20 mm. The second iodine mixer + nozzle has two throats of 7,5 mm height due to placing in it's center of the perforated 5 mm tube with the blade. The sketch of two throats nozzle is shown in Fig.1. The walls of the slit duct diverged at the angles of 2,5°. The optical resonator consists of the mirrors (9) of 45mm diameter and 5m curvature. The mirror spacing was 65 cm, as nitrogen-purged tunnels separated the mirrors from gain region. The heights of the stream in the center of the cavity were equal to 28 mm and 30 mm for distance of 55mm and 80 mm between nozzle throat and optical axes correspondingly. The mechanical pump maintains the exhaust of the active medium with 125 liter/s capacity. The vacuum tank with volume of 4 m^3 is connected quickly in parallel to the pump for creation of the high short time exhaust capacity. The nitrogen tests showed that maximum exhaust capacity was of 630 liter/s at the first second and was decreased up to 520 liter/s in 5sec.

During the laser operation the pressure in the reactor P_1, in the mixing chamber (plenum pressure) P_2, static pressure in the cavity P_3, in the iodine measuring cell P_4, total pressure in Pitot tube P_5 and pressure in the vacuum duct P_6 were measured. The ratio P_5/P_3 was used for estimation of Mach number M of gas flow in laser cavity.

The given COIL design creates the favorable conditions for improving of JSOG productivity and gives a good possibility for the scaling. It was found carrying out of BHP film from the reactor's walls in traditional version of the JSOG was the main reason that cause BHP aerosol in the gas flow [ ]. The emergence of BHP drops in the advanced Verti-JSOG is possible only due to the generation and carry-out its by gas flow from volume.

The gaseous chlorine is delivered to JSOG from the elastic plastic envelope at atmospheric pressure, where it is delivered in its turn from small balloon with liquid chlorine. The total output power W was counted equal to $W = W_1 (T_1+T_2)/T_1$, where T_1 is the transmission of the output mirror, T_2 is transmission of the second mirror.

1.3. THE COIL OPERATION WITH ONE THROAT NOZZLE

The chlorine molar flow rate in these experiments was G_c = 39.2 mmole/s. The preliminary test of JSOG showed that at pressure P_1 = 35 torr in JSOG the $O_2(^1\Delta)$ yield was more than 60% and chlorine utilization more than 90%. The ratio close to G_c:G_{NP}:G_{NS}=1:1:1 was used in COIL operation to achieve optimal pressure in JSOG P_1=35 torr. The distance between nozzle throat and optical axis was 55 mm. The maximum power 765W and chemical efficiency 21.5% were achieved for iodine molar flow rate 0.44 mmole/s and mirror transmission T_1=1% and T_2=0%. The Mach number of gas flow n cavity was estimated as 1.54. The using molar gas flow ratio G_c:G_{NP}:G_{NS}=1:2:1 resulted in off designed value of pressure in JSOG. Therefore the double throat nozzle was used to test COIL at higher primary nitrogen dilution.

1.4. THE COIL OPERATION WITH TWO THROAT NOZZLE

1.4.1 The COIL operation with 39.2 mmole/s of chlorine molar flow rate.

First of all in experiments the ratio G_c:G_{NP}:G_{NS}=1:2:1 was used. At cold laser tests with using nitrogen instead of all gases and for the flow rate of nitrogen 39,2 mmole/s through JSOG the Mach numbers were equal to 1.72 and 1.8, accordingly for distances between optical axes and the nozzle throat of 55 mm and 80 mm. Mach numbers for ideal iso-entropic expansion stream should be equal to 2,18 and 2,25, accordingly. The difference of these Mach numbers and obtained ones in the experiments is explained by the imperfect nozzle profile, existence of the boundary layers and the heat release.

Firstly the distance between throat and optical axis 55 mm was installed.

The total matrix of experiments for 39,2 mmole/s of chlorine and 55 mm distance between optical axis and nozzle throat is presented in Table 1.

In hot experiments for G_c:G_{NP}:G_{NS} = 1:2:1 and nitrogen flow rate through each mirror tunnel of 1.36 mmole/s the pressures in the reactor P_1 and in the mixing chamber P_2 were equal to 35 torr and 22.5 torr and didn't depended on molecular iodine molar flow rate G_{I2}. The estimation of the absolute gas velocity in the mixing chamber gave a value of 178 m/s. The pressure in the vacuum duct P_6 exceeded static pressure in the cavity P_3 on (1÷3) torr during the COIL run. The weak dependence plenum pressure on G_{I2} specifies by the absence of significant heat release in the duct between JSOG and nozzle where Mach number M<1. On the other hand it was found that pressures in cavity P_3 and Pitot tube P_5 increased with increasing of G_{I2}. It is due to the increase of the heat release in the supersonic part of the nozzle with increasing of G_{I2}. The dependence of output power on G_{I2} is presented in Fig.2. The additional conditions of COIL tests are indicated in the Table 2. The maximum output power 858 W (η=24,1 %) was achieved for primary nitrogen at 80°C and 798 W (η= 22,4 %) for nitrogen at room temperature.

The ratio G_c:G_{NP} = 1:1 was used to decrease the generator pressure P_1 and to increase the gas velocity in the reactor. In this case generator pressure P_1 decreased from 35 torr to 28 torr, however the supersonic stream in the cavity was unstable. At first the increase of iodine flow rate resulted in monotone growth of output power, but then the lasing failed sharply and the stream in cavity became subsonic with Mach number M = 0.66. The increase of ratio G_{NP}:G_c more, than 2:1 resulted in the growth of the reactor pressure and falling of the $O_2(^1\Delta)$ yield and of output power.

Table 1. The results of COIL testing at 39.2 mmole/s of Cl_2 molar flow rate and optical axis-throat distance 50 mm.

.Pos.	G_{NS}	GNP	G_c	P_1	P_2	P_3	P4	P5	P6	PI2	G_{I2}	T_1. %	T_2.	W 1	W	η%	M
Nitrogen flow rate for mirror purging is1.36 ммоль/с for each mirror. In first run nitrogen flows through JSOG instead chlorine																	
Variation od iodine molar flow rate																	
1	38.5	78	39.2	23.8	18.4	3.5	124	15.1	4.5	0	0	0.9	0	0	0	0	1.72
2	38.5	78	39.2	35.9	22.6	4.1	133	15.9	5.5	1.38	0.41	0.9	0	134	134	3.8	1.62
3	38.5	78	39.2	35.7	22.6	4.4	135	15.3	5.3	1.59	0.46	0.9	0	326	326	9.2	1.52
4	38.5	78	39.2	36	22.8	5	136	15.3	6	1.76	0.51	0.9	0	454	454	12.8	1.4
5	38.5	78	39.2	35	22.3	5.06	137	15.9	5.1	2,06	0.59	0.9	0	558	558	15.7	1.43
6	38.5	78	39.2	35.2	22.7	5.24	138	16.4	4.9	2.23	0.63	0.9	0	566	566	16	1.42
7	38.5	78	39.2	37	23.3	5.27	139	16.5	4.9	2.4	0.68	0.9	0	536	536	15.1	1.42
In next run nitrogen precooled																	
8	38.5	78	39.2	35.3	22	5.32	138	15.1	5.1	2.2	0.62	0.9	0	606	606	17.1	1.34
Variation of secondary nitrogen at constant iodine flow rate																	
9	46	78.4	39.2	34.7	22.9	4.58	147	16	5.6	2.06	0.64	0.9	0	571	571	16.1	1.52
10	39.2	78.4	39.2	33.6	21.2	4.54	129	15.2	4.9	2.05	0.62	0.9	0	574	574	16.2	1.48
11	31	78.4	39.2	33.6	20	4.46	108	13.9	4.77	2.01	0.57	0.9	0	556	556	15.6	1.42
12	26.8	78.4	39.2	33	18.8	4.1	87	12	4.6	2.03	0.62	0.9	0	522	522	14.7	1.36
13	53.4	78.4	39.2	35.2	24.3	4.8	173	17	5.2	2.02	0.62	0.9	0	567	567	16	1.53
Variation of iodine at constant secondary nitrogen flow rate																	
14	43	78.4	39.2	33.5	22.1	4.7	139.	15.3	5	2.04	0.63	1.3	0	621	621	17.5	1.46
15	43	78.4	39.2	33.5	21.6	5.1	140	14.8	4.8	2.22	0.68	1.3	0	619	619	17.4	1.36
16	43	78.4	44	33.6	23	4.77	137	15.7	5	2.3	0.72	1.3	0	583	583	16.4	1.47
New mirror set were installed																	
17	43	78.4	39.2	34.1	22	4.5	138	15.7	5.6	2.1	0.65	1	0	798	798	22.4	1.52
In next two run precooled primary nitrogen was used																	
18	43	78.4	39.2	34.4	22	5	138	14.3	5	2.08	0.65	1	0	850	850	23.9	1.34
19	43	78.4	39.2	33.7	21.5	4.9	137	14.6	5.64	1.88	0.59	1	0	858	858	24.1	1.38
Decreased primary nitrogen flow rate																	
20	28	39	39.2	28.3	15.6	3.55	85	8.5	3.78	1.58	0.55	1.3	0	325	325	9.15	1.2
21	35	39	39.2	28.3	16.3	3.82	107	10.6	4	1.54	0.54	1.3	0	306	306	8.6	1.32
22	35	39	39.2	28.8	16.9	8.06	108	1.4	3.73	1.95	0.68	1.3	0	0	0	0	0.92
In previous run the subsonic gas flow in cavity was obtained/ Then again increase primary nitrogen flow rate																	
23	40	78	39.2	33	22	4.4	139	14.7	5.3	2	0.7	1.3	0	342	342	9.6	1.48
It was found that in previous run mirrors were polluted and for next run they were ckeaned																	
24	40	78	39.2	32.5	21.7	4.4	140	15.2	5.56	2.1	0.73	1.3	0	642	642	18.	1.51
In next run again decreased primary nitgogen flow rate and again the subsonic operation was obtained																	
25	40	39	39.2	29.3	18.7	8.61	140	11.5	4.3	2	0.7	1.3	0	0	0	0	0.66
New mirror set																	
26	39.	79.	39.3	31.1	21.2	4.77	135	14	5.3	2.04	0.59	0.7	0.7	382	764	21.4	1.37

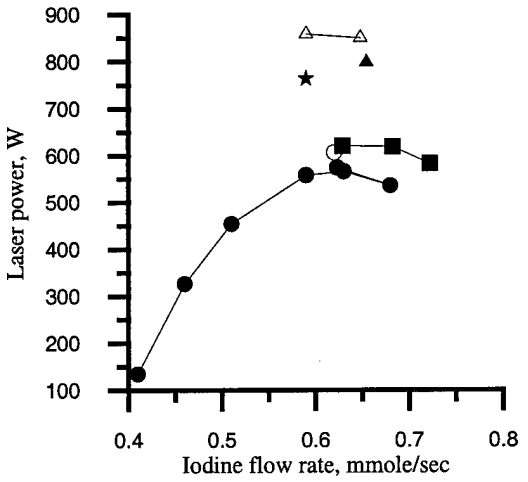

Fig. 2. Dependence of output power on iodine flow rate and mirrors set for Gc:G_{N2P}:G_{N2S} = 1:2:1.

Table 2

Symbol	T(N2P)	T_1,%	T_2,%
●	Room	0.9	0
○	Cold	0.9	0
■	Room	1.3	0
▲	Room	1	0
Δ	Cold	1	0
□	Room	0.7	0.7

Optical axis-throat distance of 80 mm. The matrix of COIL runs is presented in Table 3. The behavior of the gas flow in the cavity with growth of iodine flow rate became qualitatively another for the position of the optical axes of 80 mm from iodine mixer. The output power equal to 467 W at iodine flow rate of 0.47 mmole/s, mirrors with T_1 = 0.9 %, $T_2 \approx 0$ % and ratio G_c:G_{NP}:G_{NS} = 1:2:1 was above, than power at the optical axes position of 55 mm. The Mach number of a stream in a resonator was equal to 1.43 in this case. However, the increase iodine flow rate G_{I2} up to 0.54 mmole/s led already to the change of the supersonic stream mode in the cavity on a subsonic one and to fatal failure of the lasing. In some tests it was possible to observe the temporal change of the supersonic regime for active medium stream in the cavity on subsonic mode (Fig.3). The duct was evacuated only by the vacuum pump up to the time point t1. when the valve of vacuum tank was opened. During interval of time from t2 up to t3 the supersonic regime with M= 1.4 is realized and the lasing took place. Then the pressure in cavity increased sharply, the flow in the cavity became subsonic (M= 0.64) and lasing failed. On the contrary at similar conditions in the other test the subsonic flow in the cavity without lasing was realized in the first time after opening vacuum tank and then the flow transited to a supersonic mode with appearing of the lasing.

Such behavior of the stream in the cavity specifies by instability connected with appearing of the thermal crisis and formation of a straight shock wave in the nozzle. Thus the increase of supersonic part of the nozzle on 25 mm in these conditions results in additional heat release and heating of the active medium sufficient for the change of stream mode on subsonic one. The consequent COIL tests were conducted at the optical axes position placed on 55 mm downstream the nozzle throat.

Table 3. Results of COIL operation at 39.2 mmole/s of chlorine and optical axis-throat distance 80 mm.

Pos.	G_{NS}	GNP	G_c	P1	P2	P3	P4	P5	P6	PI2	G_{I2}	T1	T2	W_1	W_t	η,%	M	T1+ T2
Dry COIL run with nitrogen instead of chlorine																		
1	39.2	78.4	39.2	33.6	21.1	3.1	118	14.6	4.8	0	0	0.9	0	0	0	0	1.8	0.9
Variation of secondary nitrogen at constant iodine flow rate.																		
2	30	78.4	39.2	32.6	19.5	4.56	101	13.4	4.8	1.56	0.46	0.9	0	483	483	13.6	1.37	0.9
3	26	78.4	39.2	31.7	17.5	9.59 4.4	82	12.6 11.6	5.39	1.55	0.49	0.9	0	453	453	12.7	0.64 1.27	0.9
In last run at first seconds after switch on vacuum receiver the subsonic operation, then the supersonic operation																		
4	39.2	78.4	39.2	33.5	20.4	4.76	127.	15	5.6	1.53	0.47	0.9	0	467	467	13.1	1.43	0.9
5	46.6	78.4	39.2	35.3	22.9	4.57	151	15.8	5.24	1.54	0.47	0.9	0	441	441	12.4	1.51	0.9
Variation of iodine molar flow rate at maximum secondary nitrogen flow rate.																		
6	46.6 46,6	78.4 78,4	39.2 39,2	34 34	22 22	11.8 5,4	151 151	15.6 16,6	5.22	1.76	0.54	0.9	0	0 370	0 370	0 10,3	0.64 1,4	0.9
In last run the transition from supersonic to subsonic operation was observed (Fig.3)																		
7	46.6	78.4	39.2	36	23.4	4.85	152	17.8	5.6	1.8	0.55	0.9	0	435	435	12.2	1.57	0.9
8	39.2	78.4	39.2	33.4	21.6	8.6	127	14.9	5.4	1.75	0.54	0.9	0	0	0	0	0.92	0.9
9	46	78.4	39.2	34.3	22.8	10.8	148	14.7	5	2.1	0.65	0.9	0	0	0	0	0,68	0.9
10	46	78.4	39.2	34.6	23.1	11.6	147	15.1	5.1	2.07	0.65	0.9	0	0	0	0	0,63	0.9

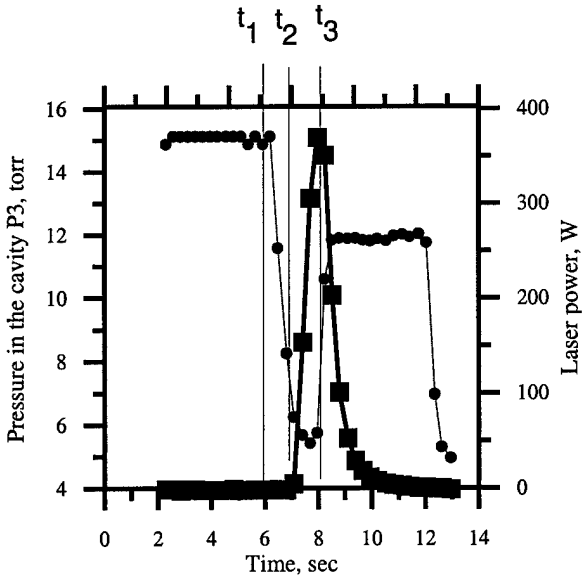

Fig.3. The time variation of the pressure in the laser cavity and the laser power during one COIL run in conditions close to the thermal crisis. ● - pressure in the cavity, P_3 , ■ - laser power

1. 4.2. COIL operation with 68 mmole/s of chlorine molar flow rate.

For chlorine flow rate 68 mmole/s the laser tests were made for gas molar flow rates ratio G_c:G_{NP}:G_{NS} = 1:2:1. The pressures P_1 and P_2 were equal to 54 torr and 36 torr, accordingly. It has been found that the increase of the nitrogen flow for purging of mirrors from 4.5 mmole/s up to 10.3mmole/s has resulted in the raise of the laser power from 890 W to 1035 W (T_1 = 0.94 %, T_2 = 0.9%) for fixed iodine flow rate of 0.71mmole/s. The pressure P_3 has increased from 7.6 torr to 9.7 torr, and the Mach number of the flow dropped from M = 1.49 to M = 1.39. The growth of P_3 and falling of the Mach number of the stream in the cavity with increasing of the nitrogen flow rate through cavity tunnels were probably connected with compression of the stream (appearing angle shocks in the cross section of the cavity inlet). The dependence of output power on total transmission of mirrors is presented in Fig. 4. An approximate estimation of the threshold mirrors' transmission is equal to 6 %.

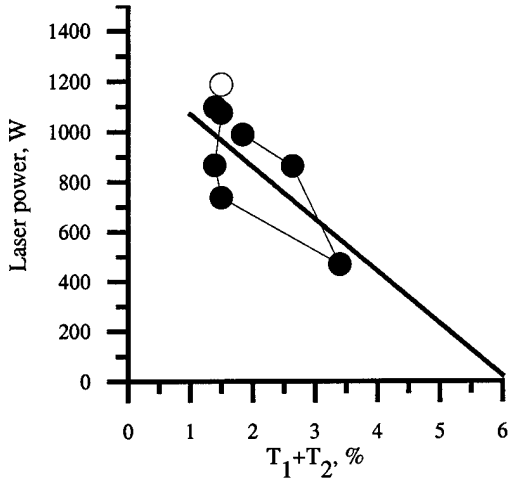

Fig. 4. Dependence of output power on the total mirrors' transmissivity for G_c = 68 mmole/s and G_{I2} =0.71 mmole/s. ● - primary nitrogen at room temperature, ○ - cold primary nitrogen.

The total matrix of COIL runs with 68 mmole/s of chlorine is presented in Table 4.

Table 4. Matrix of COIL test with 68 mmole/s of chlorine.

Pos.	G_{NS}	GNP	G_c	P1	P2	P3	P4	P5	P6	PI2	G_{I2}	T1	T2	W1	W	%	M
Variation of nitrogen flow rate for each mirror purging: first run 4.5 mmole/s, second 6.8 mmole/s, third 10.3 mmole/s.																	
1	66	132	68	58.4	37.5	7.55	226	25.5	9	2.51	0.73	0.94	0.9	459	898.	14.5	1.49
2	66	132	68	60	39	7.88	226	25.7	8.36	2.35	0.69	0.94	0.9	455	890.	14.4	1.46
3	66	132	68	53.6	36	9.85	225	28.6	11.7	2.48	0.73	0.94	0.9	508	994.	16.1	1.36
In last run the vacuum receiver was not good pumped. Repeat last run with lower initial pressure in vacuum receiver.																	
4	66	132	68	53.3	36	8.7	226	29.2	8.5	2.53	0.74	0.94	0.9	529	1035	16.8	1.48
6Install nitrogen flow rate for each mirror purging 5.7 mmole/s and change secondary nitrogen flow rate.																	
5	55	132	68	53.2	34	8	191	26.7	8.26	2.49	0.72	0.94	0.9	501	980.	15.9	1.48
6	82	132	68	54	38	8.3	241	29.3	8.46	2.5	0.76	0.94	0.9	474	927	15.1	1.53
Now change iodine flow rate at 5.7 mmole/s of nitrogen flow rate for purging of each mirror. The decrease of Mach number is observed with increase of iodine flow rate																	
7	66	132	68	54.7	37	7.22	217	28.3	8.43	2.08	0.63	0.94	0.9	452	884.	14.4	1.63
8	66	132	68	52.6	36	7.86	218	28.4	8.7	2.35	0.71	0.94	0.9	505	988.	16.0	1.55
9	66	132	68	53	36	8.06	219	26.8	8.4	2.50	0.76	0.94	0.9	457	894.	14.5	1.48
10	66	132	68	54	36.5	8.3	221	27.6	8.4	2.82	0.84	0.94	0.9	432	845	13.7	1.48
Now chage mirror transmition																	
11	66	132	68	52.4	35	7.55	219	27.2	8.31	2.28	0.69	1.7	0.94	555	861.	14	1.55
12	66	132	68	54	35	7.52	219.	26.9	8.47	2.35	0.71	1.7	1.7	234	468	7.59	1.54
13	66	132	68	56.8	36.5	7.4	219.	24.2	8.25	2.38	0.72	1.3	0.2	639	737.	11.9	1.46
14	66	132	68	54	35	7.5	219.	27.2	8.3	2.38	0.71	1.3	0.09	810	866.	14.1	1.55
15	66	132	68	55	37	7.5	220.	25.9	8.3	2.39	0.71	0.8	0.7	573	1074	17.4	1.51
In next three runs pre cooled primary nitrogen.																	
16	66	132	68	55	37.5	7	223.	22.1	8.9	2.41	0.71	0.8	0.7	631	1183	19.2	1.43
17	66	132	68	53	37	7	220	22.5	9.5	2.07	0.62	0.8	0.7	633	1186	19.3	1.45
18	66	132	68	54	37.3	7.4	223	22.2	9.3	2.57	0.76	0.8	0.7	595	1115	18.1	1.38
In next two runs the fresh mirrors were used																	
	65.7	135.	66	55.6	37.2	7.3	224	25.6	8.78	2.41	0.71	0.7	0.7	532	1064	17.8	1.52
	65.7	135.	66	57.4	38.6	7.3	225	25.7	9.48	2.9	0.85	0.7	0.7	487	974	16.3	1.53

1.4.3. COIL operation with 75mmole/s of chlorine molar flow rate.

The total matrix of experiments is presented in Table 5. In several runs the chlorine molar flow rate was 77 mmole/s because of increasing of atmospheric pressure.

The increasing of chlorine molar flow rate up to 75 mmole/s resulted in increasing of pressures P_1 and P_2 to 67 torr and 42 torr, accordingly for the ratio of the flow rates G_c:G_{NP}:G_{NS} = 1:2:1. If the iodine flow rate exceeded 0.8 mmole/s for nitrogen flow rate through each mirror's tunnel of 2,7 mmole/s the lasing has ceased although the active medium flow in the cavity was supersonic with the Mach number M = 1.5. The raise of the nitrogen flow rate through each mirror's tunnel up to 6,8 mmole/s has allowed to reach the stable COIL operation at iodine flow rate down to 0.9 mmole/s. Consequently, the resonance absorption of the stagnant zones in the mirror's tunnels has decreased with growth of the purging nitrogen flow rate. The maximum power of 1030 W was reached at iodine flow rate of 0.89 mmole/s, for given ratio of gas flow rates and at using of mirrors with T_1=0.94%, T_2=0.9%. The pressure in the cavity and the total pressure in the Pitot tube were equal to P_3=8,6 torr and P_5=29 torr. The falling of COIL chemical efficiency with increasing of chlorine flow rate from 68 mmole/s up to 75 mmole/s was due to high pressure in the reactor and smaller O_2 ($^1\Delta$) yield. The decreasing of G_{NP} from 155 mmole/s to 79 mmole/s has resulted in decreasing of P_1 to 53 torr. However the flow mode in the cavity was subsonic (with static pressure of 14,4 torr and the Mach number M = 0.78) and the lasing was absent at iodine flow rate of 0.7mmole/s. The additional diminution of G_{NS} to 44mmole/s has not allowed to convert the subsonic flow of the active medium to a supersonic mode. The primary and secondary nitrogen flow rates were increased up to 96 mmole/s and to 82 mmole/s, accordingly, for returning of the flow in the cavity to a supersonic mode. In this case P_1 was equal to 55torr only and the Mach number had reached value M=1.5. The static pressure in the cavity was P_3=7.1 torr. The fresh mirrors (T_1=0.8% and T_2=0.7%) were installed simultaneously and that has allowed to obtain the total output power of 1408 W with chemical efficiency η=20.7%. The growth of chemical efficiency with the diminution dilution of the active medium by nitrogen was observed in [3] also.

Table 4. Matrix of COIL test with 75 mmole/s of chlorine.

Pos.	G_{NS}	G_{NP}	G_c	P1	P2	P3	P4	P5	P6	PI2	G_{I2}	T1	T2	W1	W	%	M	T1+ T2
Variation of secondary nitrogen and iodine flow rates. Nitrogen flow rate for mirror purging 2.7 mmole/s																		
1	40	155	77	66	36.3	6.93	140	22.8	8.4	2.15	0.75	1.3	0	819	819	11,7	1.47	1.3
2	70	155	77	66.4	40.8	7.8	225	27.6	9.6	1.98	0.69	1.3	0	881	881	12,6	1.53	1.3
3	85.2	155	77	68.4	43.6	7.9	>241	28.9	9.7	2.1	0.73	1.3	0	871	871	12,5	1.56	1.3
4	85	155	77	67	43.2	7.8	>241	28.6	10.3	2.14	0.75	1.3	0	0	0	0	1.56	1.3
5	85	155	77	68.5	43.7	8	139	29.8	10	2.05	0.71	1.3	0	827	827	11,8	1.58	1.3
6	40	155	77	60	35.7	6.83	>241	22.6	9.74	2.56	0.89	1.3	0	740	740	10,6	1.47	1.3
7	85	155	77	67.2	43	8.1	>241	27.5	10.1	2.49	0.87	1.3	0	0	0	0	1.5	1.3
The increasing of iodine flow rate resulted in no lasing. In next runs the nitrogen flow rate for mirror purging was increased up to 6.8 mmole/s. Variation of iodine flow rate																		
8	85	155	77	69.3	44	8.45	>241	28.2	9.85	2.38	0.83	1.3	0	740	740	10,6	1.48	1.3
9	85	155	77	67	43	8.37	>241	30.1	9.63	2.06	0.72	1.3	0	626	626	9	1.55	1.3
10	70	155	77	70	42.3	7.43	231	26.9	9.3	1.93	0.67	1.3	0.9	473	800.	11,5	1.55	2.2
11	70	155	77	68.4	40.3	7.6	231	25.6	10.1	2.24	0.78	1.3	0.9	497	841.	12,1	1.49	2.2
12	70	155	77	71.8	43.5	8.1	231	26.1	9.6	2.53	0.8	1.3	0.9	400	676	9,7	1.45	2.2
13	70	155	77	68.8	43.5	8.44	231	28	9.3	2.13	0.74	0.94	0.9	444	869.	12,5	1.47	1.84
14	70	155	77	66.7	42.2	8.64	234	28.9	10.5	2.56	0.89	0.94	0.9	527	1031	14,8	1.48	1.84
15	70	155	77	68.8	42.6	8.35	231	27.6	10.5	2.14	0.75	0.94	0.9	516	1010	14,5	1.47	1.84
16	70	155	77	65.4	39.1	7.6	232	25.3	9.5	2.12	0.74	0.94	0.9	518	1013	14,5	1.48	1.84
17	80	160	77	73	50	8.2	241	31.2	10.2	2.39	0.72	0.94	0.9	427.	836.	12	1.6	1,84
18	65.7	135	75	61.6	40.3	7.66	222	25.6	8.74	2.41	0.71	0.7	0.7	533	1066	15.7	1.48	1.4
19	65.7	135	75	62.7	40.8	7.77	222	26	8.67	2.63	0.78	0.7	0.7	511	1022	15.	1.48	1.4
20	65.7	135	75	60.1	39.4	7.97	220	27.1	9.5	2.354	0.7	0.7	0.7	537	1074	15.8	1.5	1.4
21	65.7	79	75	53	34.5	15.1	220	22.6	6.95	2.33	0.7	0.7	0.7	0	0	0	0,78	1.4
Nitrogen flow rate for mirror purging 2.8 mmole/s																		
22	43.8	79	75	50.4	39.4	14.6	146	19.3	6.1	2.05	0.61	0.7	0.7	0	0	0	0,64	1.4
23	43.8	96	75	52	31	14.4	146	19	7.1	2.07	0.62	0.7	0.7	0	0	0	0,64	1.4
Nitrogen flow rate for mirror purging 4.2 mmole/s																		
24	65.7	96	75	56	36.6	256.8	213	20.7	8.2	2.06	0.64	0.8	0.7	695	1303	19.2	1.4	1.5
25	65.7	96	75	55	36	1264.2	213	19.4	7.8	2.28	0.7	0.8	0.7	0	0	0	0,68	1.5
Gc:GNp=1:1. And increase secondary nitrogen flow rate																		
26	82.1	96	75	57	39.6	7.1	241	24.2	7.78	2.3	0.69	0.8	0.7	751	1408	20.7	1.5	1.5
27	82.1	79	75	55	37.8	6.4	241	24	7.61	1.8	0.56	0.8	0.7	602	1129	16.6	1.59	1.5
28	82.1	79	75	56	38.4	8.1	241	22.1	8.47	2.28	0.7	0.8	0.7	636	1192	17.5	1.3	1.5
29	82.	79	75	56	38	6.74	241	21.7	7.28	2.07	0.62	0.8	0.7	718.5	1347	19.8	1.45	1.5
30	71.9	84	75	52.4	34.7	6.46	232	20.3	7.1	2.25	0.7	0.8	0.7	524	982	14.4	1.42	1.5

1.5. CONCLUSION

The presented results of COIL tests showed that laser output power and flow mode of the active medium in the cavity depend essentially on the primary, secondary and purging nitrogen flow rates. It's stipulated in many respects by the limited pump capacity. So static pressure P_3 in the cavity as a rule was always less than pressure P_6 in vacuum duct on (1÷3) torr in the present tests. The inlet and outlet of the cavity for a gas stream were made identical to prevent the penetration of the increased pressure from the vacuum duct. The increase of nitrogen flow rates through the mirrors' tunnels is limited by formation of angle shocks and compression of a supersonic stream. Obviously, on the other hand, that the size of stagnant zones in the mirrors' tunnels (where gas circulates, relaxes and may have the resonance absorption) should decrease with growth of the purging nitrogen flow rates.

The raise of heat release in the active medium or reduction of the gas thermal capacity lead to the thermal crisis and to the break - down of the stream to subsonic mode. It was observed when the distance between the nozzle's throat and optical axes has been made longer from 55 mm to 80mm and when the flow rates G_{NP} or G_{NS} have been decreased. The break-down of the flow to subsonic mode with higher pressure results in the failure of the lasing. The obvious explanation of this failure of lasing consists in the sharp increase of temperature, threshold $O_2(^1\Delta)$ yield, all concentrations (water vapor, atomic and molecular iodine, oxygen) and in the intensification of $O_2(^1\Delta)$ quenching and heat release. In addition singlet oxygen fraction in the mirrors' tunnels may decrease to a level which is lower than threshold value (parameter $P\tau$ increases sharply in subsonic mode) and may lead to resonance absorption in these tunnels. Unfortunately in the frame of the given work we can not explain uniquely the failure of lasing at realization of a subsonic flow in the cavity.

The final COIL test sheet is presented in Fig.5 and Table 6. The experimental results of additional COIL tests at chlorine flow rate Gc = 23,2mmole/s and $Gc:G_{NP}:G_{NS}$ = 1:2:1 are represented here also. The efficiency of the laser depends essentially on used mirrors set, that was marked earlier in other works also [8].

The most important specific parameters of COIL have been reached in the given work: specific power per unit of the stream area in the cavity of 100W/cm^2, specific power per unit of the reactor volume of 5 kW/liter and specific power per unit of the pump capacity (without using diffuser) of 2,7W/(liter/s)=2.7J/liter. The maximum specific power per unit of the stream area in the cavity, known to the present time of 400 W/cm^2 and specific power per volume of the reactor of 4,3 kW/liter are reached in the work [7]. Such performances were possible to reach as a result of the increase of a linear gas velocity in the reactor and in the cavity at large dilution of oxygen by helium. In the given work the raise of specific power per unit of the reactor volume up to 5 kW/liter is reached by increasing of JSOG pressure.

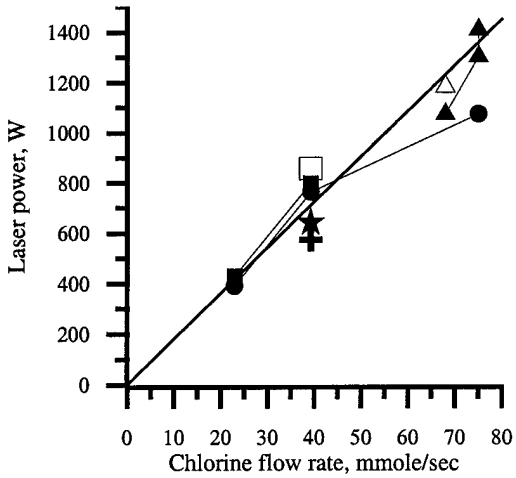

Fig.5..Dependence of laser power on chlorine flow rate. The direct line corresponds to chemical efficiency of 20%.

Table 6

G_c	G_{NS}	G_{NP}	T_1, T_2,%	W	η, %	M
23	23,2	46.5	0.7; 0.7	390 (●)	18.7	1.24
23	23,2	46.5	1; 0	429 (■)	20.6	1.24
39.2	39,2	78.4	0.9; 0	574 (✙)	16.2	1.48
39.2	43	78,4	1; 0	798 (■)	22.4	1.52
39.2	40	78,4	1.3; 0	642 (★)	18.1	1.51
39.2	39,2	78.4	0.7; 0.7	764 (●)	21.4	1.37
39.2	43	78.4*	1; 0	858 ( )	24.1	1.38
68	66	66	0.8; 0.7	1074 (▲)	17.4	1.51
68	66	66*	0.8; 0.7	1183 (Δ)	19.2	1.43
75	65.7	135.5	0.7; 0.7	1074 (●)	15.8	1.5
75	65.7	95.8	0.8; 0.7	1303 (▲)	19.2	1.4
75	82.	95.8	0.8; 0.7	1408 (▲)	20.7	1.5

*- cold primary nitrogen

References

1. J. Vetrovic, «Prospects for an Industrial Chemical Oxygen- Iodine Laser», Proc. SPIE, **3092**, pp.780-, 1996

2. Endo M., Nagatomo S., Takeda S., Wani F., Nanri K., Fujioka T.,» Advanced technologies in chemical oxygen-iodine laser for industrial applications», Proc. SPIE, **3268**, pp. 106-, 1998.

3. D.L. Carroll, D.M. King, L. Fockler, D. Stromberg, W.C.Solomon, L.H. Sentman, «Performance of a High Power Chemical Oxygen-Iodine Laser Using Nitrogen Dilution», Proc. of Lasers'98, ed. V.S.Corcoran, STS Press, McLean, VA, 1999

4. Von Bulov H., Schall W.O., « Oxygen-Iodine Laser for Industrial Applications», Proc. SPIE, **2502**, pp. 258-,1994

5. M.V. Zagidullin, V.D. Nikolaev, M.I. Svistun, N.A. Khvatov, N.I. Ufimtsev, « Highly Efficient Supersonic Chemical Oxygen-Iodine Laser with a Chlorine Flow Rate of 10 mmole/s», Quantum Electronics, **27**, 195-, 1997.

6. V.N. Azyazov, M.V. Zagidullin, V.D. Nikolaev, M.I. Svistun, N.A. Khvatov, « Oxygen-Iodine Laser with a Drop-jet generator of $O_2(^1\Delta)$ Operating at Pressure up to 90 torr», Quantum Electronics, **25**, 418-, 1995

7. W.E. McDermott, J.C. Stephens, J. Vetrovec, R. Dickerson,» Operating Experience With a High Throughput Jet Generator», AIAA Paper 97-2385, 28th Plasmadynamics and Lasers Conference, June 23-25, 1997/ Atlanta, GA

8. T.L. Rittenhouse, S.P. Phipps, C.A. Helms, K.A. Truesdell,» High Efficiency Operation of a 5 cm Gain Length Supersonic Chemical Oxygen-Iodine Laser»,Proc. SPIE, **2702**, 333 , 1996

Part 2.

An efficient supersonic COIL with more than 200 torr of the total pressure in the active medium.

Abstract

The new nozzle concept was suggested and tested for chemical oxygen-iodine laser (COIL). The nozzle bank consists of the array of cylindrical nozzles for pure N_2 flow, slit nozzles for $O_2(^1\Delta)$ flow. The N_2+I_2 jets are injected into turbulent wakes between oxygen and N_2 streams through small cylindrical orifices. The LIF was used for the visualization of the iodine mixing efficiency in the mixing chamber. It was found practically uniform distribution of iodine molecules in the supersonic flow on the distance about 60 mm downstream nozzle bank. The COIL experiments were performed with this nozzle bank and at 5 cm gain length COIL cavity. The output power 700 W or chemical efficiency 19.7% have been achieved for the chlorine molar flow rate 39.2 mmole/s. Simultaneously the static pressure 10.9 torr in laser cavity and pressure 100 torr in Pitot tube have been achieved. The estimated Mach number of the flow was equaled to 2.6 and total pressure in the laser cavity was equaled to 218 torr. High dilution of the oxygen by nitrogen 1:11 results in small growth of the stagnation temperature of the gas flow and creates good conditions for the pressure recovery in the diffuser.

P_1- pressure in reactor
P_2- in the mixing chamber (plenum pressure),
P_3static pressure in the cavity,
P_4 -pressure in iodine measurement cell,
P_5 -total pressure in Pitot tube
P_6 -pressure in the vacuum duct downstream cavity
P_{I2}- iodine partial pressure in the measuring cell
G_c - chlorine molar flow rate,
G_{NP} -primary nitrogen molar flow rate,
G_{NS} -secondary nitrogen molar flow rate,
G_{I2}- iodine molar flow rate,
G_{NM}-the total nitrogen molar flow rate through mirrors tunnels (purging)
T_1 - the transmission of the output mirror,
T_2 - transmission of the second mirror.
W_1- laser power from output mirror
W- total laser power
η_c-chemical efficiency
M- Mach number of the flow from ratio $\frac{P_5}{P_3} = \frac{166.7M^7}{\left(7M^2-1\right)^{2.5}}$

2. 1. Introduction

The increase of the stagnation pressure of the gas flow in the cavity of gas-dynamic and chemical lasers is very important for efficient exhaust of the laser gas into atmosphere [1]. The increase of the stagnation pressure should not accompanied with essential decreasing of the power and efficiency of the laser system. This problem is specific for COIL due to relatively low pressure in the singlet oxygen generator. The stagnation pressure in the Verti-COIL laser system with rotating disk SOG [2] has been increased up to 100 torr using high dilution (1:6) oxygen by helium. However high gas density in the reaction zone promotes the initiation of instabilities of the BHP film on the disks and entrainment of BHP aerosol because this method has restricted possibility for reaching high recovery pressure. The new ejector method of preparing of the COIL active medium has been suggested in [3,4]. The nozzle bank consists of conical nozzles for N_2+I_2 flow and slit or cylindrical nozzles for $O_2(^1\Delta)$ flow. The conical nozzles generate supersonic N_2+I_2 jets but slit or cylindrical nozzles generate $O_2(^1\Delta)$ sonic jets with moderate static pressure (10 torr). If the total momentum N_2+I_2 jets is much more than the momentum of oxygen jets then the full pressure of completely mixed stream will be determined mainly by N_2+I_2 flow. This scheme keeps the inner contradictions yet. Indeed, the reaching of high full pressure requests generating the N_2+I_2 flow with large supersonic velocity in the nozzles with high expansion ratio. Iodine vapor

PART 3
The results of iodine gain line scanning in COIL with slit nozzle and new nozzle bank.

Abstract

The probe diode laser was used to scan the gain line of iodine atom in supersonic flows of COILs with slit nozzle and new nozzle bank.

P_1- pressure in reactor
P_2- in the mixing chamber (plenum pressure),
P_3-static pressure in the cavity,
P_4 -pressure in iodine measurement cell,
P_5 -total pressure in Pitot tube
P_6 -pressure in the vacuum duct downstream cavity
P_{I2}- iodine partial pressure in the measuring cell
G_c - chlorine molar flow rate,
G_{NP} -primary nitrogen molar flow rate,
G_{NS} -secondary nitrogen molar flow rate,
G_{I2}- iodine molar flow rate,
G_{NM}-the total nitrogen molar flow rate through mirrors tunnels (purging)
T_1 - the transmission of the output mirror,
T_2 - transmission of the second mirror.
W_1- laser power from output mirror
W- total laser power
η_c-chemical efficiency
M- Mach number of the flow from ratio $\frac{P_5}{P_3} = \frac{166.7M^7}{\left(7M^2-1\right)^{2.5}}$

3.1. Introduction.

The operation of COIL with slit nozzle having two throats was described in Part 1 of present report. The operation of COIL with new nozzle bank (ejector scheme) was described in Part 2 of the present report. All these results with laser power optimization were obtained in the spring and summer of 1999. The results of gain scanning were obtained in November - December of 1999. Before stating of gain measurements several modifications of COIL set-up were made. The analysis of experimental result obtained in the first half of 1999 forced us to make several changes. It seemed to us that these changes of set-up would improve the operation of COIL. First of all the absorption length in iodine measuring cell was made 5 cm. It allowed us to measure more precisely iodine molar flow rate at higher level. But the new design of this cell resulted to increase of the nitrogen pressure in the measuring cell in comparison with old design at the same secondary nitrogen molar flow rate. It is necessary to take into account when one will compare the value of P_4. Another important modification was made in laser cavity duct. The geometry of the cavity in experiments of first half of 1999 was like this:

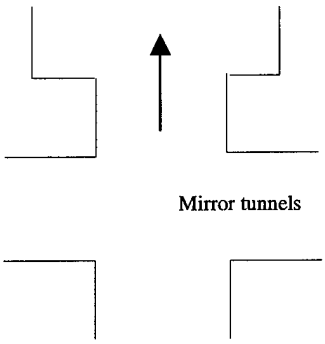

The width of inlet to cavity and outlet were 50 mm. It was due to limited pump capacity of our pump system. Usually the pressure in the vacuum tube downstream cavity was higher than the static pressure in the cavity. If we would increase the width of the outlet then the higher pressure from the vacuum tube penetrates into cavity through boundary layer. But the edges of the stream in the cavity strike about corners of outlet and some portion of the active medium blows into mirrors' tunnels where singlet oxygen is quenched and may generate the resonance absorption. Now the angles of outlet were smoothed to prevent the indicated blow and geometry of laser duct at present looks like:

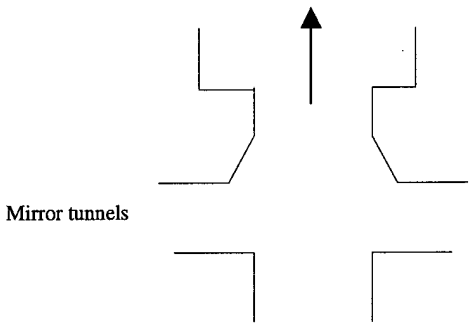

This modification of cavity was made to decrease effect of mirror purging gas on main gas flow also. Unfortunately it was impossible to increase the width of outlet from cavity because the pump rate was not enough to obtain supersonic flow in cavity with wider outlet.

3.2. The gain and temperature of active medium of the COIL with slit nozzle having two throats.

The results of COIL operation with slit nozzle having two nozzles were described in Part 1 of present report. The experimental set-up was the same like in COIL experiments instead of cavity modification described in 3.1. The probe laser beam double passed through the active medium (the total gain length was 10 cm). The experimental set-up of gain measurements is presented in fig.1. The optical axis was located 55 mm downstream from the throat of slit nozzle. The height of cavity was equal to 19 mm at the position of optical axis. The values of G_{NP}, G_{NS}, G_{NM} were close to the values early used for COIL experiments with slit nozzle. First of all the gain was measured in the point of optical axis as a function of iodine molar flow rate. The next parameters of scanning were installed: number of gain line scans per second was 25, averaging of the gain line each 0.5 sec. The example of the gain line scanning presented in Fig.2.

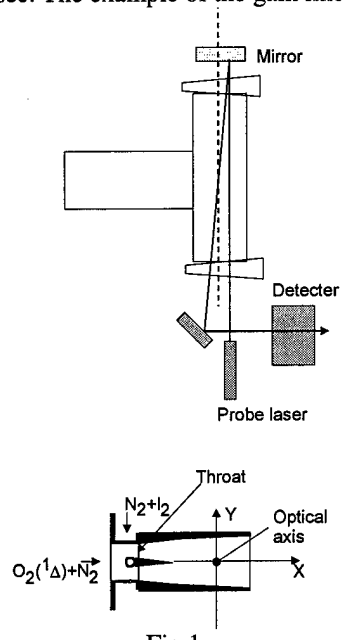

Fig.1.

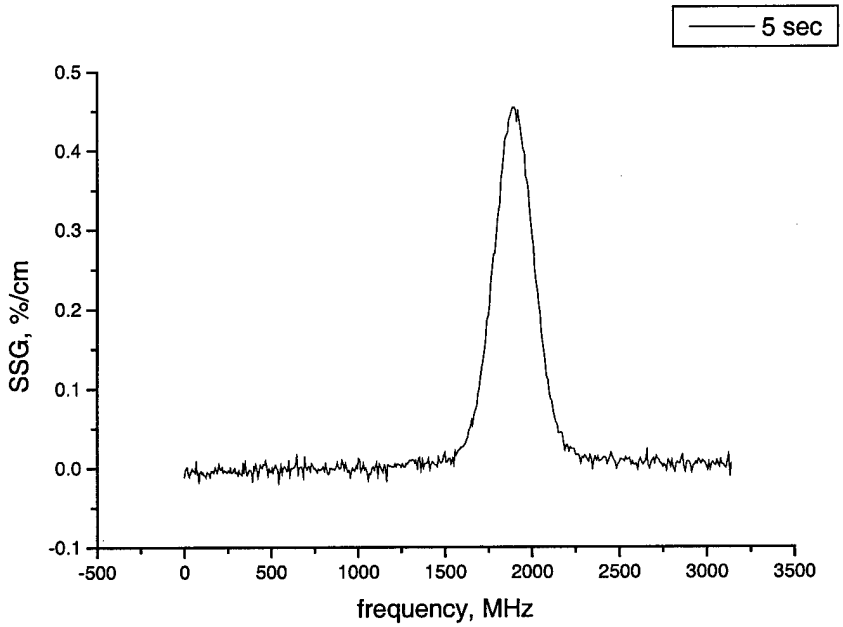

Fig.2. The gain line profile. (5 sec Table 1).

Several words about fitting of data by Foight function. The probe laser line was assumed to be δ-function, base line was cubic. The results of fitting: area A, Lorenz WL and Gauss WG widths were assumed the final parameters. The gas temperature was calculated as $T=(WG/14.49)^2$, the population inversion was calculated as

$$\Delta N(cm^{-3}) = 8\pi\left(\frac{12}{7}\right)\frac{A}{A_{34}\lambda^2} = 4.88\times10^{12}\times A(MHZ\times\%/cm)$$

The time dependence of gain and temperature is presented in Table 1. (the time resolution of Run N.4 in Table 3).

Table 1.

Time,s	Pick gain, %/cm	WG, MHZ	T, K	WL,MHz	A(MHz×(%/cm)	ΔN (cm^{-3})
2.5	-1.1	273	355	125.7	-470	-2.3×10^{15}
3	0.384	235	263	53.5	117.8	5.75×10^{14}
3.5	0.482	239	272	42.8	144	7×10^{14}
4	0.47	245	286	33.6	139	6.78×10^{14}
4.5	0.46	235	263	47	138	6.73×10^{14}
5	0.45	238	270	47	135	6.59×10^{14}
5.5	0.44	246	288	31	130	6.34×10^{14}
6	0.44	235	263	54	135	6.59×10^{14}
6.5	0.46	223	237	77	148	7.22×10^{14}
7	0.42	235	263	52	127	6.2×10^{14}

The chlorine stated to feed JSOG and COIL near 2.5 s and only mechanical vacuum pump worked, then between 2.5 and 3 s the vacuum receiver was opened and high vacuum pump rate realized, after 7 s the chlorine flow was switched off. The gain line for time 5 s is presented in Fig.2. The absorption at t=2.5 s is due to subsonic gas flow in the cavity, high temperature and possibly absorption in the mirrors' tunnels. The large absolute value of population density is due to the high static pressure in subsonic mode. The SSG decreases slowly on time. We explain this by generation of water vapor from BHP aerosols carrying out from JSOG.

3.2.1. The SSG and temperature as vs. on gas flow conditions. Probe laser beam located in the optical axis position (X=0, Y=0)

The dependence of pick gain and gas temperature on iodine molar flow rate on the optical axis (X=0, Y=0) are presented in Table 2 and Fig.3, Fig.4.. The gas temperature is correlated with estimated Mach number of gas flow: for higher M the temperature is lower. Higher iodine molar flow G_{I2}>0.85 mmole/s rate resulted in subsonic gas flow in cavity and negative gain.

Table 2. Here t_s is the time interval from the moment of vacuum receiver opening.

Run	G_c	G_{NP}	G_{NS}	P_1	P_2	P_3	P_5	G_{I2}	SSG,%/cm	WG, MHz	T,K	WL	M	t,s
1	68	130	68	58.7	37.2	6.05	28	0.666	0.316	218	226	50	1.77	2.5
2	68	123	60	54.5	34	6.4	26.8	0.628	0.431	222	235	54.3	1.67	2.5
3	68	130	60	55.1	33.4	6.7	26.1	0.713	0.504	219	228	62.3	1.65	2.5
4	68	123	60	55.7	36.4	7.3	25.2	0.807	0.564	230	252	55	1.52	2.5
5	39.2	72	40	30.6	20	4.54	14.2	0.615	0.54	235	263	36	1.42	2.5
6	39.2	72	40	31.4	20.8	4.65	14.5	0.749	0.6	227	245	51.6	1.38	2.5
7	39.2	72	40	31.8	21.7	3.5	14.5	0.484	0.141	194	179	69	1.65	2.5
8	39.2	72	40	31	21.7	3.5	14.6	0.478	0.113	210	210	58	1.68	3
9	39.2	72	40	32	21.8	3.8	14.2	0.544	0.277	218	226	56	1.57	2.5
10	39.2	72	40	31.6	20.1	4.15	13	0.606	0.387	224	239	50	1.43	2.5
11	39.2	72	40	31	20	4.55	13	0.678	0.551	229	250	50	1.34	2.5
12	39.2	72	40	31.7	20.8	4.87	13.5	0.758	0.631	229	250	49.7	1.34	2.5

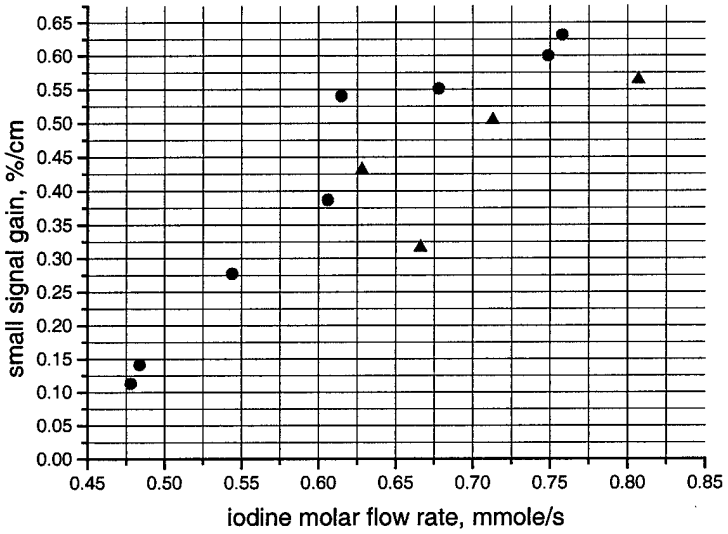

Fig.3. The dependence of SSG on iodine molar flow rate. Black tiangle for 68 mmole/s of Cl_2 molar flow rate (runs 1-4), red circle for 39.2 mmole/s of Cl_2 molar flow rate (runs 5-12).

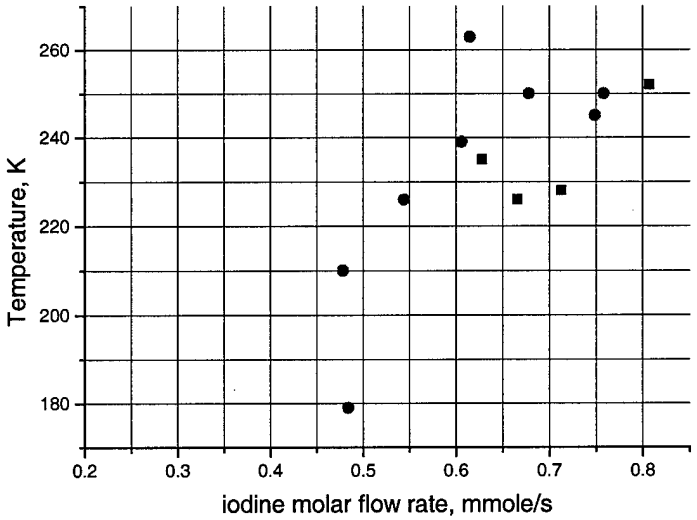

Fig.4. The dependence of temperature on iodine molar flow rate. Black tiangle for 68 mmole/s of Cl_2 molar flow rate (runs 1-4), red circle for 39.2 mmole/s of Cl_2 molar flow rate (runs 5-12).

3.1.2. The dependence of SSG and temperature on the position of the probe laser beam relatively to optical axis.

The dependence of SSG and temperature on position of probe beam relative optical axis is presented in Table 3 and Fig.5, Fig.6. The iodine molar flow rate in these runs was in the range G_{I2}=0.6÷0.7 mmole/s. This fluctuation of iodine molar flow rate resulted in additional scatter of values in Fig.5 and Fig.6. The SSG increases with increasing of distance X from the throat of slit nozzle. Thus dissociation of iodine is not complete at distances less than 55 from the throat of the nozzle. The point X=0, Y=0 is located in the wake from the central blade of slit nozzle. It's possible also that active medium in the turbulent wake with low SSG mixes with gas flow from stream core with higher SSG and as result SSG increases with raise X.

Table 3.

Run	G_c	G_{NP}	G_{NS}	P_1	P_2	P_3	P_5	G_{I2}	X, mm	Y, mm	SSG, %/cm	WG, MHz	T,K	WL	M	t,s
1	39.2	72	40	31	20	4.55	13	0.678	0	0	0.551	229	250	50	1.37	2.5
2	39.2	72	40	31.5	21.1	4.54	12.7	0.677	10	0	0.553	224	239	50.4	1.35	2.5
3	39.2	72	40	31.8	21.4	4.7	13.1	0.702	20	0	0.567	222	235	54.4	1.35	2.5
4	39.2	72	40	31.8	21.3	4.62	12.9	0.677	-10	0	0.447	238	270	46.7	1.35	2.5
5	39.2	72	40	32.7	22.5	4.69	12.8	0.67	-20	0	0.447	236	265	41	1.35	2.5
6	68	123	60	55.4	33.3	6.8	25	0.614	10	0	0.457	221	233	61	1.57	2.5
7	68	123	60	55.4	33.8	7.1	24.6	0.633	18	0	0.504	218	226	64.7	1.52	2.5
8	68	123	60	56.2	34.8	6.7	25.2	0.603	0	0	0.449	215	220	60	1.57	2.5
9	68	123	60	56.2	34	6.8	25.1	0.6	-10	0	0.389	212	214	77	1.57	2.5
10	68	123	60	56.4	35.1	6.7	25.6	0.608	-10	0	0.353	211	212	75	1.6	2.5
11	68	123	60	59.1	38.5	6.7	25.7	0.594	-20	0	0.197	209	208	73	1.61	2.5
12	68	123	60	60	38.4	6.7	25.8	0.606	-20	0	0.217	190	172	88	1.62	2.5
13	68	123	60	57.8	35.5	7	25.2	0.586	0	7	0.615	212	214	72	1.55	2.5
14	68	123	60	58.2	36	6.5	26.2	0.619	10	7	0.539	213	216	64	1.65	2.5
15	68	123	60	58.5	36.3	6.8	26.3	0.608	-10	7	0.416	214	218	48	1.63	3

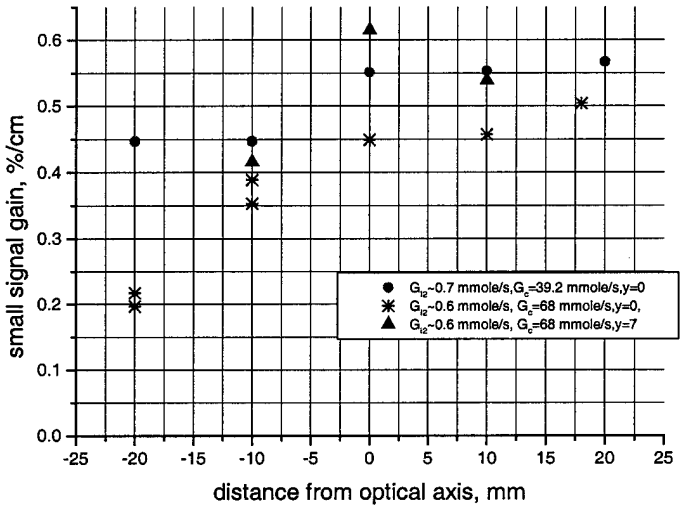

Fig.5. The dependence of SSG on the position of probe laser beam relative to optical axis. The point X=0,Y=7 mm located in the kernel of flow from one throat.

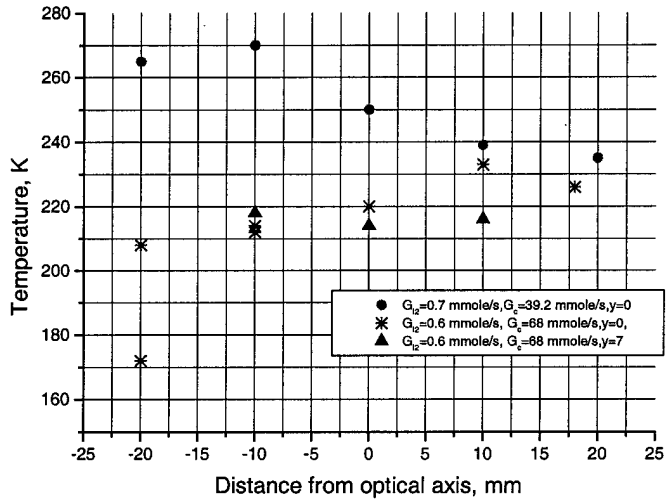

Fig. 6. The dependence of temperature on position X of the probe laser beam relative optical axis.

3.3. The gain and temperature of active medium of the COIL with new advanced nozzle bank

3.3.1 The SSG and temperature of gas flow as vs. on gas flow conditions . Probe laser beam located in the optical axis position (X=0, Y=0).

The experimental set-up was similar to set-up in 3.2 but new nozzle bank described in Part 2 was installed in COIL. The optical axis was located on 64 mm downstream from nozzle bank.

The results of gain and temperature measurements for X=0, Y=0 are presented in Table 4 and Fig.7,8. The Mach number of the flow in the cavity was much higher than for the slit nozzle system. The static temperature of gas flow was lower than for slit nozzle system also. The Pitot pressure $P_5 \approx 90$ torr was less than 100 torr pressure obtained in the laser experiments (Part 2). We believe that it was due modification of outlet of the laser cavity and decreasing static pressure in the mirrors' tunnels and in the cavity. The pressure broadening WL is approximately in two times more than for slit nozzle system. First of all it is due to higher static pressure in the cavity and lower temperature. The pressure broadening is inverse proportional to temperature WL(T)=WL(300K)(300/T) [1].

Table 4.

Run	G_c	G_{NP}	G_{NS}	G_{NM}	P_1	P_2	P_3	P_4	P_5	G_{I2}	SSG, %/cm	WG, MHz	T,K	WL, MHz	M	t,s
1	39.2	410	11	11	36.6	30.7	9.5	70	87.4	0.63	0.49	190	172	103	2.65	3
2	39.2	410	11	11	37	31	9.5	68.2	88.6	0.55	0.48	200	191	95	2.65	3
3	39.2	410	11	11	37	31	9.4	65.6	86	0.50	0.43	199	189	80	2.6	3
4	39.2	410	11	11	37	31	9.7	71	85	0.70	0.53	192	176	101	2.5	2.5
5	39.2	410	11	11	37.4	31	9.9	77.4	86	0.72	0.56	199	189	94	2.55	3
6	39.2	410	11	11	40	33.6	9	83.3	88	0.42	0.41	192	175	106	2.7	2.5
7	39.2	410	11	11	40.4	33.9	9.1	84	88	0.46	0.43	203	196	85	2.7	2.5
8	39.2	410	30	11	40.1	33	9.4	157	90	0.57	0.35	200	191	95	2.65	2.5
9	39.2	410	30	11	40	33.1	9.56	156	87	0.66	0.42	189	170	114	2.6	2.5
10	39.2	410	30	11	40	33.6	9.66	159	87	0.76	0.45	192	175	115	2.55	2.5
11	39.2	410	30	11	40.6	34	9.9	159	84	0.85	0.48	199	188	108	2.45	2.5
12	39.2	410	42	11	36.9	30.8	9.1	216	95	0.58	0.29	182	158	113	2.75	2.5
13	39.2	410	42	11	37.3	31	9.9	226	81	0.76	0.39	191	174	112	2.45	2.5
14	39.2	410	42	11	34.2	31.2	9.7	222	86	0.66	0.37	184	161	119	2.5	2.5
15	39.2	410	42	11	39.7	33	10.2	212	85	0.87	0.5	198	186	114	2.45	2.5
16	39.2	410	42	11	40.5	33	10.1	210	87	0.82	0.46	207	204	93	2.5	2.5
17	39.2	410	55	11	39.4	33	9.8	240	90	0.77	0.38	196	183	100	2.54	2.5
18	39.2	410	55	11	39.8	33.1	9.9	240	91	0.66	0.35	205	200	97	2.54	2.5
19	39.2	410	55	11	40	33.4	10.3	240	91	0.82	0.40	201	192	103	2.54	2.5
20	39.2	410	55	11	39.8	33.6	10.3	240	89	0.93	0.45	190	172	114	2.5	2.5

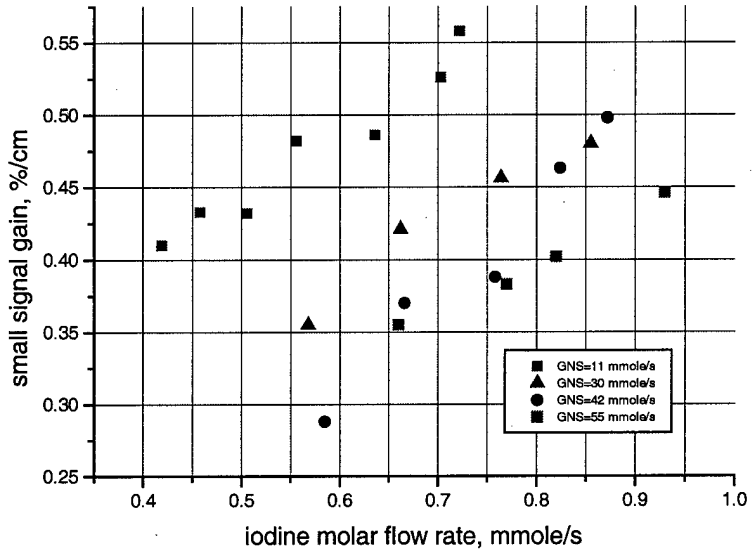

Fig.7. The dependence of SSG on iodine and secondary nitrogen molar flow rate.

Higher G_{NS} forces to increase iodine molar flow rate to achieve the same value of SSG for smaller G_{NS}. Let's consider SSG for G_{NS}=42 mmole/s and G_{I2}≈0.8 mmole/s. The value of SSG≈0.45 %/cm measured by probe laser is approximately equal to the value estimated from Rigrod curve at the same gas flow conditions (Fig.8 in Part2).

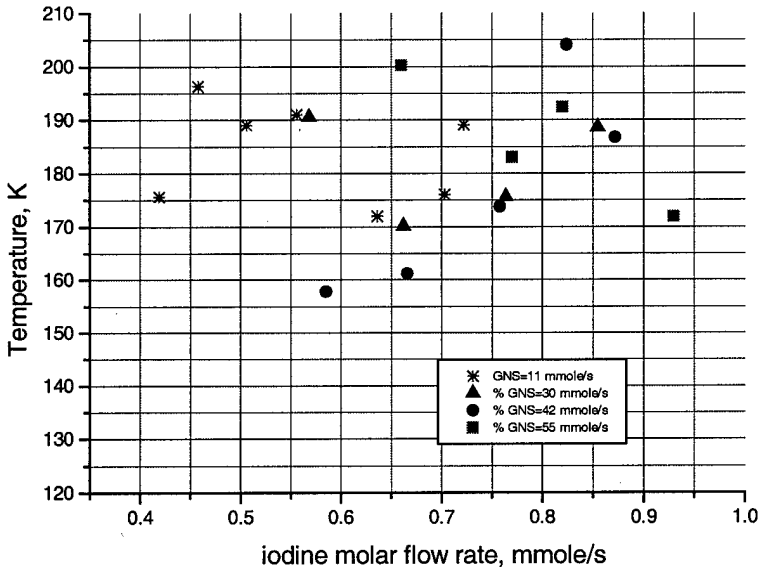

Fig.8. The dependence of gas temperature on iodine and secondary nitrogen molar flow rates.

3.3.2. The dependence of SSG and temperature on the position of probe laser beam relative to optical axis.

In COIL experiments (Part 2) with new advanced nozzle bank the Pitot pressure 100 torr has been achieved at G_{NP}=400mmole/s. The primary nitrogen molar flow rate in these experiments with probe laser was increased up to 500 mmole/s to raise the Pitot pressure up to 100 torr. The results of measurements are presented in Table 5 and Fig.9, Fig.10.

The SSG decreases with increase of distance X from the nozzle bank. The SSG is equal to

$$g\left(cm^{-1}\right)=n_I\sigma\times\frac{(K_{eq}+0.5)Y-0.5}{(K_{eq}-1)Y+1}$$

where σ is efficient cross section, n_I iodine atoms density, Y is $O_2(^1\Delta)$ fraction, $K_{eq}=3/4\exp(402/T)$.
Is it possible to explain such SSG dependence by quenching of $O_2(^1\Delta)$ or decreasing of Y? The quenching of $O_2(^1\Delta)$ is mainly due to quenching of $I(^2P_{1/2})$ by water , I_2 and N_2 (highest fraction in gas flow). The specific time of $O_2(^1\Delta)$ quenching (or decreasing of Y) is approximately

$$\tau^{-1}\approx([H_2O]K_W+[N_2]K_N+[I_2]K_I)\times[I]/[O_2],$$

where $[H_2O]$ is water vapor concentration, $K_W=2\times10^{-12}\ (T/300)^{0.5}\ cm^3/s$, $[N_2]$ - nitrogen concentration, $K_N=6.5\times10^{-17}\ (T/300)^{0.5}\ cm^3/s$, $[I_2]$ molecular iodine concentration, $K_I=3.6\times10^{-11}\ cm^3/s$, For pressure 10 torr and gas composition $I_2:H_2O:O_2:N_2=0.02:0.05:1:11$, dissociation efficiency 50% ($[O_2]:[I]=100:2$) and temperature 190K one obtains (quenching by I_2 excluded): $([H_2O]K_W+[N_2]K_N)\times[O_2]/[I]\approx100\ s^{-1}$. This value of τ corresponds to the length 500 cm for gas velocity 500 m/s. Thus quenching of I* by H2O and by N2 can't explain fast drop of gain along gas flow. Taking into account 50% of undissociated iodine resulted in estimation $\tau^{-1}\approx([I_2]K_I)\times[I]/[O_2]=200\ s^{-1}$. This quenching also can't explain the drop of SSG along the gas flow. Another possible mechanism of $O_2(^1\Delta)$ losses is the recombination of I atoms in the presence of high density of N_2 and reverse dissociation of I_2. In this case the losses of $O_2(^1\Delta)$ is proportional to $[I][I][N_2]$ but can't explain fast drop of gain also. We considered also gasdynamic origin of gain drop that is due to mirror purging gas effect. It compress main flow near the outlet of cavity and efficiently decrease the gain length. But product "active length×[I]" is constant along gas flow. Thus compressing of main flow also can't explain drop of SSG. So at present we have not adequate explanation of SSG drop along gas flow. Possible the measured SSG and temperature dependencies is result of the influence of absorbing gas circulated in the mirror tunnels. It's necessary to repeat these experiments when mirrors tunnels will be removed.

Table 5.

R	G_c	G_{NP}	G_{NS}	G_{NM}	P_1	P_2	P_3	P_4	P_5	G_{I2}	X,mm	Y,mm	SSG,%/cm	WG, MHz	T,K	M	WL, MHz	t,s
1	39.2	500	11	30	40.4	33.8	12.3	72	105	0.76	5	0	0.36	186	165	2.5	153	2.5
2	39.2	500	11	30	39	33.3	12.9	68	111	0.79	0	0	0.45	192	176	2.5	139	2.5
3	39.2	500	11	30	41	35	12.4	67	105	0.81	15	0	0.32	222	235	2.5	116	2.5
4	39.2	500	11	30	39.9	34	12.8	68.4	123	0.81	0	0	0.4	193	177	2.6	135	3
5	39.2	500	11	30	40.4	34	12.3	69	106	0.81	10	0	0.35	207	204	2.5	133	2.5
6	39.2	500	11	30	39.8	33	12.3	68.8	106	0.81	0	0	0.44	193	177	2.5	130	2.5
7	39.2	500	11	30	39.8	33.3	12.4	69.4	104	0.82	0	0	0.42	207	204	2.5	118	2.5
8	39.2	500	11	30	39.3	33	12.4	64.9	117	0.85	-15	0	0.52	195	181	2.6	125	2.5
9	39.2	500	11	30	40.3	34.4	12.1	64.4	108	0.85	0	0	0.51	194	179	2.6	126	2.5
10	39.2	500	11	30	38.3	32.5	12.4	66	111	0.86	0	0	0.44	194	179	2.5	130	2.5
11	39.2	500	11	30	40.1	33.6	12.1	65	114	0.86	-5	0	0.44	196	183	2.6	133	2.5
12	39.2	500	11	30	39.2	33.1	13	65.6	119	0.87	-20	0	0.58	177	149	2.6	157	2.5
13	39.2	500	11	30	39.9	33.3	12.4	63.7	114	0.87	5	0	0.43	194	179	2.6	138	2.5
14	39.2	500	11	30	38.6	32.6	11.9	63	98	0.87	-10	0	0.58	195	181	2.5	118	3
15	39.2	500	11	30	40	33.9	12.6	63.6	117	0.87	20	0	0.37	189	170	2.6	132	2
16	39.2	500	11	30	40.5	34.3	12.7	64.4	118	0.88	20	0	0.26	197	185	2.6	138	3
17	39.2	500	11	30	36	33	12.3	63.4	114	0.88	10	0	0.44	205	200	2.6	125	2.5
18	39.2	500	11	30	39	33	12.4	63.3	119	0.88	-10	0	0.54	180	154	2.6	146	2.5
19	39.2	500	11	30	39.3	33.3	12.7	63.5	116	0.88	20	0	0.37	225	241	2.6	92	3
20	39.2	500	11	30	39.5	33.5	12	64	104	0.89	-20	0	0.58	184	161	2.5	141	2.5
21	39.2	500	11	30	39.5	33.2	12.3	61.3	114	0.89	10	0	0.45	199	189	2.6	136	2.5
22	39.2	500	11	30	38.6	32.8	11.8	63.1	102	0.9	-15	0	0.57	183	160	2.5	135	3
23	39.2	500	11	30	38	32	11.7	61.6	95	0.90	-5	0	0.55	173	143	2.4	154	2.5
24	39.2	500	11	30	40.5	34.5	12.6	62	117	0.90	15	0	0.36	197	185	2.6	142	2.5
25	39.2	500	11	30	39.7	33.5	12.1	61.7	114	0.90	0	0	0.46	200	191	2.6	124	2.5
26	39.2	500	11	30	39.5	33.4	12.4	63	115	0.91	5	0	0.47	198	187	2.6	133	2.5
27	39.2	500	11	30	40	33.7	12.3	61.8	115	0.91	-5	0	0.48	192	176	2.6	135	2.5
28	39.2	500	11	30	39.3	33.2	12.1	64.5	114	0.92	-10	0	0.47	182	158	2.6	150	2.5
29	39.2	500	11	30	39.6	33.4	12.4	61.6	115	0.92	15	0	0.39	190	172	2.6	147	2.5

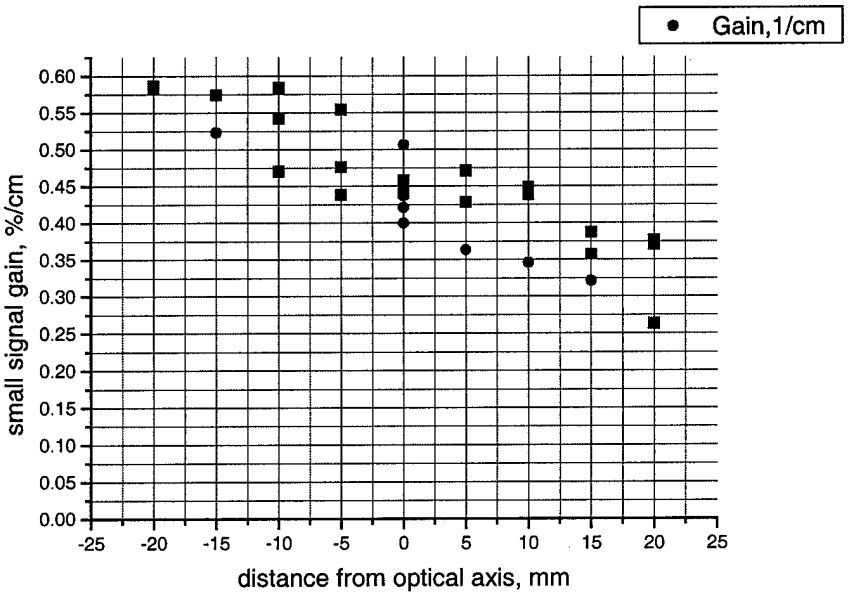

Fig.9. The dependence of SSG on the position of the probe laser beam relative to the optical axis (Y=0). (blue sqaure G_{I2}=0.76÷0.85, red circle-G_{I2}=0.86÷0.92.)

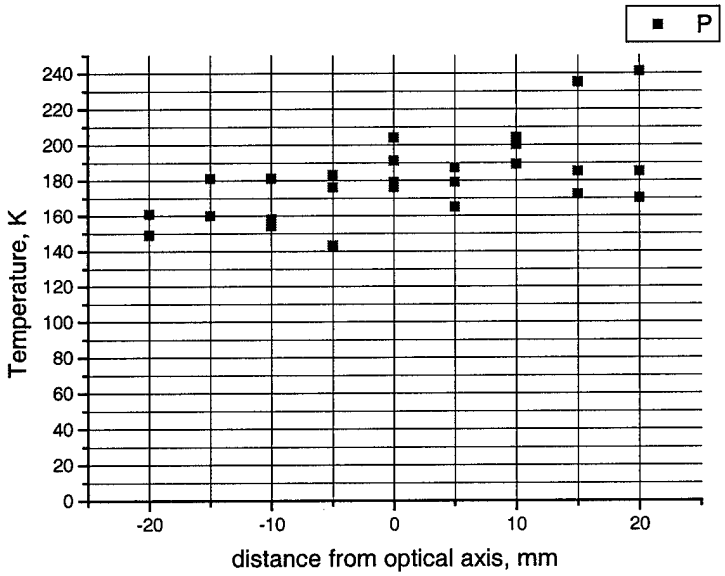

Fig.10. The dependence of gas temperature on the position of probe laser beam (Y=0).

3.3. The special run at subsonic gas flow velocity in the cavity with slit nozzle.

For comparison two special runs with slit nozzle system were performed. The gas flow rates were identical in both runs but in second run the vacuum receiver was not opened. The results of probe laser experiment (X=0, Y=0) are presented in Table 6. In the run 1 the supersonic flow and in run 2 subsonic flow.

Table 6. G_c=39.2 mmole/s, P_1=32 torr, G_{NP}=72 mmole/s, G_{NS}=40 mmole/s, G_{NM}=6 mmole/s

Run	P_2	P_3	P_5	G_{I2}	SSG, %/cm	WG, MHz	T,K	WL, MHz	A (MHz×(%/cm)	ΔN (cm^{-3})	M	t,s
1	20.1	4.15	13	0.60	0.387	224	239	50	111	5.4×10^{14}	1.42	2.5
2	28.8	27	29	0.60	-1.37	291	403	135	626	3.0510^{15}	0.32	2.5

Let's don't take into account the influence of absorption zone in the mirror tunnels in both runs on the measured value of SSG and temperature T. The SSG is equal to

$$g\left(cm^{-1}\right)=n_I\sigma\times\frac{(K_{eq}+0.5)Y-0.5}{(K_{eq}-1)Y+1}$$

In supersonic run SSG>0 and in subsonic run SSG<0. It means that in supersonic run $(Y-Y_{th})>0$ and in subsonic run $(Y-Y_{th})<0$, where $Y_{th}=(1+2K_{eq})^{-1}$. The $O_2(^1\Delta)$ fraction is equal to $Y=Y_0-Y_q-Y_d$, where Y_0 is the initial $O_2(^1\Delta)$ yield, Y_q fraction of $O_2(^1\Delta)$ lost for gas heating (this value include the quenching losses during I_2 dissociation), Y_d is the $O_2(^1\Delta)$ fraction for breaking bond of I_2 molecules ($\approx$2 $O_2(^1\Delta)$ for one I_2).

It is also possible to estimate absolute gas velocities U, threshold $O_2(^1\Delta)$ fraction $Y_{th}=(1+1.5\exp(402/T))^{-1}$ in both cases, flux of population inversion $G_{\Delta N}=\Delta N\times U$. (Table 7). The stagnation temperature is $T^*=T\,(1+0.2M^2)$. The heating of gas is due to quenching of $O_2(^1\Delta)$ (value Y_q). The initial stagnation temperature is estimated as T^*_0=300K for both runs. Thus $Y_q=(T^*-T^*_0)\times3.5*(G_{NP}+G_{NS}+G_c)/G_c/11340$. Here 11340K is $O_2(^1\Delta)$ energy in K and 3.5 is specific heat capacity of N_2 or O_2. In both runs the initial $O_2(^1\Delta)$ fraction was identical Y_0. The Y_d is less than $Y_{dmax}=2[I_2]/[O_2]=2G_{I2}/G_c$. The calculated values in Table 7.

Table 7.

Run	T^*, K	U, m/s	$G_{\Delta N}$(mmole/cm^2/s)	Y_{th}	Y_q	Y_{dmax}	$Y_{th}+Y_q+Y_{dmax}$
1	335	440	0.04	0.11	0.04	0.03	0.18
2	411	129	0.066	0.2	0.09	0.03	0.32

For obtaining absorption in subsonic gas flow the initial $O_2(^1\Delta)$ yield Y_0 should be < 0.32. In this case the available $O_2(^1\Delta)$ fraction in supersonic gas flow is only $Y_0-(Y_{th}+Y_q+Y_{dmax})=0.14$. But COIL lasing experiments (Part 2) demonstrated chemical efficiency >20%. It means that above simple analysis was not correct. This contradiction can be explained by effect of absorption zones in the mirror tunnels. This absorption should be much higher for subsonic gas flow in cavity due to much higher static pressure in cavity. In this case the measured value of SSG is the average value along optical axis. The real absorption length is higher than 5 cm. In the case of supersonic gas flow the absorption zones in the mirror tunnels smaller but also exists.

Thus if one will take into account absorption in mirror tunnels it is possible to explain high measured absorption in subsonic flow conditions. In the case of supersonic flow conditions the real local gain is higher than measured.

We plan to make experiments with probe laser without mirror tunnels. The glass wedge windows will be walls for gas flow in this case.

References

1. R.Engelman, B.A.Palmer. Transition probability and collision broadening of the 1.3 μm transition of atomic iodine. J.Opt.Soc.Am., v.73, N.11, pp. 1585-1589, 1983

Part 4.

Pulsed COIL with a Transverse dc Discharge Generation of Iodine Atoms

1. Introduction

The chemical oxygen – iodine laser (COIL) is currently considered as a promising candidate for specific industrial and other applications. Saying about industrial COIL applications one usually means CW mode of COIL operation. But for some applications the power is a crucial factor. In this case the COIL pulsed mode may be more preferable.

Indeed, the pulse mode of COIL operation allows one to get pulses which power exceeds that for CW mode. In any case the average power remains constant and its value is governed by chemicals flow rate. Such a pulsed COIL can find application working individually as well as in a complex with a CW COIL. The latter can be attractive if an exact coincidence of wavelength is required.

The different approaches are used to get pulse mode of COIL operation. It can be Q-switching or mode – locking methods applied to CW COIL. In these cases the active medium is prepared by mixing of singlet oxygen with molecular iodine. Because of fast relaxation processes it is impossible to form the active medium of significant dimensions. It is easily to show /1/ that the ratio of power of pulse W_{pulse} produced due to methods mentioned above to that of cw mode W_{cw} at the same chemicals flow rate has a limit:

$$W_{pulse} / W_{cw} = K_f \cdot [I] L / v, \qquad (1)$$

where K_f is a rate constant for forward reaction of energy exchange, [I] is a concentration of iodine atoms, L is a laser cavity length in the flow direction and v is a flow velocity. In experiment the maximal value of 16 was obtained /2/.

To generate a pulse of power as high as possible one have to form a large scale active medium with high energy store and then extract the stored energy in time as short as possible. The forming of large-scale active medium requires one to use relatively stable gas mixture at the stage of filling the active volume. It can be made using a mixture of singlet oxygen with iodides, which doesn't react practically with singlet oxygen. After the stage of filling the mixture is exposed to instantaneous action resulting in release of free iodine atoms. The photolysis, electric discharge , radiolysis can be used for iodide decomposition. This method, called as volume generation if iodine atoms, make it possible to form a meter scale active medium. Being born the iodine atoms extract the energy stored in singlet oxygen in a form of laser emission in a time τ_{pulse}

$$\tau_{pulse} \cong 1 / K_f \cdot [I], \qquad (2)$$

where K_f is a rate constant for forward reaction of energy exchange and [I] is a concentration of iodine atoms. If generation of iodine atoms doesn't activate relaxation processes the output laser energy is determined by only the value of energy stored in active volume and remains constant. But the pulse duration is reciprocal to the concentration of iodine atoms. Thus, one can shorten the pulse duration and, hence, increase the pulsed power by increasing the iodine concentration.

When photolysis was used to produce iodine atoms the specific energy of 3,3 J/ l was obtained at 3 Torr of oxygen pressure, 40% singlet oxygen yield and at CH_3I as an iodide /3/. This value of specific energy corresponds to 90% of extraction efficiency and to 23 % of chemical efficiency. The chemical efficiency of 36 % was obtained at lower oxygen pressure and, hence, higher singlet oxygen yield. These very high values of chemical efficiency at rather low yield were obtained due to saving the excited oxygen molecules being consumed to dissociate molecular iodine in the traditional CW COIL The pulse duration could be varied from 15 μs to about 500 μs at practically constant output energy. The pulse power of 300 kW was obtained from a laser with 1.4 l of active volume. Thus the active medium as long as 1 m in flow direction at singlet oxygen pressure to 3 Torr and power level of three orders of magnitude higher that in CW mode at the same chemicals flowrate were demonstrated.

Photolysis is a very convenient way to produce iodine atoms due to its selectivity. Its demerits are low efficiency and low repetition rate of flash lamps operation. The electric discharge can provide laser operation with multi kilohertz repetition rate. But *ab initio* it was not clear if electric discharge is suitable to decompose iodide and, at the same time, not to quench the singlet oxygen molecules. The experiments carried out with a longitudinal pulsed dc discharge showed the electric discharge is effective for this purpose. The specific energy of 1 J / l was obtained at 2 Torr of oxygen pressure. The total efficiency (ratio of laser output energy to that stored in capacity bank) was close to 100% /4/. The operation with repetition rate up to 20 Hz was demonstrated. Note, that repetition rate in our case was limited by the power of an available power supply.

The value of specific energy obtained with electric discharge initiation is at a disadvantage in relation to that obtained with photolysis. The possible causes of this difference could be the quenching of singlet oxygen by electrons and particle fragments as well as heating of active medium due to increased energy cost of iodine atoms produced by discharge. The energy of UV quantum causing the iodide molecule dissociation is 5 eV. Assuming the total energy stored in capacitor bank is deposited into active medium one can estimate the energy cost of iodine atom produced by discharge is as large as 25 eV.

The promising results obtained with the longitudinal pulsed COIL with volume generation of atomic iodine by using a dc discharge encouraged us to start an investigation of a transverse discharge excitation. This type of discharge make it possible to work with higher pressure of singlet oxygen provided by modern jet singlet oxygen generator. Besides, it was found that repetitively pulsed operation of longitudinal COIL worsens when repetition rate increases. This is a result of vaporization of iodine deposited on the wall of laser chamber. One can decrease this effect by minimizing the ratio of surface of laser chamber to its volume. It can be made when transverse flow transverse discharge is used.

But change over to the transverse discharge configuration meets problems. The first one is an acceptable matching of transverse discharge to power supply circuit. It is known that the best energy transfer from power supply to the load is obtained when the load resistance is equal to that of power supply. Unlike the longitudinal discharge the transverse one has usually significantly shorter discharge gap at larger area of discharge cross -section.

The resistance of the discharge is proportional to its length and reciprocal of its cross section. Thus, shortening the length of discharge gap by a factor of n one have to increase the cross section by the same factor to save the active volume. As a result the resistance of discharge reduces by a factor of $1/n^2$. To save the electric field strength one has to decrease the voltage across a discharge gap by a factor 1/n too. The latter requires one to increase the capacitance by a factor of n^2 to save the energy deposition into active medium. In its turn the change of capacitance results in decreasing the circuit resistance by a factor 1/n. (The inductances for both longitudinal and transverse discharges are assumed to be equal). Thus, one can see that discharge gap resistance changes proportionally to $1/n^2$ while that for circuit is proportional to 1/n. This difference results in impedance mismatch.

The another problem can be essential when operation pressure and discharge gap are small. In this case the length of cathode fall of voltage can occupy the major part of active volume thus shortening the area of positive column in which the processes governing the laser operation occur.

2. Experimental technique.

At present the different approaches are used to provide the transverse electric discharge to drive the gas lasers with high operation pressure (CO_2 – lasers, eximer lasers). Practically all of them use the preionization with electron beam or photoionization. To produce the latter the array of spark gaps, barrier discharge or surface discharge is used. Recently the great success was obtained in initiation of nonchain HF – laser /5/ using a system of electrodes with high edge nonuniformity and without any preionization. The uniform self-sustained volume discharge was obtained in a mixture of SF_6 with hydrocarbons C_2H_6 at total pressure of 60 Torr and the component ratio $SF_6 : C_2H_6 = 20 : 1$. The active volume of laser chamber was as large as 50 l at the length of electrodes gap 27 cm. The simple flat electrodes with rounding along its perimeter were used. The mechanism of formation of a uniform volume discharge proposed by authors allowed us to hope to obtain similar results in the case of pulsed COIL active medium. Indeed, like that in HF – laser, the COIL active medium contains the electronegative component – oxygen and easy to ionization component – RI. Note, that ionization potentials for both CH_3I – 9.5 eV and for CF_3I – 10,2 eV

are the less that for C_2H_6. Besides, the less pressure of the COIL active medium seemed to be positive to obtain the uniform discharge.

Two laser chambers with electrodes system mentioned above were designed and manufactured. The first one has 50 cm gain length and 4 cm discharge gap (fig.1) The active volume of this chamber is 800 cm3. This laser chamber is integrated with laser facility providing the operation with chlorine flowrate up to 100 mmole / s and pumping capacity to 1500 l / s. Thus, one can expect the maximal repetition rate to over 1 kHz.

Both electrodes were made of flat aluminum plates rounded along their perimeters. The cathode surface was subjected to sand-blasting.

All attempts to get a uniform discharge with this electrode system were unsuccessful. The nonuniformity increased drastically when iodide was added to oxygen. No lasing was detected within wide range of variation of electrical circuit parameters. To improve the discharge uniformity the electrode system was modified. The flat cathode was substituted for electrode with a surface discharge. The array of plasma channels produced across its surface served as a plasma cathode. Such a cathode reduces the role of negative effects in the zone of cathode voltage fall. Besides, the VUV radiation of plasma channels causes the preionization of discharge gap. As a result, the uniform discharges were obtained in the zones where the plasma channels existed. Thus the task was reduced to receiving the total filling the cathode surface with a plasma channels. This work is now in progress.

The second laser chamber was designed to work in combination with a jet singlet oxygen generator (fig. 2). It has 5 cm gain length and 2 cm electrode gap and in its first version it was equipped with a simple system of electrodes. Like that for the 50 cm laser chamber all attempts to obtain the uniform discharge were unsuccessful too.

In spite our experiments with simple electrode system without preionization were unsuccessful we believe this approach can be useful for future experiments at higher pressure and longer electrode gaps. Up to now the simple flat cathode was substituted for resistively loaded multi pin one. The satisfactory uniform discharge was obtained in recent experiments. This substitution was made on the base of results obtained with a 19-cm gain length laser chamber equipped with multi pin resistively loaded cathode. All results presented below on the pulsed COIL with generation of iodine atoms by using a transverse discharge were obtained with this laser chamber.

The experimental facility (fig.3) included the chemical singlet oxygen generator, gas handling system, pumping system, discharge power supply, optical chamber, laser chamber, control system. The quartz cylinder sparger singlet oxygen generator had 140-mm diameter and 230 mm height. It was packed with Rashig rings (12x12x1.5mm) made of Teflon. The height of packing was 130 mm. The typical working solution was prepared by mixing 750 ml of 50% hydrogen peroxide with 400 ml of 50 % KOH. The start temperature of working solution in SOG was close to -20^0 C. Typically, the duration of a run was as long as 10 – 20 sec and then it was followed with a period of cooling the working solution. The gas from SOG was transported to the laser cavity through a quartz tube of 50-mm o.d. The pressure guide, iodide injector and optical chamber inlet were located 500 mm, 640 mm and 800 mm downstream of SOG, respectively. The iodide injector was perforated torus made of Teflon. The gas flow entering the optical chamber branched into two arms ended with outlets to pumping system and cavity mirrors holders. The total length of optical chamber was 1600 mm and it was equal to the length of the laser resonator when internal mirrors were used. Previously this optical chamber was used as a laser cell of the pulsed COIL with longitudinal geometry. In the present work the 19-cm gain length laser cell was inserted into the one of the arms of optical chamber.

The laser chamber was equipped with electrodes, 1.8 cm apart, providing the transverse discharge with respect to the flow direction. It had 19-cm length cathode with 120 pins arranged in three lines. The active volume was 52 cm^3. The electric circuit (Fig.4) was fed with a positive high voltage from a power supply with a buffer capacitor C_1. The discharge capacitor C_2 could be varied within 3.4 nF....20.4 nF by variation of the number of capacitor of 3.4 nF. The electric discharge was triggered by the pulse generated with a generator S and applied to the grid of thyratron TGI1- 16 / 500.This thyratron provided the circuit operation with a voltage up to 18 kV (little over its passport limit). In its turn the pulse generator PG drove the triggering generator S. The duration of discharge was close to 200 ns.

Molecular chlorine was fed through the leaker and electromagnetic valve from a 5-liter volume flexible polyethylene bag filled from a standard cylinder with liquid chlorine. The application of a flexible bag made it possible to sustain the input pressure to be equal to atmospheric one and thus to stabilize the

chlorine flowrate. Iodides were fed through the leaker and electromagnetic valve too. CH_3I delivered from a stainless steel vessel of 8-l volume charged with 100 ml of liquid iodide. CF_3I was fed from small volume cylinder. When used the buffer gases (He, N_2, Ar, SF_6) were injected into the chlorine flow upstream of SOG. This way made it possible to reduce the chlorine partial pressure in SOG and thus increase the singlet oxygen yield at high buffer gas flowrate.

The laser emission was detected with Ge- photodiode equipped with averaging sphere. Laser emission was focused on the hole of this sphere. The signal from detector was monitored with oscilloscope and then recorded with a digital camera. The output energy was measured with a calorimeter. The losses of energy in the elements of optical system were taken into account.

3. Results and discussion.

The investigation of pulsed COIL with generation of iodine atoms in the pulsed DC discharge was performed in Troitsk in accordance with Item 2. The influence of discharge energy, discharge voltage, oxygen pressure, sort and pressure of buffer gas on laser parameters was investigated.

All experiments were performed with laser cavity formed with totally reflecting mirror and output one with 4.5 % transmission. This value of transmission was chosen on the base of preliminary experiments on resonator optimization. Pump capacity was 80 l / s. It is not the limit for our pumping system, but such a medium pumping made it possible to increase the run duration without refilling the SOG.

Specification:
P_{O2} – oxygen pressure in laser chamber
P_{He} – helium pressure
P_{Ar} – argon pressure
P_{N2} – nitrogen pressure
P_{SF6} – sulfur hexafluoride pressure
P_{RI} – iodide pressure
E_{out} – output laser energy
C_2 – discharge bank capacitance
V – capacitor bank voltage
E_{el} - energy stored in capacitor bank
$\tau_{1/2}$ – pulse duration
τ_{del} – delay time between discharge and lasing start
ε - specific energy (E_{out} / 52 cm^3)
I – intensity of singlet oxygen luminescence
($\eta = I / P_{O2}$)- relative yield

3.1. Oxygen pressure.

Experimental conditions:
C_2 = 13.6 nF
V = 18 kV
E_{el} = 4.4 J
Buffer gas – nitrogen, P_{N2} = 9 torr
Iodide – CH_3I, P_{RI} = 0.5 torr
The matrix of experiments is presented in Table 1.

Table1

P_{O2},Torr	E_{out}, mJ	η, arb. u	ε,mJ/cm^3	$\tau_{1/2}$, μs	τ_{del}, μs
0.5	18	30	0.15	10.6	5
1.0	33	25	0.63	11.3	5
1.6	42	23	0.81	10.8	5
2.0	47	22	0.9	12.6	5
3.0	40	20	0.76	9	4

One can see the variation of oxygen pressure results practically in only variation of the output energy value. Pulse duration and time delay remains constant within the limit of error (about 1 μs, the thickness of the oscilloscope beam) (Fig. 5). It means the iodide concentration remains constant for all oxygen pressures. Thus the energy deposition into active medium is governed mainly by buffer gas that pressure is in excess of that for oxygen.

Unlike the theoretical predictions the output energy doesn't increase linearly with oxygen pressure but has a maximum (Fig. 6). The reason of such a behavior is a drop of singlet oxygen yield when oxygen pressure increases. Such a drop is critical for sparger type singlet oxygen generator, and it practically negligible for jet one (at least within the pressure range investigated). Thus one can expect an appreciable increase of output energy working with jet SOG instead of sparger one. In this case the improvement of laser performance is due to increase of both the oxygen operation pressure and singlet oxygen yield. In our experiments the yield value doesn't exceed 40 % at pumping capacity 80 l / s

Nevertheless, the value 0.9 J / l of specific energy obtained is at a slight disadvantage in relation to longitudinal discharge. At the same time the pulse duration is much shorter. Note, the visual observation of discharge shows its nonuniformity. Thus one can expect the increasing of specific energy under improvement of discharge uniformity.

3.2. Sort and partial pressure of iodide.

Experimental conditions:

C_2 = 13.6 nF
V = 18 kV
E_{el} = 4.4 J
P_{O2} = 1.0 torr
Buffer gas – nitrogen, P_{N2} = 9 torr
The matrix of experiments is presented in Table 2

Table 2

P_{RI}, torr	E_{out}, mJ	$\tau_{1/2}$, μs	τ_{del}, μs	[I], 10^{14} cm^{-3}	[I] / [RI]
CH_3I					
0.2	28	16	9	8	0.12
0.4	36	12	5	10.6	0.08
0.6	37	9	4	14	0.07
0.7	37	9	4	14	0.06
CF_3I					
0.2	18	17	9	7.5	0.12
0.4	24	13	5	10	0.08
0.6	29	9	4	14	0.07
0.8	29	8	3	16	0.06
1.0	30	7,5	3	17	0.05
1.5	33	7	2	18	0.04

Low saturation pressure of CH_3I vapor limited the range of P_{RI} variation.

The results obtained show the both iodides produce iodine atoms with the same effectiveness. It results in practically identical time parameters of laser pulses obtained at the equal iodide pressures (Fig.7). The value of iodine atom concentration [I] and ratio of this value to the corresponding iodide molecules one is presented in the Table 2 too. The latter is a level of iodide dissociation. The iodine atom concentrations were evaluated from equation (2) using experimental data on pulse duration. Note that iodine atom concentration of 1.8×10^{15} cm^{-3} is close to the highest value reported for COIL operation of both CW and pulsed modes.

Thus, the increase in iodide partial pressure is a fruitful way to shorten the pulse duration. When laser operates much over threshold the output energy changes slightly (Fig. 8).

Like that for the case of photoinitiation the output energy depends in the same manner on the sort of iodide used. The CH_3I appears to be more effective iodine donor (Fig.8). It was shown /6/ that the cause of such a difference is a fast quenching of singlet oxygen by RO_2 molecules (R is a radical CH_3 or CF_3) formed after iodide dissociation But in the case of discharge the output energies obtained for these two iodides differ by only 15 % against that of about 50 % for photolysis. It can be a result of more short pulse duration.

One can see the level of dissociation drops when iodide concentration increases. As soon as iodide molecules dissociate in a process of dissociative attachment the drop of dissociation level can be result of deficit of electrons in active medium. This deficit can be eliminated due to higher voltage or discharge energy. Indeed, this effect was observed (see below).

3.3. Voltage and bank capacitance.

Experimental conditions:

P_{O2} = 1.0 torr

Buffer gas – nitrogen, P_{N2} = 9 torr

Iodide – CF_3I, P_{RI} =1.5 torr

The matrix of experiments is presented in Table 3

Table 3.

U,kV	E_{el}, J	E_{out}, mJ	$\tau_{1/2}$, μs	τ_{del}, μs	[I], 10^{14} cm^{-3}	Cost, eV
C_2 = 6.8 nF						
10	0.68	19		-	-	
10	0.68	20		-	-	
15	1.53	28		-	-	
18	2.20	34	10	5	13	203
C_2 = 20.4 nF						
10	2.04	29	8	2	16	153
15	4.59	28	7	2	18	306
18	6.60	29	6.5	2	20	396
C_2 = 3.4 nF						
10	0.34	1.2	-	24	-	
15	0.76	13	17	8	7	130
18	1.10	17	16	5	8	162
C_2 = 13.6 nF						
10	1.36	28	10	4	13	125
15	3.06	31	7.5	2.5	17	216
18	4.40	33	7	2.5	18	293

The variation of voltage at constant bank capacitance results in only variation of stored energy while, besides that, variation of C_2 changes the matching of discharge to circuit. In our case this effect is not so important. It seems the range of variation of voltage and capacitance investigated is too small to understand what parameter of discharge circuit is a critical one. The results obtained show the stored energy is a critical factor governing the value of output energy and time parameters within the range investigated.

The values of energy cost of iodine atom presented in Table 3 seem to be very large. These values are relative one. The real values of energy cost can be obtained if energy deposition into active medium is known. In its turn energy deposition is determined as a product of discharge current by voltage drop across the discharge gap. The apparatus to measure these parameters is now under manufacturing.

It was mentioned above the shortening of laser pulse can be obtained due to iodide pressure increase as well as to discharge energy increase. Indeed, one can see, the shortest pulse duration of 6.5 μs (Fig.9) was obtained at iodide pressure 1.5 torr and 6.6 J of energy store in capacitor bank.

3.4. Buffer gas.

Experimental conditions:

C_2 = 13.6 nF
P_{O2} =1.0 torr
Iodide – CH_3I, P_{RI} =0.5 torr
The matrix of experiments is presented in Table 4

Table4

P_{buffer}, torr	V, kV	E_{el}	E_{out}, mJ	$\tau_{1/2}$, μs	τ_{del}, μs
He					
3.0	10	1.36	2.5	-	-
3.0	15	3.06	8.6	-	-
3.0	18	4.40	12	-	-
5.0	10	1.36	8.6	27	17
5.0	15	3.06	17	16	9
5.0	18	4.40	19	15	7
9.0	10	1.36	20	24	9
9.0	15	3.06	27	17	6
9.0	18	4.40	29	16	5
Ar					
3.0	10	1.36	6.1	-	-
3.0	15	3.06	9.8	-	-
3.0	18	4.40	12	-	-
5.0	10	1.36	9.2	-	-
5.0	15	3.06	15	-	-
5.0	18	4.40	15	-	-
9.0	10	1.36	13	18	8
9.0	15	3.06	16	14	6
9.0	18	4.40	14		
N_2					
3.0	10	1.36	5.5	-	-
3.0	15	3.06	11	19	10
3.0	18	4.40	13	16	8
5.0	10	1.36	12	23	11
5.0	15	3.06	18	17	6
5.0	18	4.40	21	14	6
9.0	10	1.36	24	18	7
9.0	15	3.06	27	12	4
9.0	18	4.40	27	11	4
SF_6					
3.0	10	1.36	13	24	12
3.0	15	3.06	18	-	-
3.0	18	4.40	18	-	-
5.0	10	1.36	22	20	9
5.0	15	3.06	22	-	8
5.0	18	4.40	22	11	6
7.0	10	1.37	26	17	7

Unlike that for pulsed COIL with photolysis the role of buffer gas in a discharge initiated laser is more complex. In this case buffer gas not only increases the heat capacity of active medium but change the parameters of discharge plasma. In particular, the increase of operation pressure due to buffer gas make it possible to increase the discharge resistance and thus improve the energy deposition into active medium. Indeed, one can see from table 4, the higher buffer gas pressure results in shortening of both pulse duration and time delay. As it was shown above, both these effects are governed by mainly iodine atom concentration in active medium.

The efficiency of buffer gas depends on its sort. Fig10 demonstrates the dependence of output energy on buffer gas partial pressure for V = 15 kV. One can see the buffer gas heat capacity is not the only parameter governing the laser performance. Indeed, helium and argon having the same heat capacity result in different output energy. It is positive that cheap nitrogen is not at a disadvantage in relation to expensive helium.

The high efficiency of SF_6 seems to be very promising. It is known that SF_6 dissociates in a discharge, forming free fluorine atoms F. Thus one has opportunity to use chemical generation of iodine atoms. When HI or DI is used as an iodine atom donor free fluorine atoms can react with iodide forming free iodine atoms /7/.

$$F + HI(DI) \rightarrow I + HF(DF) \qquad (3)$$

Thus, high concentration of iodine atoms can be obtained due to increase of SF_6 partial pressure instead of iodide one. Besides, this way allows one to reduce the expenses for laser operation.

Unfortunately, our facility didn't allowed us to increase SF_6 pressure over 7 torr. Because of insufficient conductivity of our pipe line and high SF_6 viscosity the input pressure over 1 atm was required to provide necessary SF_6 flowrate. But this high pressure blocked the chlorine flow driven by atmospheric pressure pressing the chlorine bag.

.4. Conclusion.

Investigation of the pulsed COIL with volume generation of iodine atoms using a transverse DC discharge was performed. The influence of oxygen pressure, iodide sort and pressure, discharge energy, sort and pressure of buffer gas on the output energy and time parameters of the laser pulse was studied. The aim of investigation was to search for the ways making it possible to generate a laser pulse as powerful as possible. It was shown the increase of oxygen pressure and singlet oxygen yield resulted in output energy growth at conserved pulse duration. At the same time increase of both iodide concentration and discharge energy resulted in growth of iodine atom concentration and thus in shortening of the pulse duration. The pulse duration of 6.5 μs is reported. This value corresponds to the iodine atom concentration close to the highest one reported for the COIL of both CW and pulsed type.

Following this way one can produce the iodine atom concentration close to that of singlet oxygen. In this case the significant fraction of energy is stored in iodine atoms. If Q-modulation method is applied this energy can be extracted in a form of nanosecond scale pulse.

Specific energy of 0.9 J / l, that is close to that obtained with longitudinal discharge, and specific power of 75 kW / l was obtained. The ways to increase these values were proposed.

Hexafluoride was shown to be a very promising buffer gas. Having rather high heat capacity this gas generates fluorine atoms when exposed to discharge. Thus, application of this buffer gas make it possible to use chemical generation of iodine atoms via reaction of fluorine atoms with HI or DI used as iodine donor.

References

1. Yuryshev N.N. "Chemically Pumped Oxygen-Iodine Laser", Quantum electronics, **26(7),** pp 567-584 (1996).
2. Highland R, Crowell P and Hager G, Proc. SPIE Int, Soc. Opt. Eng. **1225** 512 (1990)
3. Frolov M, Ishkov D, Kryukov P, Pazyuk V, Podmar'kov Yu, Vagin N and Yuryshev N, Proc. SPIE Int, Soc. Opt. Eng. **2502** 291 (1995)
4. Vagin N, Pazyuk V and Yuryshev N. Quantum Electronics **25**(8) 746 (1995).
5. Apollonov V.V., Firsov K.N., Kazantsev S.Yu. and Oreshkin V.F., Proc. SPIE Int, Soc. Opt. Eng. **3574** 374 (1998)
6. Yuryshev N. Proc. SPIE Int, Soc. Opt. Eng. **139** 221 (1991).
7. Jiraser J, Spalek O. and Kodymova J "Kinetic and Thermodinamic Aspects of Chemical Generation Chemical Generation of Atomic iIodine for a COIL and their Consequences for Experiments", Proc. Of COIL R&D Workshop, 11 – 12 Oct. 1999.

Part 5

The study of production iodine atoms from CH_3I in RF discharge.

The volume production of iodine atoms using transverse RF discharge in the mixture of a iodide (RI) with singlet oxygen is very attractive method for creation active medium for the Q-switched COIL. The existing RF power supply with the next output parameters has been modified for realization such possibility:

CW power	1.5 kW,
frequency	16MHz,
CW maximal voltage	8.5 kV,
pulse duration	variable,
pulse repetition frequency	1kHz

Peak pulse power at pulse duration about 10 μs exceeded CW power in several times only.

The major problem of this investigation consists in the determination of the iodide dissociation efficiency. There are two methods:

1) to use COIL lasing;
2) to use probe laser for the measurement iodine atom concentration.

The first method means the work in the dark conditions without any information about iodine atom concentration, if lasing is absent. Second method can't be used at the conditions of the pulse repetition mode of the supersonic COIL. Requested pulse duration is $\tau \le 0.1 L_{gain}/U_{gas} \approx 10$ μs because the period of the probe laser frequency scanning $T_{scan} =$ 40ms $>> \tau$. Taking into account these circumstances the efficiency of iodine atoms generation is studied at CW mode of RF discharge and subsonic flow. Conditions of the subsonic flow give possibility to increase the interaction of gas with plasma of RF discharge and to reach more higher iodine concentration from one hand and to use smaller iodide flow rates at the requested iodide partial pressures. The typical portion of the dissociated iodide in the **axial flow** pulse repetition COIL with DC discharge equal to approximately (1÷3)% because iodide and chlorine flow rates are close with each other. This means that the obtaining the requested iodide partial pressure in the subsonic mode operation is possible at significantly less iodide molar flow rate than at supersonic mode. The special discharge chamber has been manufactured. The electrodes with square 6×6 cm have been manufactured from the glass plastic with copper cover. The thickness of the glass plastic plates was 1.5mm. The distance between these the glass plastic plates equal to 30 mm. The Plexiglas nozzles' blades with thickness 5 mm were inserted in the discharge chamber forming the gap of

20mm. The nitrogen and then argon were used as carriers iodide molecules. At first the nitrogen molar flow rate was 20 mmole/s, iodide flow rate (CH_3J) – 4.3 mmole/sec, the static pressure in the discharge chamber without discharge was 3.2 torr and increased up to 3.4÷3.9 torr when the discharge was switched in. The current, voltage and the phase shift between its were measured . The input power in the gap was calculated and was changed in the limits 150W ÷ 1500W but we could not say exactly what portion of this power is power input in the gas flow because the resistance of plastic glass plates and nozzle's blades is unknown. The voltage was varied from 2 to 8.2 kV. The discharge was homogeneous. The probe laser beam was used for determination of the iodine atoms' absorption which appeared at input power more 250 W. The probe laser beam was located in the center of discharge chamber. The absorption value had weak dependence on the input power in the limits (250 ÷ 1500) W and was $2\alpha L$=(0.35 ÷0.5)% although the line width changed from 250MHz to 285 MHz. At increasing twice nitrogen flow rates and static pressure in the discharge gap the absorption value equaled to 0,4% at maximal possible input power. The typical best absorption lines are presented in fig.1÷fig.4 and experimental conditions - in the Table 1. The change nitrogen on argon at the same flow rate resulted in the decreasing of the absorption value. The maximal absorption 0.3% was reached in one run only. The reached maximal iodide dissociation efficiency is one order of magnitude less than the requested one for successful COIL operation. It's worth nothing that the discharge gap constitutes close to reactive load and the phase shift between voltage and current differs from 90° on small value. It means bad impedance match power supply and load. It's necessary to develop the special RF power supply with high peak pulse power and small impedance. Decreasing the static pressure and increasing voltage for raising discharge parameter (E/P_{cavity}) had not sense because low static pressure has not interest but large voltage is very danger at real COIL operation conditions when BHP aerosol may provide the conductivity the duct walls. The further investigation of this method for production of iodine atoms were stopped.

Table1

M_{CH3I}, mmole/s	M_{N2}, mmole/s	P_{cavity}, torr	U, kV	I, A	W_{disch}, W	α, %/cm
4.3	20	3.4	5.5	2	525	0.0437
4.3	20	3.4	5.9	2.5	840	0.0494
4.3	39	6.56	4.6	2.5	1350	0.0405
4.3	40	6.6	4.6	2.5	1500	0.04

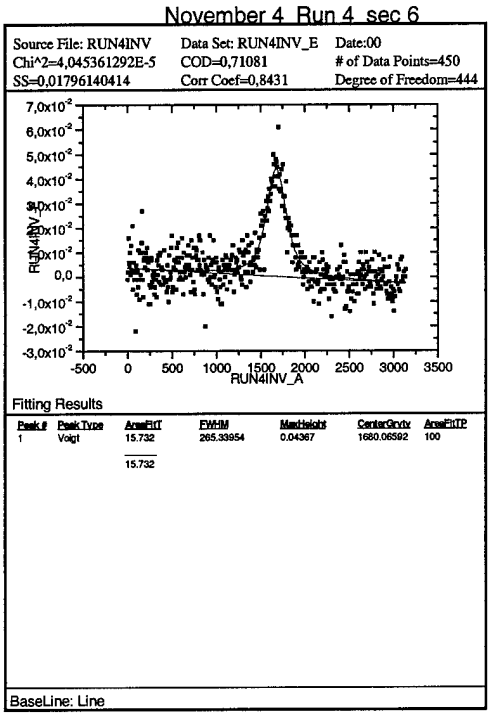
November 4 Run 4 sec 6
Source File: RUN4INV
Data Set: RUN4INV_E
Date:00
Chi^2=4,045361292E-5
COD=0,71081
# of Data Points=450
SS=0,01796140414
Corr Coef=0,8431
Degree of Freedom=444
RUN4INV_A
Fitting Results
Peak # Peak Type AreaFitT FWHM MaxHeight CenterGrvty AreaFitTP
1 Voigt 15.732 265.33954 0.04367 1680.06592 100
15.732
BaseLine: Line

Fig.1

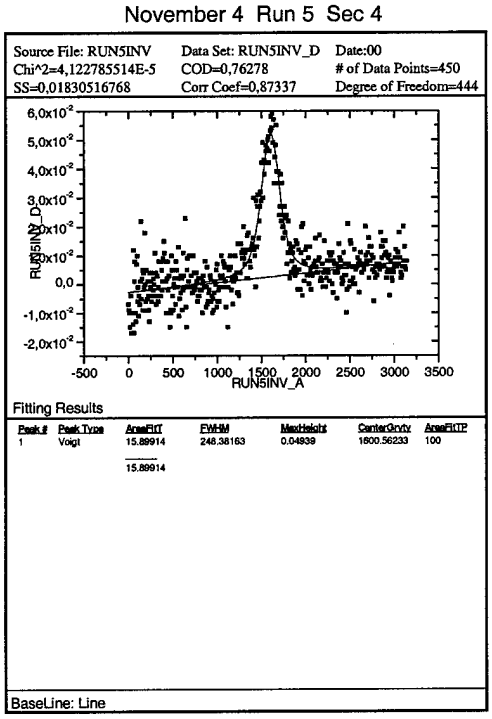
November 4 Run 5 Sec 4
Source File: RUN5INV
Data Set: RUN5INV_D
Date:00
Chi^2=4,122785514E-5
COD=0,76278
# of Data Points=450
SS=0,01830516768
Corr Coef=0,87337
Degree of Freedom=444
RUN5INV_A
Fitting Results
Peak # Peak Type AreaFitT FWHM MaxHeight CenterGrvty AreaFitTP
1 Voigt 15.89914 248.38163 0.04939 1800.56233 100
15.89914
BaseLine: Line

Fig. 2

November 4 Run 8 Sec 8

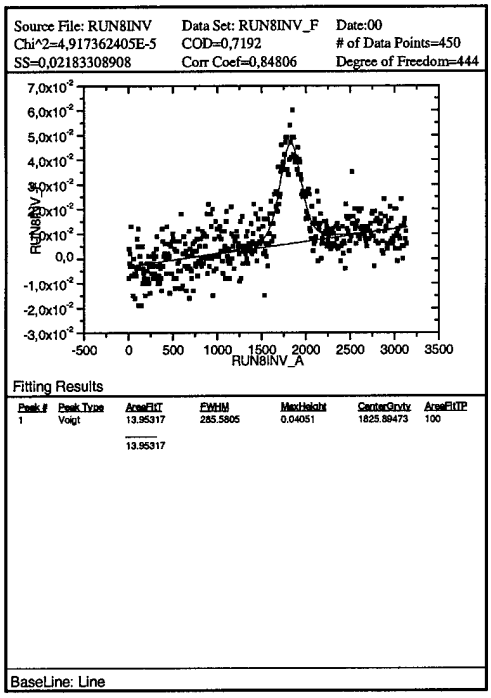

Fig.3

November 4 Run 9 sec 8

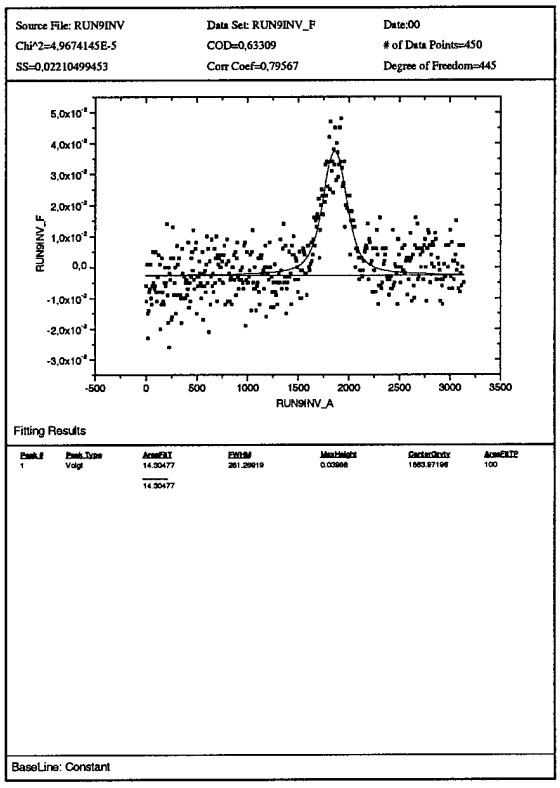

Fig. 4

Part 2.

An efficient supersonic COIL with more than 200 torr of the total pressure in the active medium.

Abstract

The new nozzle concept was suggested and tested for chemical oxygen-iodine laser (COIL). The nozzle bank consists of the array of cylindrical nozzles for pure N_2 flow, slit nozzles for $O_2(^1\Delta)$ flow. The N_2+I_2 jets are injected into turbulent wakes between oxygen and N_2 streams through small cylindrical orifices. The LIF was used for the visualization of the iodine mixing efficiency in the mixing chamber. It was found practically uniform distribution of iodine molecules in the supersonic flow on the distance about 60 mm downstream nozzle bank. The COIL experiments were performed with this nozzle bank and at 5 cm gain length COIL cavity. The output power 700 W or chemical efficiency 19.7% have been achieved for the chlorine molar flow rate 39.2 mmole/s. Simultaneously the static pressure 10.9 torr in laser cavity and pressure 100 torr in Pitot tube have been achieved. The estimated Mach number of the flow was equaled to 2.6 and total pressure in the laser cavity was equaled to 218 torr. High dilution of the oxygen by nitrogen 1:11 results in small growth of the stagnation temperature of the gas flow and creates good conditions for the pressure recovery in the diffuser.

P_1- pressure in reactor
P_2- in the mixing chamber (plenum pressure),
P_3static pressure in the cavity,
P_4 -pressure in iodine measurement cell,
P_5 -total pressure in Pitot tube
P_6 -pressure in the vacuum duct downstream cavity
P_{I2}- iodine partial pressure in the measuring cell
G_c - chlorine molar flow rate,
G_{NP} -primary nitrogen molar flow rate,
G_{NS} -secondary nitrogen molar flow rate,
G_{I2}- iodine molar flow rate,
G_{NM}-the total nitrogen molar flow rate through mirrors tunnels (purging)
T_1 - the transmission of the output mirror,
T_2 - transmission of the second mirror.
W_1- laser power from output mirror
W- total laser power
η_c-chemical efficiency
M- Mach number of the flow from ratio $\frac{P_5}{P_3} = \frac{166.7M^7}{\left(7M^2-1\right)^{2.5}}$

2. 1. Introduction

The increase of the stagnation pressure of the gas flow in the cavity of gas-dynamic and chemical lasers is very important for efficient exhaust of the laser gas into atmosphere [1]. The increase of the stagnation pressure should not accompanied with essential decreasing of the power and efficiency of the laser system. This problem is specific for COIL due to relatively low pressure in the singlet oxygen generator. The stagnation pressure in the Verti-COIL laser system with rotating disk SOG [2] has been increased up to 100 torr using high dilution (1:6) oxygen by helium. However high gas density in the reaction zone promotes the initiation of instabilities of the BHP film on the disks and entrainment of BHP aerosol because this method has restricted possibility for reaching high recovery pressure. The new ejector method of preparing of the COIL active medium has been suggested in [3,4]. The nozzle bank consists of conical nozzles for N_2+I_2 flow and slit or cylindrical nozzles for $O_2(^1\Delta)$ flow. The conical nozzles generate supersonic N_2+I_2 jets but slit or cylindrical nozzles generate $O_2(^1\Delta)$ sonic jets with moderate static pressure (10 torr). If the total momentum N_2+I_2 jets is much more than the momentum of oxygen jets then the full pressure of completely mixed stream will be determined mainly by N_2+I_2 flow. This scheme keeps the inner contradictions yet. Indeed, the reaching of high full pressure requests generating the N_2+I_2 flow with large supersonic velocity in the nozzles with high expansion ratio. Iodine vapor

condensation inside nozzles may take place at high expansion ratio. This contradiction may be eliminated by using nozzles with low expansion for N_2+I_2 flow and installation of additional supersonic nozzles to generate supersonic flow of pure nitrogen with high stagnation pressure. Thus the new nozzle bank consists of array of three types nozzles to inject gases into the mixing chamber and the laser cavity. The jet type SOG can produce oxygen at pressures up to 100 torr with high $O_2(^1\Delta)$ yield and chlorine utilization [5]. Using it provides good conditions to obtain supersonic flow with high stagnation pressure in COIL. The main goals of present investigation were the study of gasdynamic parameters of the gas flow, mixing efficiency and efficiency of lasing in COIL with new advanced nozzle bank.

2.2 The experimental set-up

The new nozzle bank consists of 7 parallel slits 15 mm in height and 2.5 mm in width for injection of oxygen (gas containing the stored energy) from the JSOG. The flow of pure N_2 (primary) at high pressure (gas providing major momentum) flows out from 56 cylindrical nozzles located in 8 rows. The diameter of nozzle is 1 mm. The I_2 (gas containing gain particles) with carrier secondary N_2 gas flows out from holes drilled in 14 nickel tubes located between oxygen and nitrogen nozzles. The number of holes in each nickel tube is 15 and the diameter of holes is 0.5 mm. The fragment of the new nozzle bank is presented in Fig.1.

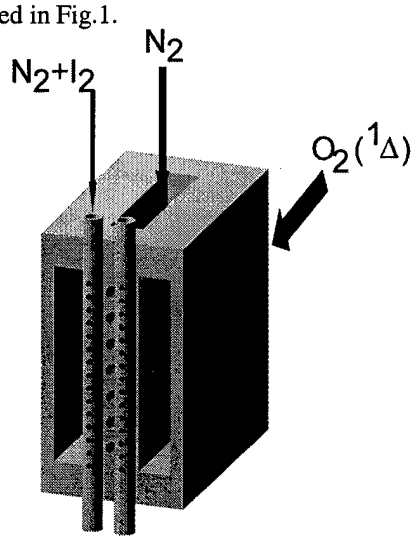

Fig.1. The fragment of nozzle bank.

The experimental COIL set-up is presented in Fig.2. The free gas jets from each array of nozzles expand and mix in the mixing chamber with initial cross section 50×15 mm^2. The angle between wide walls of mixing chamber and direction of flow can be varied from 0° to 2°. In COIL experiments this nozzle bank was connected to the Verti-JSOG earlier used for energy supply of COIL with slit nozzle [6]. This Verti-JSOG is described in Part 1 of present report in detail. The mixing chamber and laser cavity were manufactured from Plexiglas. Therefore it was possible to observe a picture of the bright yellow emission from the iodine dissociation zone. In the presented COIL design the minimal distance of 64mm between optical axis and nozzle bank can be made. The longer distance was not limited. The laser cavity was the same as in COIL experiments with slit nozzle [6,7]. The pumping out of active medium through the cavity is made by mechanical pump with capacity 125 L/s. To create high volume pump rate in the cavity during short time (~10 s) the vacuum receiver 4 m^3 is opened on. The next pressures were measured during COIL run: the pressure in JSOG P_1, the plenum pressure P_2 upstream oxygen nozzles, static pressure in the cavity P_3, pressure in the Pitot tube P_5 at the exit cross section of the cavity. The Mach number of gas flow in the cavity was estimated from ratio: $\frac{P_5}{P_3} = \frac{166.7M^7}{\left(7M^2-1\right)^{2.5}}$. The full (stagnation) pressure was estimated from the wellknown formula $P^*=(1+0.2M^2)^{3.5}P_3$. The output power was assumed to be equal to $W=W_1(T_1+T_2)/T_1$, where W_1 is the measured output power through the mirror with highest transmission T_1.

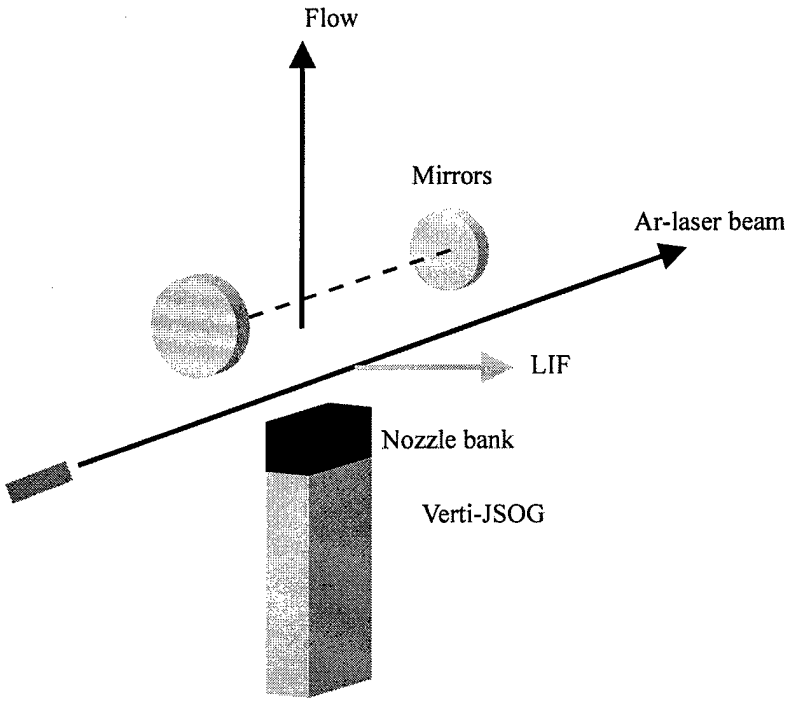

Fig.2. The experimental set-up.

2. 3 The cold tests of the new nozzle bank.

The first stage of the study new nozzle bank for supersonic COIL consists in determination gas flow conditions in the laser cavity for nominal gas flow rates. The angle between the walls of the mixing chamber and the flow direction was 2°. The experiment was performed with 40 mmole/s of the air flow rate through the oxygen nozzles. The plenum pressure (upstream of nozzles for oxygen) was equal to 17 torr for zero both primary and secondary nitrogen flow rates through the nozzle bank. But the plenum pressure increased up to 27 torr for 500 mmole/s of primary nitrogen and zero secondary nitrogen. Simultaneously the static pressure P_3 in the cavity on the distance of 64 mm downstream nozzle bank and pressure P_5 in Pitot tube located 90 mm downstream nozzle bank were equal to 8 torr and 87 torr accordingly. The estimated Mach number M of the gas flow in the laser cavity was equaled approximately to 2.7. The additional flow of the secondary nitrogen of 11 mmole/s resulted in 9.3 torr static pressure in cavity and 92 torr pressure in Pitiot tube. Then the additional nitrogen flow of 15 mmole/s through each mirror tunnel resulted in 10.4 torr static pressure in cavity and 111 torr pressure in Pitot tube. The rise of the plenum pressure from 17 torr to 27 torr when the primary nitrogen flow rate increases from 0 to 500 mmole/s is explained by choking of air flow by primary nitrogen streams. The small purging nitrogen flow through the mirrors' tunnels compresses gas stream, increases significantly static and Pitot pressures. These cold experiments demonstrated that the nozzle bank with the simple geometry of nozzles could generate the supersonic gas flow in the cavity.

2.4 The observation and study of the mixing iodine jets downstream the new nozzle bank.

The second stage of the study of the new nozzle bank consists in the qualitative observation of iodine distribution of iodine molecules in the mixing chamber. The main goal was to observe at what distance from the nozzle bank the distribution of the iodine molecules was approximately uniform in the direction of optical axis. The LIF method was used to observe the efficiency of mixing iodine I_2 with two other streams. In this method the green light near 5145A from Ar-laser excites the iodine molecules from $X^1\Sigma$ state to $B^3\Pi$ state and then excited iodine molecules emit the yellow light [7]. This LIF visualizes the iodine molecules distribution in the gas flow. In these experiments the special mixing chamber with windows for Ar-laser beam and observation of LIF was installed. The angle between walls and gas flow direction was 0°. It was possible to observe LIF of iodine molecules at distance 25 mm and more downstream from nozzle bank. The Ar-laser beam (5145A) 3mm in diameter was directed across the gas flow and was centered in the middle between walls of the mixing chamber. The LIF fluorescence was observed in direction perpendicularly to the Ar-laser beam and gas flow direction. It was possible to move Ar-laser beam position relatively to the nozzle bank. The LIF picture was recorded by Kodak film in dark conditions with optical filter to remove scattering radiation from Ar -laser beam.

Several LIF experiments were performed for the gas flow conditions in mixing chamber similar to conditions of COIL operation. The nitrogen gas was used instead of oxygen $O_2(^1\Delta)$ in LIF experiments. The molar flow rate of nitrogen through oxygen slits was varied from 40 to 75 mmole/s, primary nitrogen molar flow rate was varied from 200 to 400 mmole/s, and secondary nitrogen molar flow rate was varied from 20 to 40 mmole/s.. In these ranges of gases

molar flow rates the Mach number of the flow varied from 1.7 to 2 and static pressure of flow varied from 10 to 20 torr. The results of the visualization LIF of I_2 are presented in Fig.3. This particular experiment was performed for molar flow rate of nitrogen through oxygen slits 75 mmole/s, primary nitrogen molar flow rate 400 mmole/s, secondary nitrogen molar flow rate 40 mmole/s.. The intensity of LIF was approximately uniform for distance 62 mm for all gas flow conditions tested in experiments. The high difference in the gas velocities of flows resulted in high efficient mixing of the all gas components. So it was expected highly efficient mixing of O_2 flow from JSOG with N_2 and N_2+I_2 flows in COIL experiments.

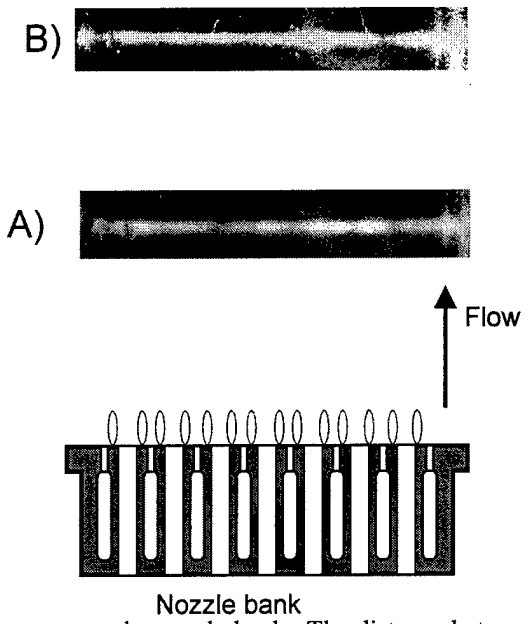

Fig.3. LIF of iodine molecules downstream the nozzle bank.. The distance between nozzle bank and Ar-laser beam 37 mm (A) and 62 mm (B).

2.5 COIL experiments.

The COIL set-up with the new nozzle bank is presented in Fig.2. The Verti-JSOG was described in details in Part 1 of present report and in [6]. The $O_2(^1\Delta)$ was transported from Verti - JSOG through rectangular duct with 10*50mm^2 cross section. The duct height increased up to 15 mm on small distance before the nozzle bank. The length of the duct between generator and nozzle bank was 30 mm. The initial cross section of the mixing duct was 15*50 mm^2. The experiments have been made for two expanding angles of the mixing duct wide walls (θ=1°and 2°) and for two distances between the optical axis and nozzle bank (L=64mm and 89 mm).

θ=1°, L=89 mm. LIF experiments have showed good mixing at this distance. The height of the mixing duct was 18 mm at this position of the optical axis. The chlorine flow rate through Verti-JSOG was 39.2 mmole/s, the primary nitrogen flow rate through cylindrical nozzles was 400mmole/s, the secondary nitrogen (carrier of I_2) flow rate through the nickel tubes was 40mmole/s, the total nitrogen flow rate through mirrors' tunnels was 20 mmole/s.. It was found that the pressure in the cavity was equal to 20 torr, in the Pitot tube was equal to 96 torr and the estimated Mach number of gas flow in cavity was close to 1.8 for iodine molar flow rate 0.6 mmole/s.

The output power was equal to 350 W (9.8% efficiency) only for mirrors with transmittances T_1=0.8%, T_2=0%. The attempts to increase the iodine molar flow rate resulted in the subsonic flow mode in the cavity. We explain that by large thickness of the boundary layers on the walls and by the heat release in the gas flow. The angle between wide walls and the flow direction was increased up to 2° for diminishing of the boundary layers' influence.

θ=2°, L=89 mm. The height of the channel was 22 mm at this position of the optical axis. The gas flow conditions were the same as in previous case. The results obtained for these conditions are presented in Table 1 and in Fig. 4÷6. The first run was the check of the gas flow conditions in the laser cavity for zero iodine molar flow rate. The optimal iodine molar flow rate was found in 2-6 runs with not good quality mirrors. The new mirrors with different transmissions were installed in 7-12 runs for obtaining the Rigrod curve.

Table 1

Run	P_1, Torr	P_2, torr	P_3, torr	P_5, torr	M	G_{I2}, mmole/s	T_1, %	T_2, %	Power, W	η_c, %
1	35.3	28.5	7.8	97	3.05	0	0	0	0	0
2	37.4	28.3	8.7	94	2.85	0.41	0.8	0.014	122	3.43
3	35.8	28.8	8	95	2.97	0.4	0.8	0.014	36.	1.03
4	35.9	28.9	9.12	86	2.65	0.51	0.8	0.014	335	9.45
5	36.1	29.2	10.3	84.3	2.45	0.67	0.8	0.014	372	10.4
6	37.3	30	10.6	84.8	2.42	0.76	0.8	0.014	317	8.93
7	41.1	35.2	11.9	81	2.2	0.68	0.94	0	603	17
8	38.4	31.6	11.2	80	2.27	0.70	1.3	0	570	16.0
9	37.8	31.5	11.5	78	2.21	0.71	4.8	0	0	0
10	38	31.6	11.4	78	2.22	0.73	0.7	0.7	400	11.2
11	38.7	31.4	11.2	78	2.24	0.74	1.7	0.94	416	11.7
12	37.7	31.5	11.2	78	2.24	0.71	1.7	1.7	36	1.0

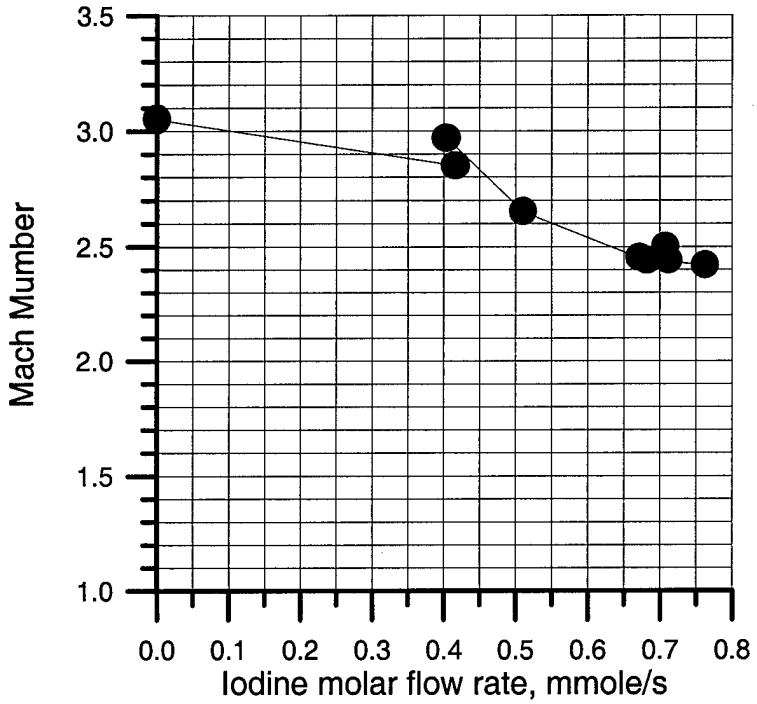

Fig.4. The dependence of the Mach number on the iodine molar flow rate

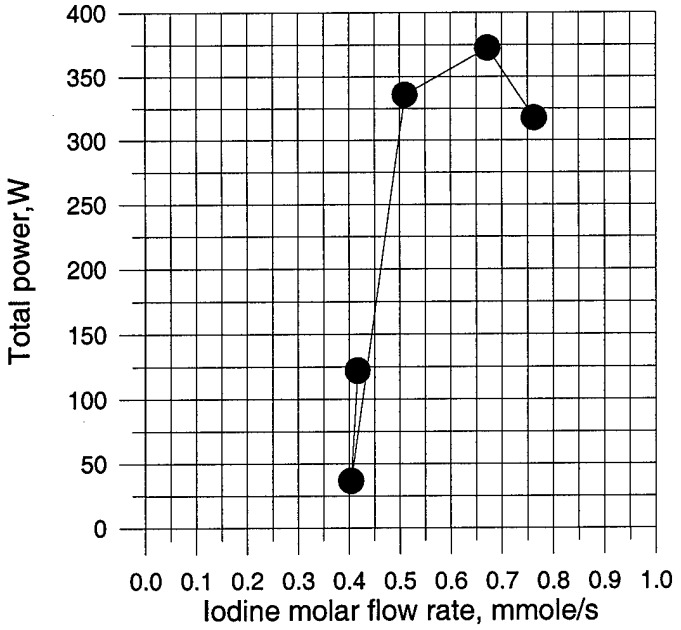

Fig.5. The dependence of the power on the iodine molar flow rate.

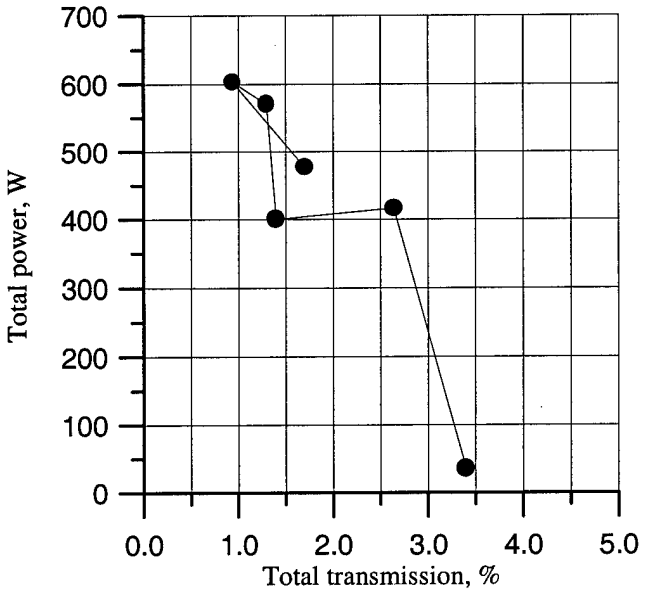

Fig.6 . The dependence of the output power on the total mirror transmission . Iodine molar flow rate is close to 0.7mmole/s.

The optimal iodine molar flow rate close to 0.7 mmole/s has been found. The maximum power 603 W (17% chemical efficiency) was achieved with mirrors T_1=0.94%, T_2=0%. Video recoder of the green-yellow emission in the mixing chamber in the laser experiments indicated that the bright yellow emmision is completed on the distances 5÷6 cm downstream from the nozzle bank. The length of bright yellow emission is close to the length of iodine dissociation along gas flow. The estimation of absolute gas velocity gives value approximately 550 m/s (Mach number 2.2). It means that time of iodine dissociation was near 100μs. Thus LIF experiments and laser experiments with L=89 mm demonstrated fast dissociation and mixing of iodine in COIL with new nozzle bank.

θ=2°, L=64 mm. It was evident to place optical axis at closer distance from nozzle bank to decrease $O_2(^1\Delta)$ quenching losses. The experimental results for the new optical axis position are presented in Table 2 and in Fig. 7 and Fig 8. The full (stagnation) pressure of the gas flow in cavity was calculated as $P^*=(1+0.2M^2)^{3.5}P_3$. The optimal molar flow rate close to 0.8mmole/s have been found.

Table 2.

Run	P_1, torr	P_2, torr	P_3, torr	P_5, torr	M	P^*	G_{I2} mmole/s	T_1, %	T_2, %	Power, W	η_c %
1	39.5	33	11.2	101	2,57	211	0.73	0.94	0.18	643	18.1
2	39.4	32.5	10.9	100	2,6	218	0.74	0.94	0.18	700	19.7
3	39	32.5	11.3	100	2,55	210	0.85	0.94	0.18	657	18.5
4	39.4	32.6	11	101	2,6	220	0.68	0.94	0.18	673	18.9
5	38.9	32.4	10.9	102	2,62	227	0.65	0.94	0.18	660	18.6
6	39	32.4	10.7	102	2,62	214	0.54	0.94	0.18	604	17.
7	39.7	32.9	11.4	100	2,5	200	0.74	0.94	0	598	16.8
8	39.3	32.5	11.4	101	2,5	200	0.75	1.3	0	563	15.8
9	39.3	32.7	11.4	102	2,55	207	0.75	1.7	0	565	15.9
10	39.7	32.6	11.3	103	2,55	205	0.78	4.8	0	0	0
11	39.8	33	11.3	102	2,55	205	0.76	1	0	618	17.4
12	39.8	33	11.4	102	2,55	207	0.77	1.7	0.94	489	13.7
13	40.2	33	11.3	103	2,55	205	0.77	1.7	1.3	405	11.4
14	39.7	32.9	11.1	101	2,55	204	0.76	1.7	1.7	0	0
15	39.6	32.8	9.47	98.3	2,9	300	0	0	0	0	0

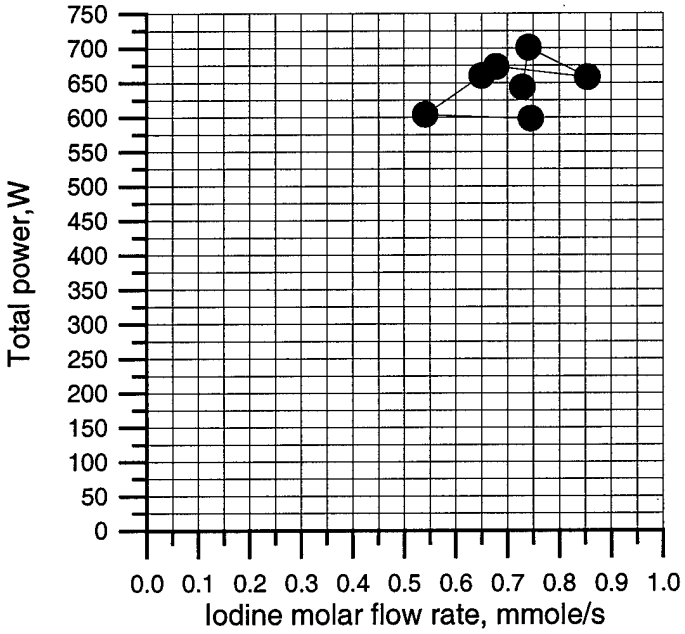

Fig.7. The dependence of output power on the iodine molar flow rate.

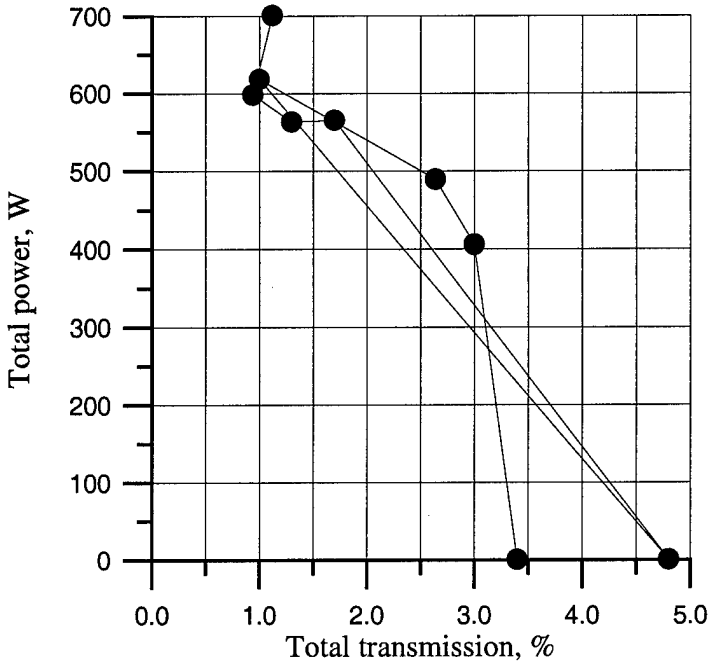

Fig.8. The dependence of the output power on the mirror transmission. The iodine molar flow rate is close to 0.77mmole/s.

Thus the displacment of the optical axis closer to nozzle block gave possibility to increase output power to 700W and chemical efficiency to 19.7% and to achieve the total pressure more than 200 torr.

2. 6. Conclusions.

The new nozzle bank for preparing of active medium for supersonic COIL was design and tested. New nozzle bank consists of three types array of nozzles: the first array of the slit nozzles for energy $O_2(^1\Delta)$ flow, second array of rake type nozzles for I_2+N_2 flow and third array of cylindrical nozzles for N_2 flow with high velocity head. All nozzles have simple geometry without special profiles. The preliminary "cold" experiments demonstrated high Mach number of supersonic flow formed by new nozzle bank. The LIF experiments demonstrated fast and efficient mixing of three flows at gas conditions close to those which realize at COIL operation. The observation of bright yellow emission from iodine dissociation zone during COIL operation demonstrated also the fast iodine dissociation in the supersonic flow. The primary nitrogen flow provides formation of the active medium with stagnation pressure in the cavity more 200 torr and recovery pressure about 100 torr.

The output power 700 W and the chemical efficiency 19.7% have been achieved in COIL with the new nozzle bank. This power was obtained at the static pressure in the cavity equal to 10.9 torr, Mach number 2.6, Pitot pressure 100torr. The full pressure of the gas flow in the cavity was estimated as 218 torr.

High stagnation pressure and high dilution oxygen by nitrogen 1:11.5 creates good conditions for diffuser operation. At present gas flow conditions the total gas flow rate in the cavity was 0.5 mole/s or 9100liter*torr/s at room temperature. Let's assume that downstream the laser cavity the supersonic diffuser is installed and recovery pressure equal to the pressure obtained in Pitot tube (100 torr). In this case one obtains estimation of the vacuum pump rate with the Q=9100liter*torr/s /100torr=91 liter/sec for successful COIL operation. It's correspondent to specific power (per unit of the pumping capacity) W/Q=700 W/91 liter/s = 7.7 J/liter. New method of the preparing of the COIL active medium allows to obtain simultaneously the high stretched gain zone and large value of the specific power. The recovery pressure 100 torr and more gives possibility to use for the exhaust gas the water sealed pump only (one pump step without liquid nitrogen trap).

Problems and solutions. The designed pressure in JSOG is P_1=30 torr for 39.2 mmole/s of chlorine. But the choking of oxygen flow by primary nitrogen resulted in higher pressure of oxygen in JSOG P_1=40. It is necessary to decrease the pressure P1 down to 30 torr to increase $O_2(^1\Delta)$ yield and chemical efficiency of COIL. There are two way: to design new JSOG for existing nozzle bank or to design new nozzle bank for existing JSOG.

References

1. Handbook of chemical lasers. Ed. By R.W.F.Gross, J.F. Bott, 1976, John Wiley&Sons, Inc.

2. T.L. Rittenhouse, S.P. Phipps, C.A. Helms, K.A. Truesdell,» High Efficiency Operation of a 5 cm Gain Length Supersonic Chemical Oxygen-Iodine Laser»,Proc. SPIE, **2702**, 333 -, 1996

3. V.D. Nikolaev, "Comparative analysis of the different methods of preparing active medium in supersonic COIL", SPIE Proceedings Vol. 3268, pp.157-162

4. M.V.Zagidullin, V.D.Nikolaev, M.I.Svistun, V.S.Safonof, N.I.Ufimtsev , N.A.Khvatov , «The study of buffer gas mixing with active gas on chemical oxygen-iodine laser performance with jet type SOG», *Proc.SPIE*, 1996, vol. 2702, pp.310-319.

5. V.N.Azyazov, M.V.Zagidullin, V.D.Nikolaev, M.I.Svistun, N.A.Khvatov, «Jet $O_2(^1\Delta)$ generator with oxygen pressure up to 13,3 kpa», *Quantun Electronics,* Vol.24, pp.120-123, Feb. 1994

6. V.D. Nikolaev, M.V. Zagidullin, "Completely Scaleable 1kW Class COIL with Verti-JSOG and Nitrogen buffer Gasses", AIAA 99-3815

7. N.L.Rapagnani, S.J.Davis. Laser-induced I_2fluorescence measurements in a chemical laser flowfield. AIAA Journal, vol. 17, N.12, pp. 1402-1404, 1979.

PART 3
The results of iodine gain line scanning in COIL with slit nozzle and new nozzle bank.

Abstract

The probe diode laser was used to scan the gain line of iodine atom in supersonic flows of COILs with slit nozzle and new nozzle bank.

P_1- pressure in reactor
P_2- in the mixing chamber (plenum pressure),
P_3-static pressure in the cavity,
P_4 -pressure in iodine measurement cell,
P_5 -total pressure in Pitot tube
P_6 -pressure in the vacuum duct downstream cavity
P_{I2}- iodine partial pressure in the measuring cell
G_c - chlorine molar flow rate,
G_{NP} -primary nitrogen molar flow rate,
G_{NS} -secondary nitrogen molar flow rate,
G_{I2}- iodine molar flow rate,
G_{NM}-the total nitrogen molar flow rate through mirrors tunnels (purging)
T_1 - the transmission of the output mirror,
T_2 - transmission of the second mirror.
W_1- laser power from output mirror
W- total laser power
η_c-chemical efficiency
M- Mach number of the flow from ratio $\frac{P_5}{P_3} = \frac{166.7M^7}{\left(7M^2-1\right)^{2.5}}$

3.1. Introduction.

The operation of COIL with slit nozzle having two throats was described in Part 1 of present report. The operation of COIL with new nozzle bank (ejector scheme) was described in Part 2 of the present report. All these results with laser power optimization were obtained in the spring and summer of 1999. The results of gain scanning were obtained in November - December of 1999. Before stating of gain measurements several modifications of COIL set-up were made. The analysis of experimental result obtained in the first half of 1999 forced us to make several changes. It seemed to us that these changes of set-up would improve the operation of COIL. First of all the absorption length in iodine measuring cell was made 5 cm. It allowed us to measure more precisely iodine molar flow rate at higher level. But the new design of this cell resulted to increase of the nitrogen pressure in the measuring cell in comparison with old design at the same secondary nitrogen molar flow rate. It is necessary to take into account when one will compare the value of P_4. Another important modification was made in laser cavity duct. The geometry of the cavity in experiments of first half of 1999 was like this:

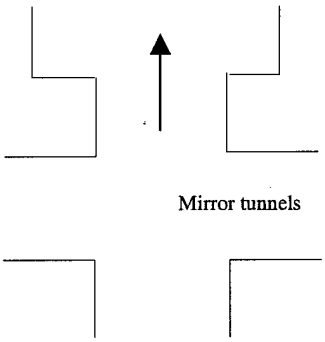

The width of inlet to cavity and outlet were 50 mm. It was due to limited pump capacity of our pump system. Usually the pressure in the vacuum tube downstream cavity was higher than the static pressure in the cavity. If we would increase the width of the outlet then the higher pressure from the vacuum tube penetrates into cavity through boundary layer. But the edges of the stream in the cavity strike about corners of outlet and some portion of the active medium blows into mirrors' tunnels where singlet oxygen is quenched and may generate the resonance absorption. Now the angles of outlet were smoothed to prevent the indicated blow and geometry of laser duct at present looks like:

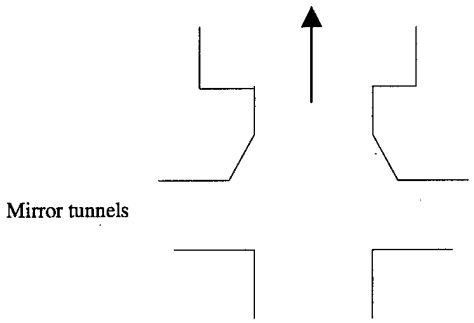

This modification of cavity was made to decrease effect of mirror purging gas on main gas flow also. Unfortunately it was impossible to increase the width of outlet from cavity because the pump rate was not enough to obtain supersonic flow in cavity with wider outlet.

3.2. The gain and temperature of active medium of the COIL with slit nozzle having two throats.

The results of COIL operation with slit nozzle having two nozzles were described in Part 1 of present report. The experimental set-up was the same like in COIL experiments instead of cavity modification described in 3.1. The probe laser beam double passed through the active medium (the total gain length was 10 cm). The experimental set-up of gain measurements is presented in fig.1. The optical axis was located 55 mm downstream from the throat of slit nozzle. The height of cavity was equal to 19 mm at the position of optical axis. The values of G_{NP}, G_{NS}, G_{NM} were close to the values early used for COIL experiments with slit nozzle. First of all the gain was measured in the point of optical axis as a function of iodine molar flow rate. The next parameters of scanning were installed: number of gain line scans per second was 25, averaging of the gain line each 0.5 sec. The example of the gain line scanning presented in Fig.2.

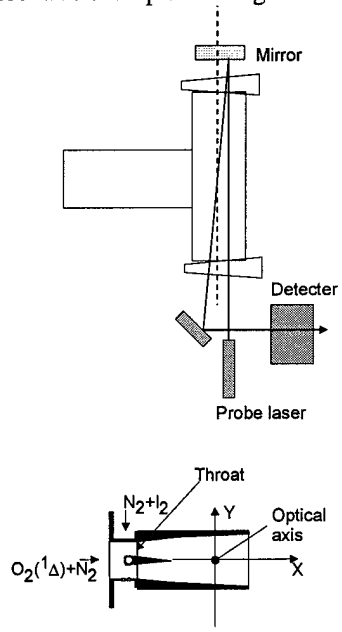

Fig.1.

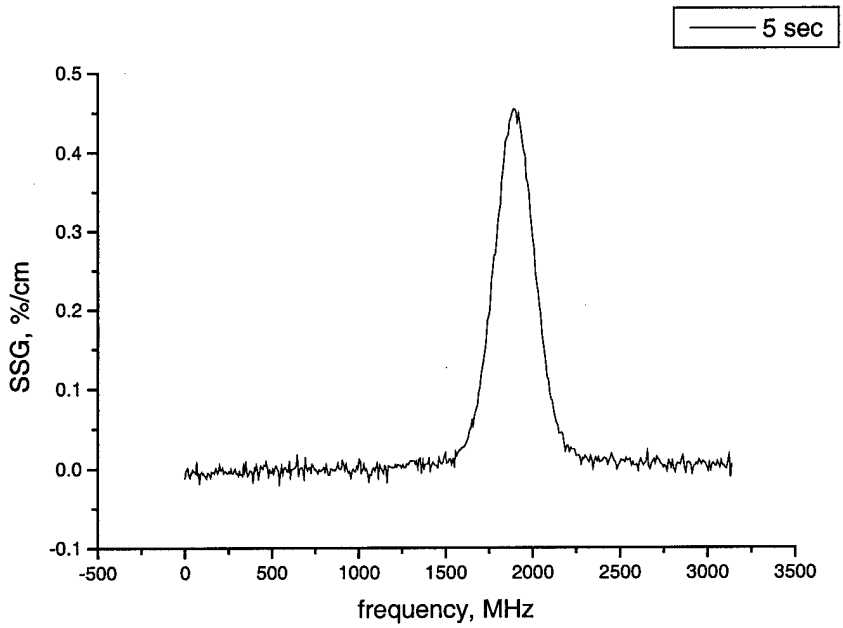

Fig.2. The gain line profile. (5 sec Table 1).

Several words about fitting of data by Foight function. The probe laser line was assumed to be δ-function, base line was cubic. The results of fitting: area A, Lorenz WL and Gauss WG widths were assumed the final parameters. The gas temperature was calculated as $T=(WG/14.49)^2$, the population inversion was calculated as

$$\Delta N(cm^{-3}) = 8\pi\left(\frac{12}{7}\right)\frac{A}{A_{34}\lambda^2} = 4.88\times10^{12}\times A(MHZ\times\%/cm)$$

The time dependence of gain and temperature is presented in Table 1. (the time resolution of Run N.4 in Table 3).

Table 1.

Time,s	Pick gain, %/cm	WG, MHZ	T, K	WL,MHz	A(MHz×(%/cm)	ΔN (cm^{-3})
2.5	-1.1	273	355	125.7	-470	-2.3×10^{15}
3	0.384	235	263	53.5	117.8	5.75×10^{14}
3.5	0.482	239	272	42.8	144	7×10^{14}
4	0.47	245	286	33.6	139	6.78×10^{14}
4.5	0.46	235	263	47	138	6.73×10^{14}
5	0.45	238	270	47	135	6.59×10^{14}
5.5	0.44	246	288	31	130	6.34×10^{14}
6	0.44	235	263	54	135	6.59×10^{14}
6.5	0.46	223	237	77	148	7.22×10^{14}
7	0.42	235	263	52	127	6.2×10^{14}

The chlorine stated to feed JSOG and COIL near 2.5 s and only mechanical vacuum pump worked, then between 2.5 and 3 s the vacuum receiver was opened and high vacuum pump rate realized, after 7 s the chlorine flow was switched off. The gain line for time 5 s is presented in Fig.2. The absorption at t=2.5 s is due to subsonic gas flow in the cavity, high temperature and possibly absorption in the mirrors' tunnels. The large absolute value of population density is due to the high static pressure in subsonic mode. The SSG decreases slowly on time. We explain this by generation of water vapor from BHP aerosols carrying out from JSOG.

3.2.1. The SSG and temperature as vs. on gas flow conditions. Probe laser beam located in the optical axis position (X=0, Y=0)

The dependence of pick gain and gas temperature on iodine molar flow rate on the optical axis (X=0, Y=0) are presented in Table 2 and Fig.3, Fig.4.. The gas temperature is correlated with estimated Mach number of gas flow: for higher M the temperature is lower. Higher iodine molar flow G_{I2}>0.85 mmole/s rate resulted in subsonic gas flow in cavity and negative gain.

Table 2. Here t_s is the time interval from the moment of vacuum receiver opening.

Run	G_c	G_{NP}	G_{NS}	P_1	P_2	P_3	P_5	G_{I2}	SSG,%/cm	WG, MHz	T,K	WL	M	t,s
1	68	130	68	58.7	37.2	6.05	28	0.666	0.316	218	226	50	1.77	2.5
2	68	123	60	54.5	34	6.4	26.8	0.628	0.431	222	235	54.3	1.67	2.5
3	68	130	60	55.1	33.4	6.7	26.1	0.713	0.504	219	228	62.3	1.65	2.5
4	68	123	60	55.7	36.4	7.3	25.2	0.807	0.564	230	252	55	1.52	2.5
5	39.2	72	40	30.6	20	4.54	14.2	0.615	0.54	235	263	36	1.42	2.5
6	39.2	72	40	31.4	20.8	4.65	14.5	0.749	0.6	227	245	51.6	1.38	2.5
7	39.2	72	40	31.8	21.7	3.5	14.5	0.484	0.141	194	179	69	1.65	2.5
8	39.2	72	40	31	21.7	3.5	14.6	0.478	0.113	210	210	58	1.68	3
9	39.2	72	40	32	21.8	3.8	14.2	0.544	0.277	218	226	56	1.57	2.5
10	39.2	72	40	31.6	20.1	4.15	13	0.606	0.387	224	239	50	1.43	2.5
11	39.2	72	40	31	20	4.55	13	0.678	0.551	229	250	50	1.34	2.5
12	39.2	72	40	31.7	20.8	4.87	13.5	0.758	0.631	229	250	49.7	1.34	2.5

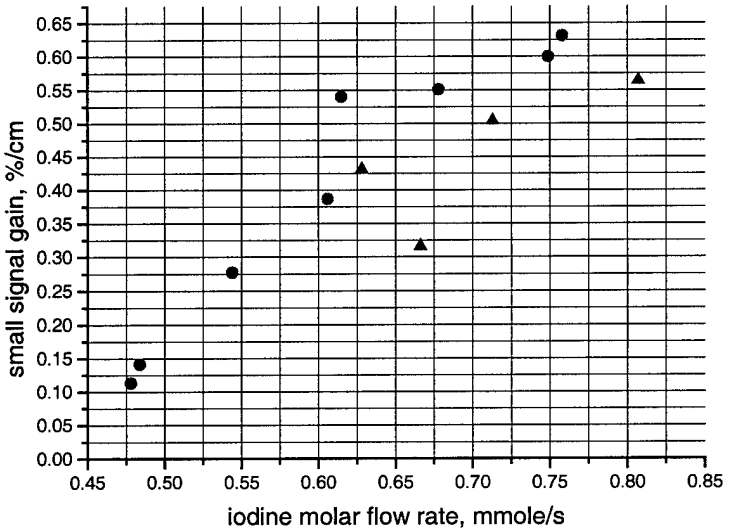

Fig.3. The dependence of SSG on iodine molar flow rate. Black tiangle for 68 mmole/s of Cl_2 molar flow rate (runs 1-4), red circle for 39.2 mmole/s of Cl_2 molar flow rate (runs 5-12).

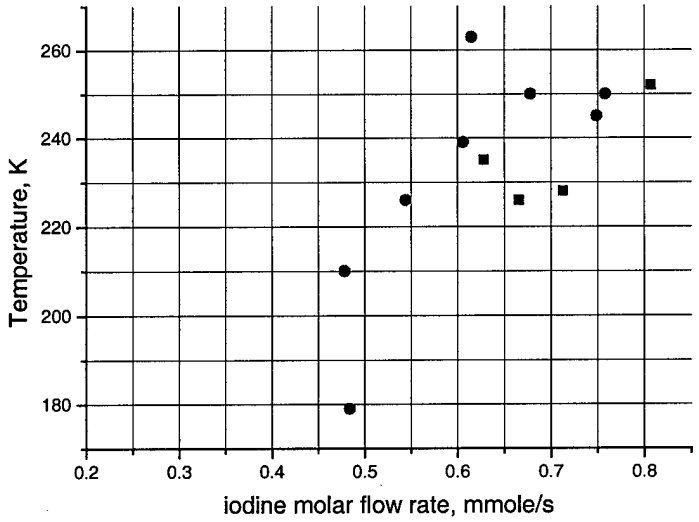

Fig.4. The dependence of temperature on iodine molar flow rate. Black tiangle for 68 mmole/s of Cl_2 molar flow rate (runs 1-4), red circle for 39.2 mmole/s of Cl_2 molar flow rate (runs 5-12).

3.1.2. The dependence of SSG and temperature on the position of the probe laser beam relatively to optical axis.

The dependence of SSG and temperature on position of probe beam relative optical axis is presented in Table 3 and Fig.5, Fig.6. The iodine molar flow rate in these runs was in the range G_{I2}=0.6÷0.7 mmole/s. This fluctuation of iodine molar flow rate resulted in additional scatter of values in Fig.5 and Fig.6. The SSG increases with increasing of distance X from the throat of slit nozzle. Thus dissociation of iodine is not complete at distances less than 55 from the throat of the nozzle. The point X=0, Y=0 is located in the wake from the central blade of slit nozzle. It's possible also that active medium in the turbulent wake with low SSG mixes with gas flow from stream core with higher SSG and as result SSG increases with raise X.

Table 3.

Run	G_c	G_{NP}	G_{NS}	P_1	P_2	P_3	P_5	G_{I2}	X, mm	Y, mm	SSG, %/cm	WG, MHz	T,K	WL	M	t,s
1	39.2	72	40	31	20	4.55	13	0.678	0	0	0.551	229	250	50	1.37	2.5
2	39.2	72	40	31.5	21.1	4.54	12.7	0.677	10	0	0.553	224	239	50.4	1.35	2.5
3	39.2	72	40	31.8	21.4	4.7	13.1	0.702	20	0	0.567	222	235	54.4	1.35	2.5
4	39.2	72	40	31.8	21.3	4.62	12.9	0.677	-10	0	0.447	238	270	46.7	1.35	2.5
5	39.2	72	40	32.7	22.5	4.69	12.8	0.67	-20	0	0.447	236	265	41	1.35	2.5
6	68	123	60	55.4	33.3	6.8	25	0.614	10	0	0.457	221	233	61	1.57	2.5
7	68	123	60	55.4	33.8	7.1	24.6	0.633	18	0	0.504	218	226	64.7	1.52	2.5
8	68	123	60	56.2	34.8	6.7	25.2	0.603	0	0	0.449	215	220	60	1.57	2.5
9	68	123	60	56.2	34	6.8	25.1	0.6	-10	0	0.389	212	214	77	1.57	2.5
10	68	123	60	56.4	35.1	6.7	25.6	0.608	-10	0	0.353	211	212	75	1.6	2.5
11	68	123	60	59.1	38.5	6.7	25.7	0.594	-20	0	0.197	209	208	73	1.61	2.5
12	68	123	60	60	38.4	6.7	25.8	0.606	-20	0	0.217	190	172	88	1.62	2.5
13	68	123	60	57.8	35.5	7	25.2	0.586	0	7	0.615	212	214	72	1.55	2.5
14	68	123	60	58.2	36	6.5	26.2	0.619	10	7	0.539	213	216	64	1.65	2.5
15	68	123	60	58.5	36.3	6.8	26.3	0.608	-10	7	0.416	214	218	48	1.63	3

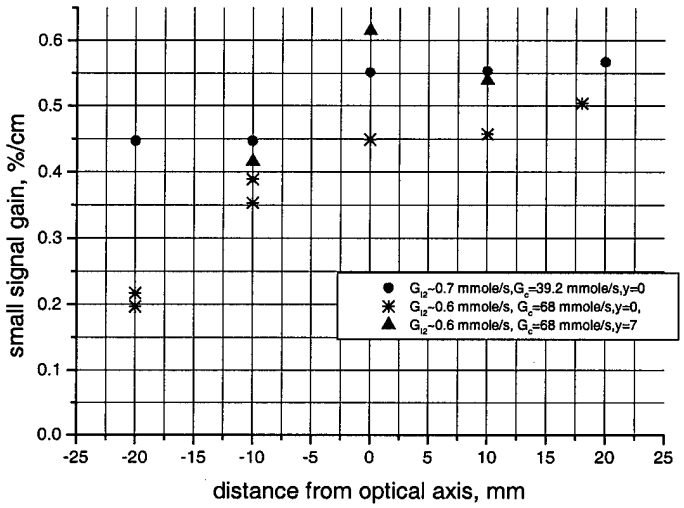

Fig.5. The dependence of SSG on the position of probe laser beam relative to optical axis. The point X=0,Y=7 mm located in the kernel of flow from one throat.

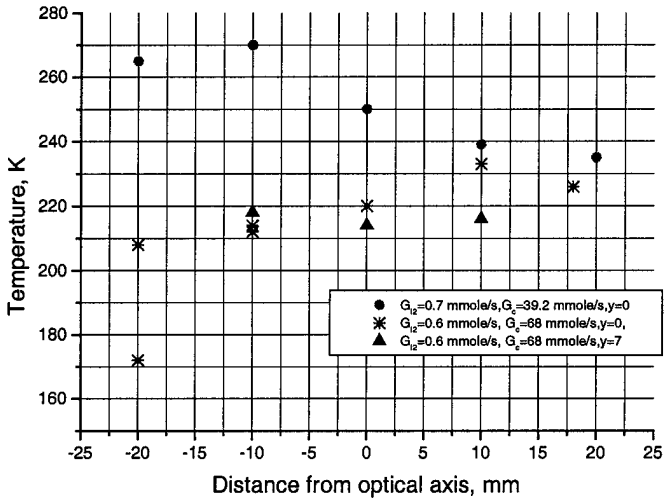

Fig. 6. The dependence of temperature on position X of the probe laser beam relative optical axis.

3.3. The gain and temperature of active medium of the COIL with new advanced nozzle bank

3.3.1 The SSG and temperature of gas flow as vs. on gas flow conditions . Probe laser beam located in the optical axis position (X=0, Y=0).

The experimental set-up was similar to set-up in 3.2 but new nozzle bank described in Part 2 was installed in COIL. The optical axis was located on 64 mm downstream from nozzle bank.

The results of gain and temperature measurements for X=0, Y=0 are presented in Table 4 and Fig.7,8. The Mach number of the flow in the cavity was much higher than for the slit nozzle system. The static temperature of gas flow was lower than for slit nozzle system also. The Pitot pressure $P_5 \approx 90$ torr was less than 100 torr pressure obtained in the laser experiments (Part 2). We believe that it was due modification of outlet of the laser cavity and decreasing static pressure in the mirrors' tunnels and in the cavity. The pressure broadening WL is approximately in two times more than for slit nozzle system. First of all it is due to higher static pressure in the cavity and lower temperature. The pressure broadening is inverse proportional to temperature WL(T)=WL(300K)(300/T) [1].

Table 4.

Run	G_c	G_{NP}	G_{NS}	G_{NM}	P_1	P_2	P_3	P_4	P_5	G_{I2}	SSG, %/cm	WG, MHz	T,K	WL, MHz	M	t,s
1	39.2	410	11	11	36.6	30.7	9.5	70	87.4	0.63	0.49	190	172	103	2.65	3
2	39.2	410	11	11	37	31	9.5	68.2	88.6	0.55	0.48	200	191	95	2.65	3
3	39.2	410	11	11	37	31	9.4	65.6	86	0.50	0.43	199	189	80	2.6	3
4	39.2	410	11	11	37	31	9.7	71	85	0.70	0.53	192	176	101	2.5	2.5
5	39.2	410	11	11	37.4	31	9.9	77.4	86	0.72	0.56	199	189	94	2.55	3
6	39.2	410	11	11	40	33.6	9	83.3	88	0.42	0.41	192	175	106	2.7	2.5
7	39.2	410	11	11	40.4	33.9	9.1	84	88	0.46	0.43	203	196	85	2.7	2.5
8	39.2	410	30	11	40.1	33	9.4	157	90	0.57	0.35	200	191	95	2.65	2.5
9	39.2	410	30	11	40	33.1	9.56	156	87	0.66	0.42	189	170	114	2.6	2.5
10	39.2	410	30	11	40	33.6	9.66	159	87	0.76	0.45	192	175	115	2.55	2.5
11	39.2	410	30	11	40.6	34	9.9	159	84	0.85	0.48	199	188	108	2.45	2.5
12	39.2	410	42	11	36.9	30.8	9.1	216	95	0.58	0.29	182	158	113	2.75	2.5
13	39.2	410	42	11	37.3	31	9.9	226	81	0.76	0.39	191	174	112	2.45	2.5
14	39.2	410	42	11	34.2	31.2	9.7	222	86	0.66	0.37	184	161	119	2.5	2.5
15	39.2	410	42	11	39.7	33	10.2	212	85	0.87	0.5	198	186	114	2.45	2.5
16	39.2	410	42	11	40.5	33	10.1	210	87	0.82	0.46	207	204	93	2.5	2.5
17	39.2	410	55	11	39.4	33	9.8	240	90	0.77	0.38	196	183	100	2.54	2.5
18	39.2	410	55	11	39.8	33.1	9.9	240	91	0.66	0.35	205	200	97	2.54	2.5
19	39.2	410	55	11	40	33.4	10.3	240	91	0.82	0.40	201	192	103	2.54	2.5
20	39.2	410	55	11	39.8	33.6	10.3	240	89	0.93	0.45	190	172	114	2.5	2.5

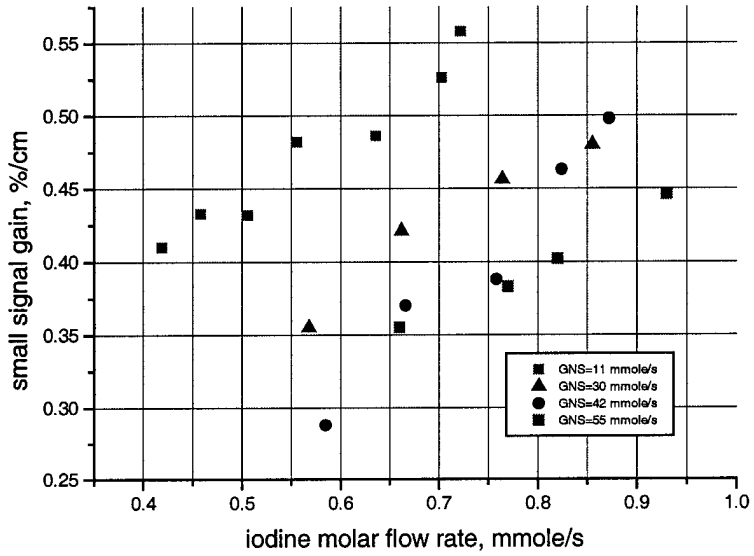

Fig.7. The dependence of SSG on iodine and secondary nitrogen molar flow rate.

Higher G_{NS} forces to increase iodine molar flow rate to achieve the same value of SSG for smaller G_{NS}. Let's consider SSG for G_{NS}=42 mmole/s and G_{I2}≈0.8 mmole/s. The value of SSG≈0.45 %/cm measured by probe laser is approximately equal to the value estimated from Rigrod curve at the same gas flow conditions (Fig.8 in Part2).

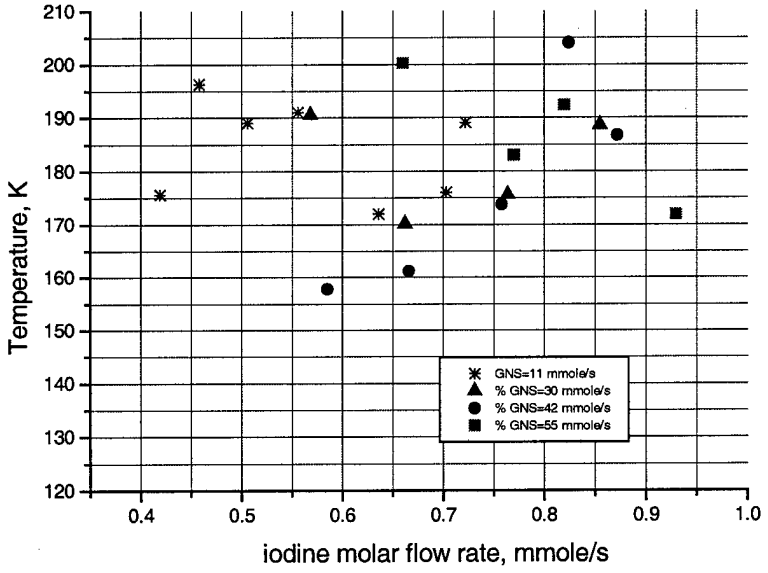

Fig.8. The dependence of gas temperature on iodine and secondary nitrogen molar flow rates.

3.3.2. The dependence of SSG and temperature on the position of probe laser beam relative to optical axis.

In COIL experiments (Part 2) with new advanced nozzle bank the Pitot pressure 100 torr has been achieved at G_{NP}=400mmole/s. The primary nitrogen molar flow rate in these experiments with probe laser was increased up to 500 mmole/s to raise the Pitot pressure up to 100 torr. The results of measurements are presented in Table 5 and Fig.9, Fig.10.

The SSG decreases with increase of distance X from the nozzle bank. The SSG is equal to

$$g\left(cm^{-1}\right)=n_I\sigma\times\frac{(K_{eq}+0.5)Y-0.5}{(K_{eq}-1)Y+1}$$

where σ is efficient cross section, n_I iodine atoms density, Y is $O_2(^1\Delta)$ fraction, $K_{eq}=3/4\exp(402/T)$.
Is it possible to explain such SSG dependence by quenching of $O_2(^1\Delta)$ or decreasing of Y? The quenching of $O_2(^1\Delta)$ is mainly due to quenching of $I(^2P_{1/2})$ by water , I_2 and N_2 (highest fraction in gas flow). The specific time of $O_2(^1\Delta)$ quenching (or decreasing of Y) is approximately

$$\tau^{-1}\approx([H_2O]K_W+[N_2]K_N+[I_2]K_I)\times[I]/[O_2],$$

where $[H_2O]$ is water vapor concentration, $K_W=2\times10^{-12}(T/300)^{0.5}$ cm^3/s, $[N_2]$ - nitrogen concentration, $K_N=6.5\times10^{-17}(T/300)^{0.5}$ cm^3/s, $[I_2]$ molecular iodine concentration, $K_I=3.6\times10^{-11}$ cm^3/s, For pressure 10 torr and gas composition $I_2:H_2O:O_2:N_2=0.02:0.05:1:11$, dissociation efficiency 50% ($[O_2]:[I]=100:2$) and temperature 190K one obtains (quenching by I_2 excluded): $([H_2O]K_W+[N_2]K_N)\times[O_2]/[I]\approx100$ s^{-1}. This value of τ corresponds to the length 500 cm for gas velocity 500 m/s. Thus quenching of I* by H2O and by N2 can't explain fast drop of gain along gas flow. Taking into account 50% of undissociated iodine resulted in estimation $\tau^{-1}\approx([I_2]K_I)\times[I]/[O_2]=200$ s^{-1}. This quenching also can't explain the drop of SSG along the gas flow. Another possible mechanism of $O_2(^1\Delta)$ losses is the recombination of I atoms in the presence of high density of N_2 and reverse dissociation of I_2. In this case the losses of $O_2(^1\Delta)$ is proportional to $[I][I][N_2]$ but can't explain fast drop of gain also. We considered also gasdynamic origin of gain drop that is due to mirror purging gas effect. It compress main flow near the outlet of cavity and efficiently decrease the gain length. But product "active length×[I]" is constant along gas flow. Thus compressing of main flow also can't explain drop of SSG. So at present we have not adequate explanation of SSG drop along gas flow. Possible the measured SSG and temperature dependencies is result of the influence of absorbing gas circulated in the mirror tunnels. It's necessary to repeat these experiments when mirrors tunnels will be removed.

Table 5.

R	G_c	G_{NP}	G_{NS}	G_{NM}	P_1	P_2	P_3	P_4	P_5	G_{I2}	X,mm	Y,mm	SSG,%/cm	WG, MHz	T,K	M	WL, MHz	t,s
1	39.2	500	11	30	40.4	33.8	12.3	72	105	0.76	5	0	0.36	186	165	2.5	153	2.5
2	39.2	500	11	30	39	33.3	12.9	68	111	0.79	0	0	0.45	192	176	2.5	139	2.5
3	39.2	500	11	30	41	35	12.4	67	105	0.81	15	0	0.32	222	235	2.5	116	2.5
4	39.2	500	11	30	39.9	34	12.8	68.4	123	0.81	0	0	0.4	193	177	2.6	135	3
5	39.2	500	11	30	40.4	34	12.3	69	106	0.81	10	0	0.35	207	204	2.5	133	2.5
6	39.2	500	11	30	39.8	33	12.3	68.8	106	0.81	0	0	0.44	193	177	2.5	130	2.5
7	39.2	500	11	30	39.8	33.3	12.4	69.4	104	0.82	0	0	0.42	207	204	2.5	118	2.5
8	39.2	500	11	30	39.3	33	12.4	64.9	117	0.85	-15	0	0.52	195	181	2.6	125	2.5
9	39.2	500	11	30	40.3	34.4	12.1	64.4	108	0.85	0	0	0.51	194	179	2.6	126	2.5
10	39.2	500	11	30	38.3	32.5	12.4	66	111	0.86	0	0	0.44	194	179	2.5	130	2.5
11	39.2	500	11	30	40.1	33.6	12.1	65	114	0.86	-5	0	0.44	196	183	2.6	133	2.5
12	39.2	500	11	30	39.2	33.1	13	65.6	119	0.87	-20	0	0.58	177	149	2.6	157	2.5
13	39.2	500	11	30	39.9	33.3	12.4	63.7	114	0.87	5	0	0.43	194	179	2.6	138	2.5
14	39.2	500	11	30	38.6	32.6	11.9	63	98	0.87	-10	0	0.58	195	181	2.5	118	3
15	39.2	500	11	30	40	33.9	12.6	63.6	117	0.87	20	0	0.37	189	170	2.6	132	2
16	39.2	500	11	30	40.5	34.3	12.7	64.4	118	0.88	20	0	0.26	197	185	2.6	138	3
17	39.2	500	11	30	36	33	12.3	63.4	114	0.88	10	0	0.44	205	200	2.6	125	2.5
18	39.2	500	11	30	39	33	12.4	63.3	119	0.88	-10	0	0.54	180	154	2.6	146	2.5
19	39.2	500	11	30	39.3	33.3	12.7	63.5	116	0.88	20	0	0.37	225	241	2.6	92	3
20	39.2	500	11	30	39.5	33.5	12	64	104	0.89	-20	0	0.58	184	161	2.5	141	2.5
21	39.2	500	11	30	39.5	33.2	12.3	61.3	114	0.89	10	0	0.45	199	189	2.6	136	2.5
22	39.2	500	11	30	38.6	32.8	11.8	63.1	102	0.9	-15	0	0.57	183	160	2.5	135	3
23	39.2	500	11	30	38	32	11.7	61.6	95	0.90	-5	0	0.55	173	143	2.4	154	2.5
24	39.2	500	11	30	40.5	34.5	12.6	62	117	0.90	15	0	0.36	197	185	2.6	142	2.5
25	39.2	500	11	30	39.7	33.5	12.1	61.7	114	0.90	0	0	0.46	200	191	2.6	124	2.5
26	39.2	500	11	30	39.5	33.4	12.4	63	115	0.91	5	0	0.47	198	187	2.6	133	2.5
27	39.2	500	11	30	40	33.7	12.3	61.8	115	0.91	-5	0	0.48	192	176	2.6	135	2.5
28	39.2	500	11	30	39.3	33.2	12.1	64.5	114	0.92	-10	0	0.47	182	158	2.6	150	2.5
29	39.2	500	11	30	39.6	33.4	12.4	61.6	115	0.92	15	0	0.39	190	172	2.6	147	2.5

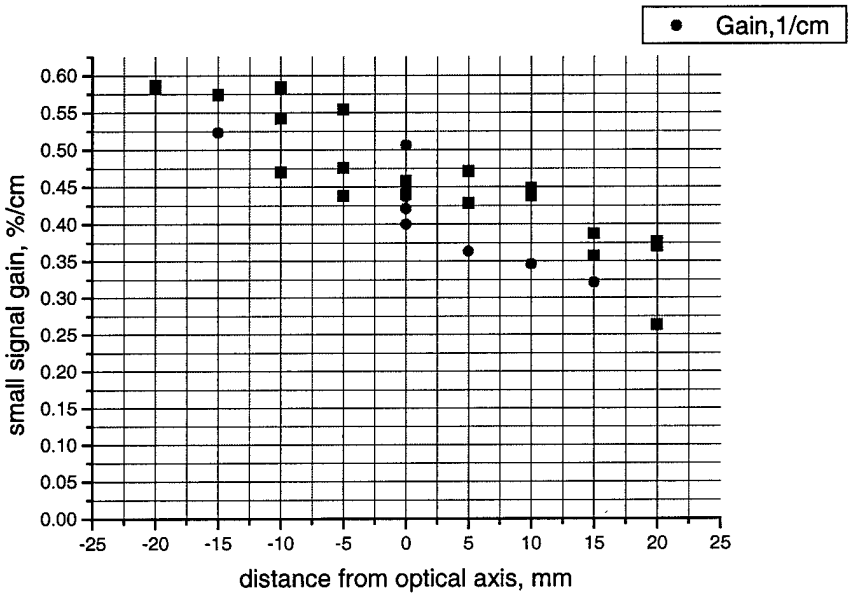

Fig.9. The dependence of SSG on the position of the probe laser beam relative to the optical axis (Y=0). (blue sqaure G_{I2}=0.76÷0.85, red circle-G_{I2}=0.86÷0.92.)

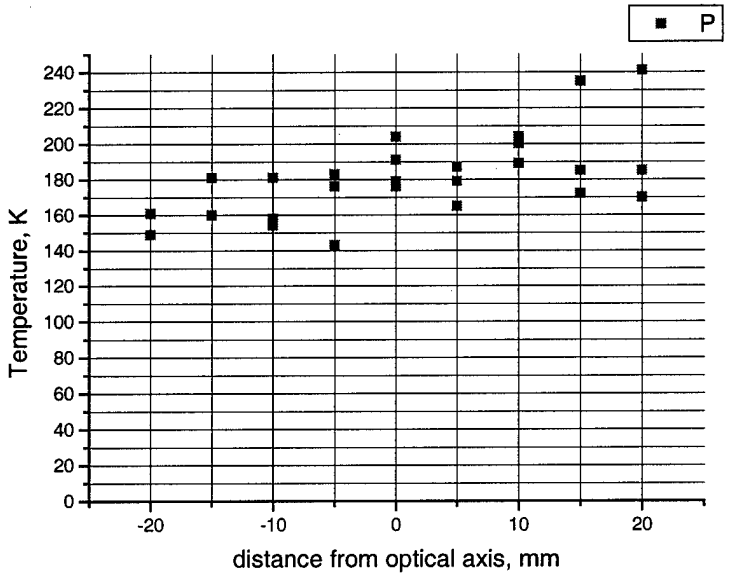

Fig.10. The dependence of gas temperature on the position of probe laser beam (Y=0).

3.3. The special run at subsonic gas flow velocity in the cavity with slit nozzle.

For comparison two special runs with slit nozzle system were performed. The gas flow rates were identical in both runs but in second run the vacuum receiver was not opened. The results of probe laser experiment (X=0, Y=0) are presented in Table 6. In the run 1 the supersonic flow and in run 2 subsonic flow.

Table 6. G_c=39.2 mmole/s, P_1=32 torr, G_{NP}=72 mmole/s, G_{NS}=40 mmole/s, G_{NM}=6 mmole/s

Run	P_2	P_3	P_5	G_{I2}	SSG, %/cm	WG, MHz	T,K	WL, MHz	A (MHz×(%/cm)	ΔN (cm^{-3})	M	t,s
1	20.1	4.15	13	0.60	0.387	224	239	50	111	5.4×10^{14}	1.42	2.5
2	28.8	27	29	0.60	-1.37	291	403	135	626	3.0510^{15}	0.32	2.5

Let's don't take into account the influence of absorption zone in the mirror tunnels in both runs on the measured value of SSG and temperature T. The SSG is equal to

$$g\left(cm^{-1}\right)=n_I\sigma\times\frac{(K_{eq}+0.5)Y-0.5}{(K_{eq}-1)Y+1}$$

In supersonic run SSG>0 and in subsonic run SSG<0. It means that in supersonic run $(Y-Y_{th})>0$ and in subsonic run $(Y-Y_{th})<0$, where $Y_{th}=(1+2K_{eq})^{-1}$. The $O_2(^1\Delta)$ fraction is equal to $Y=Y_0-Y_q-Y_d$, where Y_0 is the initial $O_2(^1\Delta)$ yield, Y_q fraction of $O_2(^1\Delta)$ lost for gas heating (this value include the quenching losses during I_2 dissociation), Y_d is the $O_2(^1\Delta)$ fraction for breaking bond of I_2 molecules ($\approx$2 $O_2(^1\Delta)$ for one I_2).

It is also possible to estimate absolute gas velocities U, threshold $O_2(^1\Delta)$ fraction $Y_{th}=(1+1.5\exp(402/T))^{-1}$ in both cases, flux of population inversion $G_{\Delta N}=\Delta N\times U$. (Table 7). The stagnation temperature is $T^*=T\ (1+0.2M^2)$. The heating of gas is due to quenching of $O_2(^1\Delta)$ (value Y_q). The initial stagnation temperature is estimated as T^*_0=300K for both runs. Thus $Y_q=(T^*-T^*_0)\times3.5*(G_{NP}+G_{NS}+G_c)/G_c/11340$. Here 11340K is $O_2(^1\Delta)$ energy in K and 3.5 is specific heat capacity of N_2 or O_2. In both runs the initial $O_2(^1\Delta)$ fraction was identical Y_0. The Y_d is less than $Y_{dmax}=2[I_2]/[O_2]=2G_{I2}/G_c$. The calculated values in Table 7.

Table 7.

Run	T^*, K	U, m/s	$G_{\Delta N}$(mmole/cm^2/s)	Y_{th}	Y_q	Y_{dmax}	$Y_{th}+Y_q+Y_{dmax}$
1	335	440	0.04	0.11	0.04	0.03	0.18
2	411	129	0.066	0.2	0.09	0.03	0.32

For obtaining absorption in subsonic gas flow the initial $O_2(^1\Delta)$ yield Y_0 should be < 0.32. In this case the available $O_2(^1\Delta)$ fraction in supersonic gas flow is only $Y_0-(Y_{th}+Y_q+Y_{dmax})=0.14$. But COIL lasing experiments (Part 2) demonstrated chemical efficiency >20%. It means that above simple analysis was not correct. This contradiction can be explained by effect of absorption zones in the mirror tunnels. This absorption should be much higher for subsonic gas flow in cavity due to much higher static pressure in cavity. In this case the measured value of SSG is the average value along optical axis. The real absorption length is higher than 5 cm. In the case of supersonic gas flow the absorption zones in the mirror tunnels smaller but also exists.

Thus if one will take into account absorption in mirror tunnels it is possible to explain high measured absorption in subsonic flow conditions. In the case of supersonic flow conditions the real local gain is higher than measured.

We plan to make experiments with probe laser without mirror tunnels. The glass wedge windows will be walls for gas flow in this case.

References

1. R.Engelman, B.A.Palmer. Transition probability and collision broadening of the 1.3 μm transition of atomic iodine. J.Opt.Soc.Am., v.73, N.11, pp. 1585-1589, 1983

Part 4.

Pulsed COIL with a Transverse dc Discharge Generation of Iodine Atoms

1. Introduction

The chemical oxygen – iodine laser (COIL) is currently considered as a promising candidate for specific industrial and other applications. Saying about industrial COIL applications one usually means CW mode of COIL operation. But for some applications the power is a crucial factor. In this case the COIL pulsed mode may be more preferable.

Indeed, the pulse mode of COIL operation allows one to get pulses which power exceeds that for CW mode. In any case the average power remains constant and its value is governed by chemicals flow rate. Such a pulsed COIL can find application working individually as well as in a complex with a CW COIL. The latter can be attractive if an exact coincidence of wavelength is required.

The different approaches are used to get pulse mode of COIL operation. It can be Q-switching or mode – locking methods applied to CW COIL. In these cases the active medium is prepared by mixing of singlet oxygen with molecular iodine. Because of fast relaxation processes it is impossible to form the active medium of significant dimensions. It is easily to show /1/ that the ratio of power of pulse W_{pulse} produced due to methods mentioned above to that of cw mode W_{cw} at the same chemicals flow rate has a limit:

$$W_{pulse} / W_{cw} = K_f \cdot [I] L / v, \qquad (1)$$

where K_f is a rate constant for forward reaction of energy exchange, [I] is a concentration of iodine atoms, L is a laser cavity length in the flow direction and v is a flow velocity. In experiment the maximal value of 16 was obtained /2/.

To generate a pulse of power as high as possible one have to form a large scale active medium with high energy store and then extract the stored energy in time as short as possible. The forming of large-scale active medium requires one to use relatively stable gas mixture at the stage of filling the active volume. It can be made using a mixture of singlet oxygen with iodides, which doesn't react practically with singlet oxygen. After the stage of filling the mixture is exposed to instantaneous action resulting in release of free iodine atoms. The photolysis, electric discharge , radiolysis can be used for iodide decomposition. This method, called as volume generation if iodine atoms, make it possible to form a meter scale active medium. Being born the iodine atoms extract the energy stored in singlet oxygen in a form of laser emission in a time τ_{pulse}

$$\tau_{pulse} \cong 1 / K_f \cdot [I], \qquad (2)$$

where K_f is a rate constant for forward reaction of energy exchange and [I] is a concentration of iodine atoms. If generation of iodine atoms doesn't activate relaxation processes the output laser energy is determined by only the value of energy stored in active volume and remains constant. But the pulse duration is reciprocal to the concentration of iodine atoms. Thus, one can shorten the pulse duration and, hence, increase the pulsed power by increasing the iodine concentration.

When photolysis was used to produce iodine atoms the specific energy of 3,3 J/ l was obtained at 3 Torr of oxygen pressure, 40% singlet oxygen yield and at CH_3I as an iodide /3/. This value of specific energy corresponds to 90% of extraction efficiency and to 23 % of chemical efficiency. The chemical efficiency of 36 % was obtained at lower oxygen pressure and, hence, higher singlet oxygen yield. These very high values of chemical efficiency at rather low yield were obtained due to saving the excited oxygen molecules being consumed to dissociate molecular iodine in the traditional CW COIL The pulse duration could be varied from 15 μs to about 500 μs at practically constant output energy. The pulse power of 300 kW was obtained from a laser with 1.4 l of active volume. Thus the active medium as long as 1 m in flow direction at singlet oxygen pressure to 3 Torr and power level of three orders of magnitude higher that in CW mode at the same chemicals flowrate were demonstrated.

Photolysis is a very convenient way to produce iodine atoms due to its selectivity. Its demerits are low efficiency and low repetition rate of flash lamps operation. The electric discharge can provide laser operation with multi kilohertz repetition rate. But *ab initio* it was not clear if electric discharge is suitable to decompose iodide and, at the same time, not to quench the singlet oxygen molecules. The experiments carried out with a longitudinal pulsed dc discharge showed the electric discharge is effective for this purpose. The specific energy of 1 J / l was obtained at 2 Torr of oxygen pressure. The total efficiency (ratio of laser output energy to that stored in capacity bank) was close to 100% /4/. The operation with repetition rate up to 20 Hz was demonstrated. Note, that repetition rate in our case was limited by the power of an available power supply.

The value of specific energy obtained with electric discharge initiation is at a disadvantage in relation to that obtained with photolysis. The possible causes of this difference could be the quenching of singlet oxygen by electrons and particle fragments as well as heating of active medium due to increased energy cost of iodine atoms produced by discharge. The energy of UV quantum causing the iodide molecule dissociation is 5 eV. Assuming the total energy stored in capacitor bank is deposited into active medium one can estimate the energy cost of iodine atom produced by discharge is as large as 25 eV.

The promising results obtained with the longitudinal pulsed COIL with volume generation of atomic iodine by using a dc discharge encouraged us to start an investigation of a transverse discharge excitation. This type of discharge make it possible to work with higher pressure of singlet oxygen provided by modern jet singlet oxygen generator. Besides, it was found that repetitively pulsed operation of longitudinal COIL worsens when repetition rate increases. This is a result of vaporization of iodine deposited on the wall of laser chamber. One can decrease this effect by minimizing the ratio of surface of laser chamber to its volume. It can be made when transverse flow transverse discharge is used.

But change over to the transverse discharge configuration meets problems. The first one is an acceptable matching of transverse discharge to power supply circuit. It is known that the best energy transfer from power supply to the load is obtained when the load resistance is equal to that of power supply. Unlike the longitudinal discharge the transverse one has usually significantly shorter discharge gap at larger area of discharge cross -section.

The resistance of the discharge is proportional to its length and reciprocal of its cross section. Thus, shortening the length of discharge gap by a factor of n one have to increase the cross section by the same factor to save the active volume. As a result the resistance of discharge reduces by a factor of $1/n^2$. To save the electric field strength one has to decrease the voltage across a discharge gap by a factor 1/n too. The latter requires one to increase the capacitance by a factor of n^2 to save the energy deposition into active medium. In its turn the change of capacitance results in decreasing the circuit resistance by a factor 1/n. (The inductances for both longitudinal and transverse discharges are assumed to be equal). Thus, one can see that discharge gap resistance changes proportionally to $1/n^2$ while that for circuit is proportional to 1/n. This difference results in impedance mismatch.

The another problem can be essential when operation pressure and discharge gap are small. In this case the length of cathode fall of voltage can occupy the major part of active volume thus shortening the area of positive column in which the processes governing the laser operation occur.

2. Experimental technique.

At present the different approaches are used to provide the transverse electric discharge to drive the gas lasers with high operation pressure (CO_2 – lasers, eximer lasers). Practically all of them use the preionization with electron beam or photoionization. To produce the latter the array of spark gaps, barrier discharge or surface discharge is used. Recently the great success was obtained in initiation of nonchain HF – laser /5/ using a system of electrodes with high edge nonuniformity and without any preionization. The uniform self-sustained volume discharge was obtained in a mixture of SF_6 with hydrocarbons C_2H_6 at total pressure of 60 Torr and the component ratio $SF_6 : C_2H_6 = 20 : 1$. The active volume of laser chamber was as large as 50 l at the length of electrodes gap 27 cm. The simple flat electrodes with rounding along its perimeter were used. The mechanism of formation of a uniform volume discharge proposed by authors allowed us to hope to obtain similar results in the case of pulsed COIL active medium. Indeed, like that in HF – laser, the COIL active medium contains the electronegative component – oxygen and easy to ionization component – RI. Note, that ionization potentials for both CH_3I – 9.5 eV and for CF_3I – 10,2 eV

are the less that for C_2H_6. Besides, the less pressure of the COIL active medium seemed to be positive to obtain the uniform discharge.

Two laser chambers with electrodes system mentioned above were designed and manufactured. The first one has 50 cm gain length and 4 cm discharge gap (fig.1) The active volume of this chamber is 800 cm3. This laser chamber is integrated with laser facility providing the operation with chlorine flowrate up to 100 mmole / s and pumping capacity to 1500 l / s. Thus, one can expect the maximal repetition rate to over 1 kHz.

Both electrodes were made of flat aluminum plates rounded along their perimeters. The cathode surface was subjected to sand-blasting.

All attempts to get a uniform discharge with this electrode system were unsuccessful. The nonuniformity increased drastically when iodide was added to oxygen. No lasing was detected within wide range of variation of electrical circuit parameters. To improve the discharge uniformity the electrode system was modified. The flat cathode was substituted for electrode with a surface discharge. The array of plasma channels produced across its surface served as a plasma cathode. Such a cathode reduces the role of negative effects in the zone of cathode voltage fall. Besides, the VUV radiation of plasma channels causes the preionization of discharge gap. As a result, the uniform discharges were obtained in the zones where the plasma channels existed. Thus the task was reduced to receiving the total filling the cathode surface with a plasma channels. This work is now in progress.

The second laser chamber was designed to work in combination with a jet singlet oxygen generator (fig. 2). It has 5 cm gain length and 2 cm electrode gap and in its first version it was equipped with a simple system of electrodes. Like that for the 50 cm laser chamber all attempts to obtain the uniform discharge were unsuccessful too.

In spite our experiments with simple electrode system without preionization were unsuccessful we believe this approach can be useful for future experiments at higher pressure and longer electrode gaps. Up to now the simple flat cathode was substituted for resistively loaded multi pin one. The satisfactory uniform discharge was obtained in recent experiments. This substitution was made on the base of results obtained with a 19-cm gain length laser chamber equipped with multi pin resistively loaded cathode. All results presented below on the pulsed COIL with generation of iodine atoms by using a transverse discharge were obtained with this laser chamber.

The experimental facility (fig.3) included the chemical singlet oxygen generator, gas handling system, pumping system, discharge power supply, optical chamber, laser chamber, control system. The quartz cylinder sparger singlet oxygen generator had 140-mm diameter and 230 mm height. It was packed with Rashig rings (12x12x1.5mm) made of Teflon. The height of packing was 130 mm. The typical working solution was prepared by mixing 750 ml of 50% hydrogen peroxide with 400 ml of 50 % KOH. The start temperature of working solution in SOG was close to -20^0 C. Typically, the duration of a run was as long as 10 – 20 sec and then it was followed with a period of cooling the working solution. The gas from SOG was transported to the laser cavity through a quartz tube of 50-mm o.d. The pressure guide, iodide injector and optical chamber inlet were located 500 mm, 640 mm and 800 mm downstream of SOG, respectively. The iodide injector was perforated torus made of Teflon. The gas flow entering the optical chamber branched into two arms ended with outlets to pumping system and cavity mirrors holders. The total length of optical chamber was 1600 mm and it was equal to the length of the laser resonator when internal mirrors were used. Previously this optical chamber was used as a laser cell of the pulsed COIL with longitudinal geometry. In the present work the 19-cm gain length laser cell was inserted into the one of the arms of optical chamber.

The laser chamber was equipped with electrodes, 1.8 cm apart, providing the transverse discharge with respect to the flow direction. It had 19-cm length cathode with 120 pins arranged in three lines. The active volume was 52 cm^3. The electric circuit (Fig.4) was fed with a positive high voltage from a power supply with a buffer capacitor C_1. The discharge capacitor C_2 could be varied within 3.4 nF....20.4 nF by variation of the number of capacitor of 3.4 nF. The electric discharge was triggered by the pulse generated with a generator S and applied to the grid of thyratron TGI1- 16 / 500.This thyratron provided the circuit operation with a voltage up to 18 kV (little over its passport limit). In its turn the pulse generator PG drove the triggering generator S. The duration of discharge was close to 200 ns.

Molecular chlorine was fed through the leaker and electromagnetic valve from a 5-liter volume flexible polyethylene bag filled from a standard cylinder with liquid chlorine. The application of a flexible bag made it possible to sustain the input pressure to be equal to atmospheric one and thus to stabilize the

chlorine flowrate. Iodides were fed through the leaker and electromagnetic valve too. CH_3I delivered from a stainless steel vessel of 8-l volume charged with 100 ml of liquid iodide. CF_3I was fed from small volume cylinder. When used the buffer gases (He, N_2, Ar, SF_6) were injected into the chlorine flow upstream of SOG. This way made it possible to reduce the chlorine partial pressure in SOG and thus increase the singlet oxygen yield at high buffer gas flowrate.

The laser emission was detected with Ge- photodiode equipped with averaging sphere. Laser emission was focused on the hole of this sphere. The signal from detector was monitored with oscilloscope and then recorded with a digital camera. The output energy was measured with a calorimeter. The losses of energy in the elements of optical system were taken into account.

3. Results and discussion.

The investigation of pulsed COIL with generation of iodine atoms in the pulsed DC discharge was performed in Troitsk in accordance with Item 2. The influence of discharge energy, discharge voltage, oxygen pressure, sort and pressure of buffer gas on laser parameters was investigated.

All experiments were performed with laser cavity formed with totally reflecting mirror and output one with 4.5 % transmission. This value of transmission was chosen on the base of preliminary experiments on resonator optimization. Pump capacity was 80 l / s. It is not the limit for our pumping system, but such a medium pumping made it possible to increase the run duration without refilling the SOG.

Specification:
P_{O2} – oxygen pressure in laser chamber
P_{He} – helium pressure
P_{Ar} – argon pressure
P_{N2} – nitrogen pressure
P_{SF6} – sulfur hexafluoride pressure
P_{RI} – iodide pressure
E_{out} – output laser energy
C_2 – discharge bank capacitance
V – capacitor bank voltage
E_{el} - energy stored in capacitor bank
$\tau_{1/2}$ – pulse duration
τ_{del} – delay time between discharge and lasing start
ε - specific energy (E_{out} / 52 cm^3)
I – intensity of singlet oxygen luminescence
($\eta = I / P_{O2}$)- relative yield

3.1. Oxygen pressure.

Experimental conditions:
C_2 = 13.6 nF
V = 18 kV
E_{el} = 4.4 J
Buffer gas – nitrogen, P_{N2} = 9 torr
Iodide – CH_3I, P_{RI} = 0.5 torr
The matrix of experiments is presented in Table 1.

Table1

P_{O2},Torr	E_{out}, mJ	η, arb. u	ε,mJ/cm^3	$\tau_{1/2}$, μs	τ_{del}, μs
0.5	18	30	0.15	10.6	5
1.0	33	25	0.63	11.3	5
1.6	42	23	0.81	10.8	5
2.0	47	22	0.9	12.6	5
3.0	40	20	0.76	9	4

One can see the variation of oxygen pressure results practically in only variation of the output energy value. Pulse duration and time delay remains constant within the limit of error (about 1 μs, the thickness of the oscilloscope beam) (Fig. 5). It means the iodide concentration remains constant for all oxygen pressures. Thus the energy deposition into active medium is governed mainly by buffer gas that pressure is in excess of that for oxygen.

Unlike the theoretical predictions the output energy doesn't increase linearly with oxygen pressure but has a maximum (Fig. 6). The reason of such a behavior is a drop of singlet oxygen yield when oxygen pressure increases. Such a drop is critical for sparger type singlet oxygen generator, and it practically negligible for jet one (at least within the pressure range investigated). Thus one can expect an appreciable increase of output energy working with jet SOG instead of sparger one. In this case the improvement of laser performance is due to increase of both the oxygen operation pressure and singlet oxygen yield. In our experiments the yield value doesn't exceed 40 % at pumping capacity 80 l / s

Nevertheless, the value 0.9 J / l of specific energy obtained is at a slight disadvantage in relation to longitudinal discharge. At the same time the pulse duration is much shorter. Note, the visual observation of discharge shows its nonuniformity. Thus one can expect the increasing of specific energy under improvement of discharge uniformity.

3.2. Sort and partial pressure of iodide.

Experimental conditions:

C_2 = 13.6 nF
V = 18 kV
E_{el} = 4.4 J
P_{O2} = 1.0 torr
Buffer gas – nitrogen, P_{N2} = 9 torr
The matrix of experiments is presented in Table 2

Table 2

P_{RI}, torr	E_{out}, mJ	$\tau_{1/2}$, μs	τ_{del}, μs	[I], 10^{14} cm^{-3}	[I] / [RI]
CH_3I					
0.2	28	16	9	8	0.12
0.4	36	12	5	10.6	0.08
0.6	37	9	4	14	0.07
0.7	37	9	4	14	0.06
CF_3I					
0.2	18	17	9	7.5	0.12
0.4	24	13	5	10	0.08
0.6	29	9	4	14	0.07
0.8	29	8	3	16	0.06
1.0	30	7,5	3	17	0.05
1.5	33	7	2	18	0.04

Low saturation pressure of CH_3I vapor limited the range of P_{RI} variation.

The results obtained show the both iodides produce iodine atoms with the same effectiveness. It results in practically identical time parameters of laser pulses obtained at the equal iodide pressures (Fig.7). The value of iodine atom concentration [I] and ratio of this value to the corresponding iodide molecules one is presented in the Table 2 too. The latter is a level of iodide dissociation. The iodine atom concentrations were evaluated from equation (2) using experimental data on pulse duration. Note that iodine atom concentration of 1.8×10^{15} cm^{-3} is close to the highest value reported for COIL operation of both CW and pulsed modes.

Thus, the increase in iodide partial pressure is a fruitful way to shorten the pulse duration. When laser operates much over threshold the output energy changes slightly (Fig. 8).

Like that for the case of photoinitiation the output energy depends in the same manner on the sort of iodide used. The CH_3I appears to be more effective iodine donor (Fig.8). It was shown /6/ that the cause of such a difference is a fast quenching of singlet oxygen by RO_2 molecules (R is a radical CH_3 or CF_3) formed after iodide dissociation But in the case of discharge the output energies obtained for these two iodides differ by only 15 % against that of about 50 % for photolysis. It can be a result of more short pulse duration.

One can see the level of dissociation drops when iodide concentration increases. As soon as iodide molecules dissociate in a process of dissociative attachment the drop of dissociation level can be result of deficit of electrons in active medium. This deficit can be eliminated due to higher voltage or discharge energy. Indeed, this effect was observed (see below).

3.3. Voltage and bank capacitance.

Experimental conditions:

P_{O2} = 1.0 torr

Buffer gas – nitrogen, P_{N2} = 9 torr

Iodide – CF_3I, P_{RI} =1.5 torr

The matrix of experiments is presented in Table 3

Table 3.

U,kV	E_{el}, J	E_{out}, mJ	$\tau_{1/2}$, μs	τ_{del}, μs	[I], 10^{14} cm^{-3}	Cost, eV
C_2 = 6.8 nF						
10	0.68	19		-	-	
10	0.68	20		-	-	
15	1.53	28		-	-	
18	2.20	34	10	5	13	203
C_2 = 20.4 nF						
10	2.04	29	8	2	16	153
15	4.59	28	7	2	18	306
18	5.60	29	6.5	2	20	396
C_2 = 3.4 nF						
10	0.34	1.2	-	24	-	
15	0.76	13	17	8	7	130
18	1.10	17	16	5	8	162
C_2 = 13.6 nF						
10	1.36	28	10	4	13	125
15	3.06	31	7.5	2.5	17	216
18	4.40	33	7	2.5	18	293

The variation of voltage at constant bank capacitance results in only variation of stored energy while, besides that, variation of C_2 changes the matching of discharge to circuit. In our case this effect is not so important. It seems the range of variation of voltage and capacitance investigated is too small to understand what parameter of discharge circuit is a critical one. The results obtained show the stored energy is a critical factor governing the value of output energy and time parameters within the range investigated.

The values of energy cost of iodine atom presented in Table 3 seem to be very large. These values are relative one. The real values of energy cost can be obtained if energy deposition into active medium is known. In its turn energy deposition is determined as a product of discharge current by voltage drop across the discharge gap. The apparatus to measure these parameters is now under manufacturing.

It was mentioned above the shortening of laser pulse can be obtained due to iodide pressure increase as well as to discharge energy increase. Indeed, one can see, the shortest pulse duration of 6.5 μs (Fig.9) was obtained at iodide pressure 1.5 torr and 6.6 J of energy store in capacitor bank.

3.4. Buffer gas.

Experimental conditions:

C_2 = 13.6 nF
P_{O2} =1.0 torr
Iodide – CH_3I, P_{RI} =0.5 torr
The matrix of experiments is presented in Table 4

Table4

P_{buffer}, torr	V, kV	E_{el}	E_{out}, mJ	$\tau_{1/2}$, μs	τ_{del}, μs
He					
3.0	10	1.36	2.5	-	-
3.0	15	3.06	8.6	-	-
3.0	18	4.40	12	-	-
5.0	10	1.36	8.6	27	17
5.0	15	3.06	17	16	9
5.0	18	4.40	19	15	7
9.0	10	1.36	20	24	9
9.0	15	3.06	27	17	6
9.0	18	4.40	29	16	5
Ar					
3.0	10	1.36	6.1	-	-
3.0	15	3.06	9.8	-	-
3.0	18	4.40	12	-	-
5.0	10	1.36	9.2	-	-
5.0	15	3.06	15	-	-
5.0	18	4.40	15	-	-
9.0	10	1.36	13	18	8
9.0	15	3.06	16	14	6
9.0	18	4.40	14		
N_2					
3.0	10	1.36	5.5	-	-
3.0	15	3.06	11	19	10
3.0	18	4.40	13	16	8
5.0	10	1.36	12	23	11
5.0	15	3.06	18	17	6
5.0	18	4.40	21	14	6
9.0	10	1.36	24	18	7
9.0	15	3.06	27	12	4
9.0	18	4.40	27	11	4
SF_6					
3.0	10	1.36	13	24	12
3.0	15	3.06	18	-	-
3.0	18	4.40	18	-	-
5.0	10	1.36	22	20	9
5.0	15	3.06	22	-	8
5.0	18	4.40	22	11	6
7.0	10	1.37	26	17	7

Unlike that for pulsed COIL with photolysis the role of buffer gas in a discharge initiated laser is more complex. In this case buffer gas not only increases the heat capacity of active medium but change the parameters of discharge plasma. In particular, the increase of operation pressure due to buffer gas make it possible to increase the discharge resistance and thus improve the energy deposition into active medium. Indeed, one can see from table 4, the higher buffer gas pressure results in shortening of both pulse duration and time delay. As it was shown above, both these effects are governed by mainly iodine atom concentration in active medium.

The efficiency of buffer gas depends on its sort. Fig10 demonstrates the dependence of output energy on buffer gas partial pressure for V = 15 kV. One can see the buffer gas heat capacity is not the only parameter governing the laser performance. Indeed, helium and argon having the same heat capacity result in different output energy. It is positive that cheap nitrogen is not at a disadvantage in relation to expensive helium.

The high efficiency of SF_6 seems to be very promising. It is known that SF_6 dissociates in a discharge, forming free fluorine atoms F. Thus one has opportunity to use chemical generation of iodine atoms. When HI or DI is used as an iodine atom donor free fluorine atoms can react with iodide forming free iodine atoms /7/.

$$F + HI(DI) \rightarrow I + HF(DF) \qquad (3)$$

Thus, high concentration of iodine atoms can be obtained due to increase of SF_6 partial pressure instead of iodide one. Besides, this way allows one to reduce the expenses for laser operation.

Unfortunately, our facility didn't allowed us to increase SF_6 pressure over 7 torr. Because of insufficient conductivity of our pipe line and high SF_6 viscosity the input pressure over 1 atm was required to provide necessary SF_6 flowrate. But this high pressure blocked the chlorine flow driven by atmospheric pressure pressing the chlorine bag.

.4. Conclusion.

Investigation of the pulsed COIL with volume generation of iodine atoms using a transverse DC discharge was performed. The influence of oxygen pressure, iodide sort and pressure, discharge energy, sort and pressure of buffer gas on the output energy and time parameters of the laser pulse was studied. The aim of investigation was to search for the ways making it possible to generate a laser pulse as powerful as possible. It was shown the increase of oxygen pressure and singlet oxygen yield resulted in output energy growth at conserved pulse duration. At the same time increase of both iodide concentration and discharge energy resulted in growth of iodine atom concentration and thus in shortening of the pulse duration. The pulse duration of 6.5 μs is reported. This value corresponds to the iodine atom concentration close to the highest one reported for the COIL of both CW and pulsed type.

Following this way one can produce the iodine atom concentration close to that of singlet oxygen. In this case the significant fraction of energy is stored in iodine atoms. If Q-modulation method is applied this energy can be extracted in a form of nanosecond scale pulse.

Specific energy of 0.9 J / l, that is close to that obtained with longitudinal discharge, and specific power of 75 kW / l was obtained. The ways to increase these values were proposed.

Hexafluoride was shown to be a very promising buffer gas. Having rather high heat capacity this gas generates fluorine atoms when exposed to discharge. Thus, application of this buffer gas make it possible to use chemical generation of iodine atoms via reaction of fluorine atoms with HI or DI used as iodine donor.

References

1. Yuryshev N.N. "Chemically Pumped Oxygen-Iodine Laser", Quantum electronics, **26(7),** pp 567-584 (1996).
2. Highland R, Crowell P and Hager G, Proc. SPIE Int, Soc. Opt. Eng. **1225** 512 (1990)
3. Frolov M, Ishkov D, Kryukov P, Pazyuk V, Podmar'kov Yu, Vagin N and Yuryshev N, Proc. SPIE Int, Soc. Opt. Eng. **2502** 291 (1995)
4. Vagin N, Pazyuk V and Yuryshev N. Quantum Electronics **25**(8) 746 (1995).
5. Apollonov V.V., Firsov K.N., Kazantsev S.Yu. and Oreshkin V.F., Proc. SPIE Int, Soc. Opt. Eng. **3574** 374 (1998)
6. Yuryshev N. Proc. SPIE Int, Soc. Opt. Eng. **139** 221 (1991).
7. Jiraser J, Spalek O. and Kodymova J "Kinetic and Thermodinamic Aspects of Chemical Generation Chemical Generation of Atomic iIodine for a COIL and their Consequences for Experiments", Proc. Of COIL R&D Workshop, 11 – 12 Oct. 1999.

Part 5

The study of production iodine atoms from CH_3I in RF discharge.

The volume production of iodine atoms using transverse RF discharge in the mixture of a iodide (RI) with singlet oxygen is very attractive method for creation active medium for the Q-switched COIL. The existing RF power supply with the next output parameters has been modified for realization such possibility:

CW power	1.5 kW,
frequency	16MHz,
CW maximal voltage	8.5 kV,
pulse duration	variable,
pulse repetition frequency	1kHz

Peak pulse power at pulse duration about 10 μs exceeded CW power in several times only.

The major problem of this investigation consists in the determination of the iodide dissociation efficiency. There are two methods:

1) to use COIL lasing;
2) to use probe laser for the measurement iodine atom concentration.

The first method means the work in the dark conditions without any information about iodine atom concentration, if lasing is absent. Second method can't be used at the conditions of the pulse repetition mode of the supersonic COIL. Requested pulse duration is $\tau \le 0.1 L_{gain}/U_{gas} \approx 10$ μs because the period of the probe laser frequency scanning $T_{scan} =$ 40ms $>> \tau$. Taking into account these circumstances the efficiency of iodine atoms generation is studied at CW mode of RF discharge and subsonic flow. Conditions of the subsonic flow give possibility to increase the interaction of gas with plasma of RF discharge and to reach more higher iodine concentration from one hand and to use smaller iodide flow rates at the requested iodide partial pressures. The typical portion of the dissociated iodide in the **axial flow** pulse repetition COIL with DC discharge equal to approximately (1÷3)% because iodide and chlorine flow rates are close with each other. This means that the obtaining the requested iodide partial pressure in the subsonic mode operation is possible at significantly less iodide molar flow rate than at supersonic mode. The special discharge chamber has been manufactured. The electrodes with square 6×6 cm have been manufactured from the glass plastic with copper cover. The thickness of the glass plastic plates was 1.5mm. The distance between these the glass plastic plates equal to 30 mm. The Plexiglas nozzles' blades with thickness 5 mm were inserted in the discharge chamber forming the gap of

20mm. The nitrogen and then argon were used as carriers iodide molecules. At first the nitrogen molar flow rate was 20 mmole/s, iodide flow rate (CH_3J) – 4.3 mmole/sec, the static pressure in the discharge chamber without discharge was 3.2 torr and increased up to 3.4÷3.9 torr when the discharge was switched in. The current, voltage and the phase shift between its were measured . The input power in the gap was calculated and was changed in the limits 150W ÷ 1500W but we could not say exactly what portion of this power is power input in the gas flow because the resistance of plastic glass plates and nozzle's blades is unknown. The voltage was varied from 2 to 8.2 kV. The discharge was homogeneous. The probe laser beam was used for determination of the iodine atoms' absorption which appeared at input power more 250 W. The probe laser beam was located in the center of discharge chamber. The absorption value had weak dependence on the input power in the limits (250 ÷ 1500) W and was $2\alpha L$=(0.35 ÷0.5)% although the line width changed from 250MHz to 285 MHz. At increasing twice nitrogen flow rates and static pressure in the discharge gap the absorption value equaled to 0,4% at maximal possible input power. The typical best absorption lines are presented in fig.1÷fig.4 and experimental conditions - in the Table 1. The change nitrogen on argon at the same flow rate resulted in the decreasing of the absorption value. The maximal absorption 0.3% was reached in one run only. The reached maximal iodide dissociation efficiency is one order of magnitude less than the requested one for successful COIL operation. It's worth nothing that the discharge gap constitutes close to reactive load and the phase shift between voltage and current differs from 90° on small value. It means bad impedance match power supply and load. It's necessary to develop the special RF power supply with high peak pulse power and small impedance. Decreasing the static pressure and increasing voltage for raising discharge parameter (E/P_{cavity}) had not sense because low static pressure has not interest but large voltage is very danger at real COIL operation conditions when BHP aerosol may provide the conductivity the duct walls. The further investigation of this method for production of iodine atoms were stopped.

Table1

M_{CH3I}, mmole/s	M_{N2}, mmole/s	P_{cavity}, torr	U, kV	I, A	W_{disch}, W	α, %/cm
4.3	20	3.4	5.5	2	525	0.0437
4.3	20	3.4	5.9	2.5	840	0.0494
4.3	39	6.56	4.6	2.5	1350	0.0405
4.3	40	6.6	4.6	2.5	1500	0.04

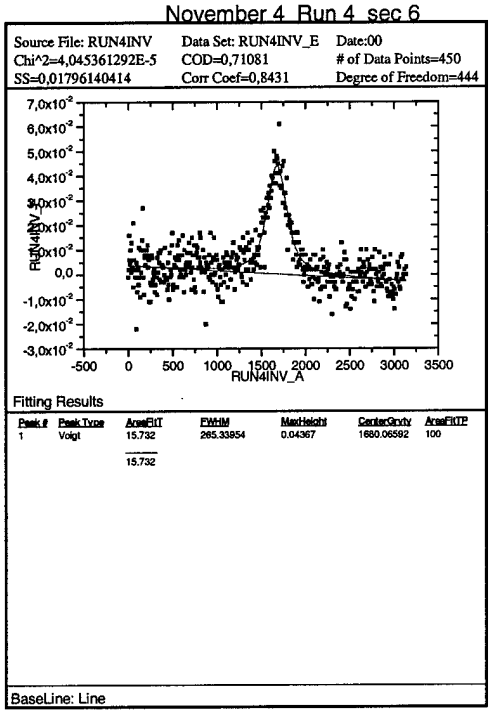
November 4 Run 4 sec 6
Source File: RUN4INV
Data Set: RUN4INV_E
Date:00
Chi^2=4,045361292E-5
COD=0,71081
# of Data Points=450
SS=0,01796140414
Corr Coef=0,8431
Degree of Freedom=444
RUN4INV_A
Fitting Results
Peak # Peak Type AreaFitT FWHM MaxHeight CenterGrvty AreaFitTP
1 Voigt 15.732 265.33854 0.04367 1680.06592 100
15.732
BaseLine: Line

Fig.1

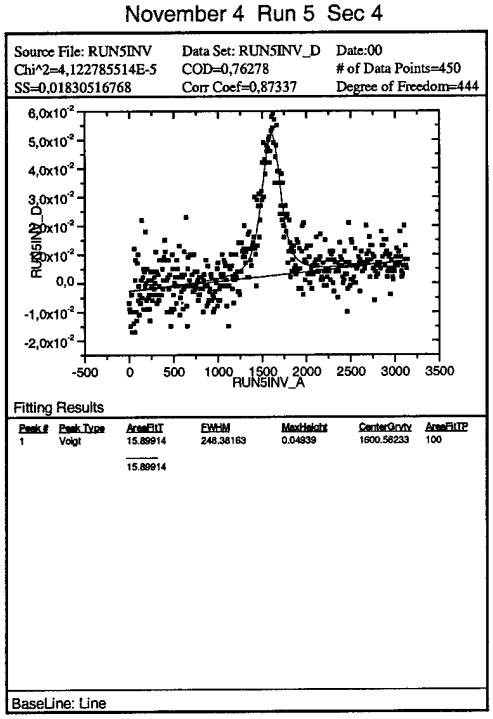
November 4 Run 5 Sec 4
Source File: RUN5INV
Data Set: RUN5INV_D
Date:00
Chi^2=4,122785514E-5
COD=0,76278
# of Data Points=450
SS=0,01830516768
Corr Coef=0,87337
Degree of Freedom=444
RUN5INV_A
Fitting Results
Peak # Peak Type AreaFitT FWHM MaxHeight CenterGrvty AreaFitTP
1 Voigt 15.89914 248.38163 0.04939 1600.58233 100
15.89914
BaseLine: Line

Fig. 2

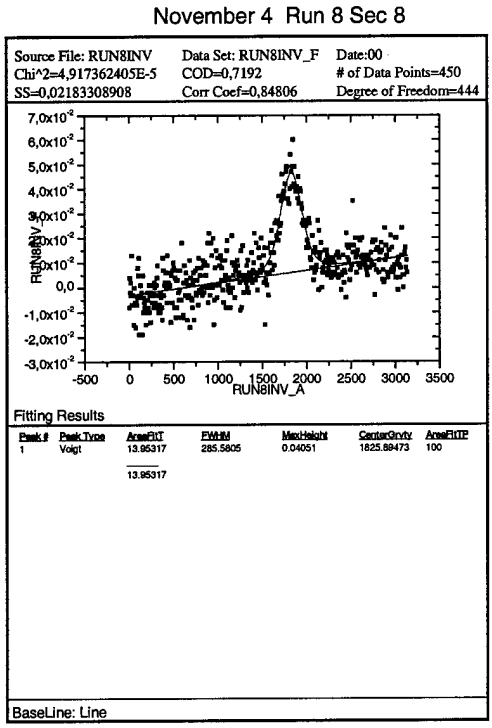
November 4 Run 8 Sec 8
Source File: RUN8INV
Data Set: RUN8INV_F
Date:00
Chi^2=4,917362405E-5
COD=0,7192
# of Data Points=450
SS=0,02183308908
Corr Coef=0,84806
Degree of Freedom=444
RUN8INV_F
RUN8INV_A
Fitting Results
Peak # Peak Type AreaFIT FWHM MaxHeight CenterGrvty AreaFITP
1 Voigt 13.95317 285.5805 0.04051 1825.89473 100
13.95317
BaseLine: Line

Fig.3

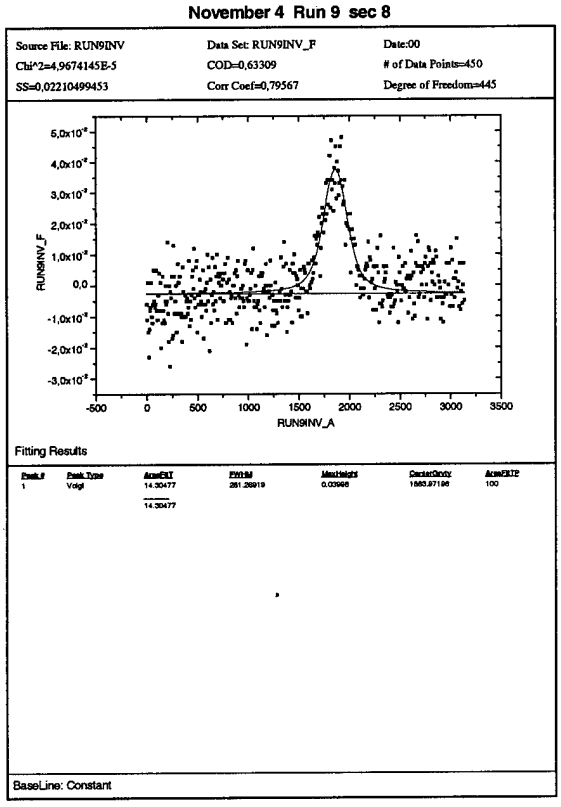
November 4 Run 9 sec 8
Source File: RUN9INV
Data Set: RUN9INV_F
Date:00
Chi^2=4,9674145E-5
COD=0,63309
# of Data Points=450
SS=0,02210499453
Corr Coef=0,79567
Degree of Freedom=445
RUN9INV_F
RUN9INV_A
Fitting Results
BaseLine: Constant

Fig. 4

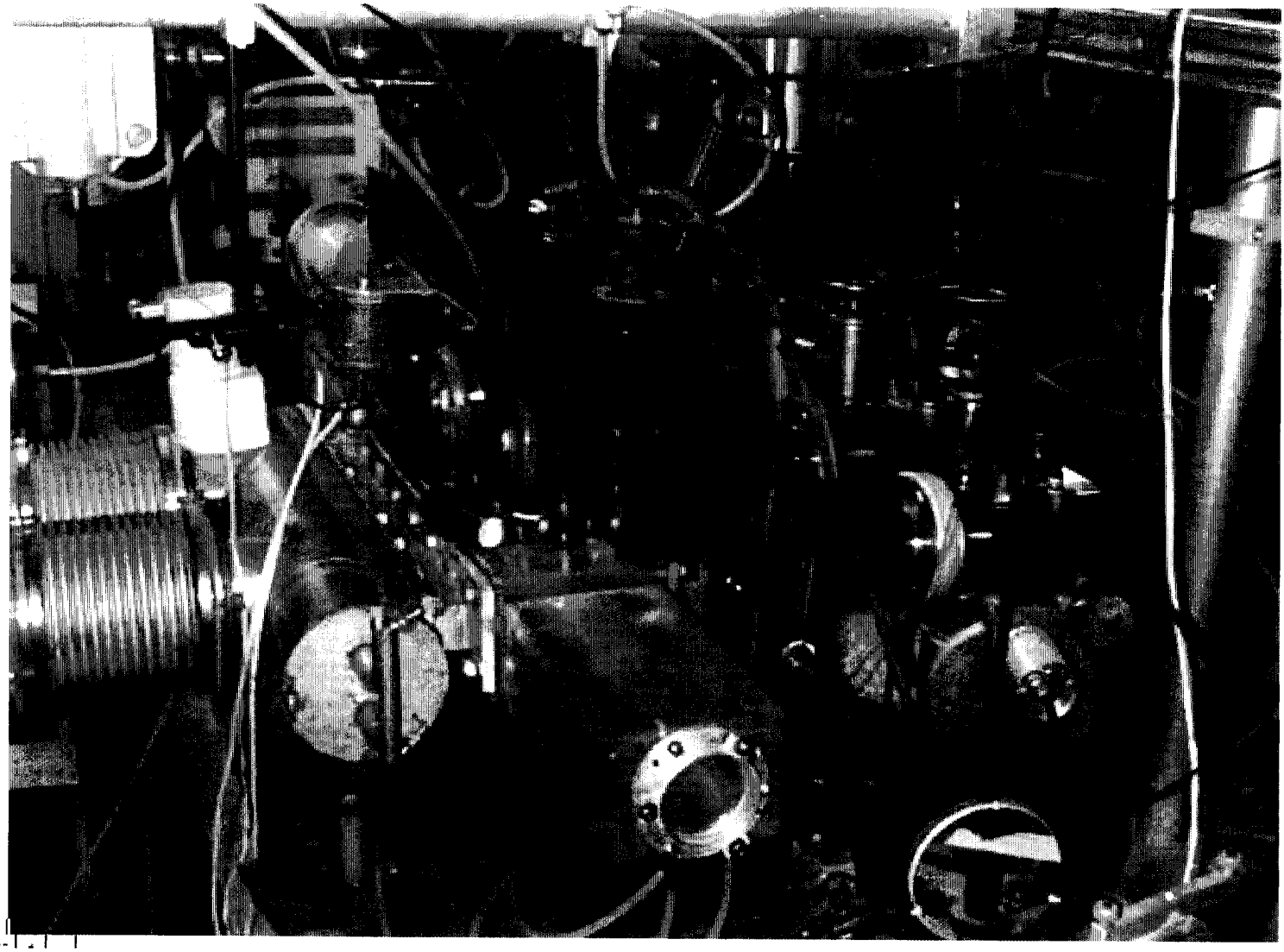

Fig. 2. The small-scale laser chamber with a Jet SOG

Fig. 2. The small-scale laser chamber with a Jet SOG

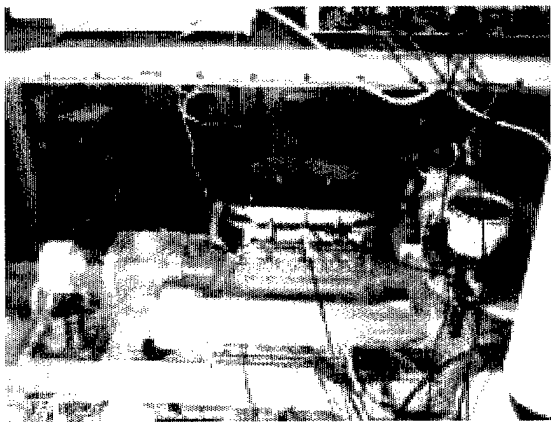

Fig 3. The view of the left arm of optical chamber with a laser chamber

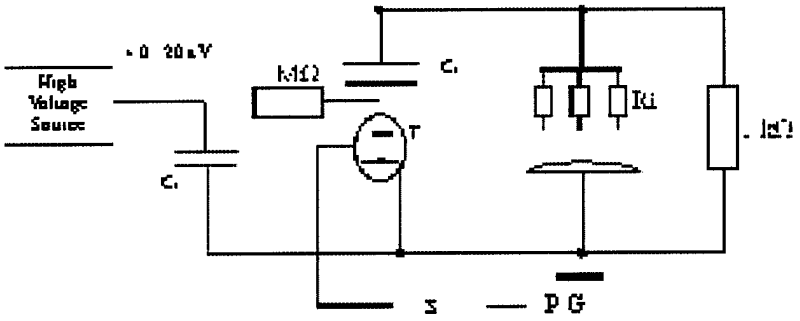

Fig 4. The diagram of electric circuit.

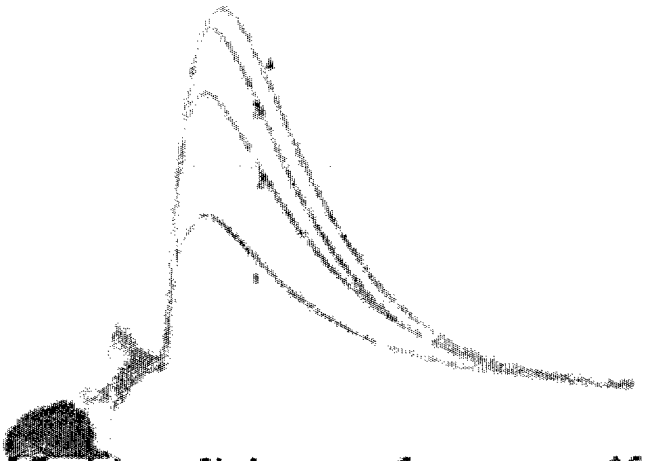

Fig 5 Time base traces of the laser energy for oxygen pressure 0.5 mm (1), 1.0 mm (2), 1.6 mm (3), and 2.0 mm (4). Time scale—5 μs/div

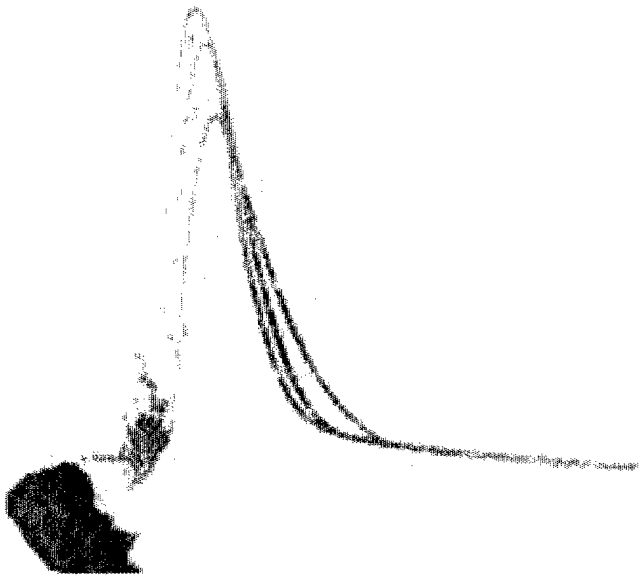

Fig. 6. Influence of discharge energy on pulse compression. P_{O_2} = 1.0 mm, R_1 = 1.5 mm, R_2 = CF; C_c = 20 pF, V = 10 kV (1), 15 kV (2), 18 kV (3). Time scale—5 μs/div